Diagrammatic Monte Carlo as an exact tool for a problem of a complex object interacting with bosons. What else can be done?

A. S. Mishchenko
Japan Science and Technology Agency, AIST, Tsukuba

1. Shortly about the methods and physical systems which one can handle without approximations
2. More about the methods
3. Franck-Condon principle. Is it good for optical spectroscopy?
4. ARPES and optical spectra of High Tc materials at low doppings. Electron-phonon?

Diagrammatic Monte Carlo method

Example: polaron.

$$\hat{H}_0 = \sum_{\mathbf{k}} \epsilon(\mathbf{k}) a^{\dagger}_{\mathbf{k}} a_{\mathbf{k}} + \sum_{\mathbf{q}} \omega_{\mathbf{q}} b^{\dagger}_{\mathbf{q}} b_{\mathbf{q}}$$

$$\hat{H}_{\text{int}} = \sum_{\mathbf{k},\mathbf{q}} V(\mathbf{k},\mathbf{q}) (b^{\dagger}_{\mathbf{q}} - b_{-\mathbf{q}}) a^{\dagger}_{\mathbf{k}-\mathbf{q}} a_{\mathbf{k}} + h.c.$$

Green function:

$$G_{\mathbf{k}}(\tau) = \langle \text{vac} \mid a_{\mathbf{k}}(\tau) a^{\dagger}_{\mathbf{k}} \mid \text{vac} \rangle$$

Green function contains a lot of information about the system and the only problem left is how to calculate it without approximations and how to extract that information

Feynman expansion:

$$G_{\mathbf{k}}(\tau) = \left\langle \text{vac} \left| T_{\tau} \left[a_{\mathbf{k}}(\tau) a^{\dagger}_{\mathbf{k}}(0) \exp\left\{ - \int_0^{\infty} \hat{H}_{\text{int}}(\tau') d\tau' \right\} \right] \right| \text{vac} \right\rangle_{\text{con}}$$

DMC is a method which sums the Feynman expansion for systems in the thermodynamic limit without truncation of Feynman series or any other approximation

Problems suitable for DMC: one or few particles in bosonic bathes.

Exciton

$$\hat{H}_0^{\text{par}} = \sum_{\mathbf{k}} \varepsilon_a(\mathbf{k}) a_{\mathbf{k}}^{\dagger} a_{\mathbf{k}} + \sum_{\mathbf{k}} \varepsilon_h(\mathbf{k}) h_{\mathbf{k}} h_{\mathbf{k}}^{\dagger}$$

$$\hat{H}_{\text{a-h}} = -N^{-1} \sum_{\mathbf{pkk'}} \mathcal{U}(\mathbf{p}, \mathbf{k}, \mathbf{k'}) a_{\mathbf{p}+\mathbf{k}}^{\dagger} h_{\mathbf{p}-\mathbf{k}}^{\dagger} h_{\mathbf{p}-\mathbf{k'}} a_{\mathbf{p}+\mathbf{k'}}$$

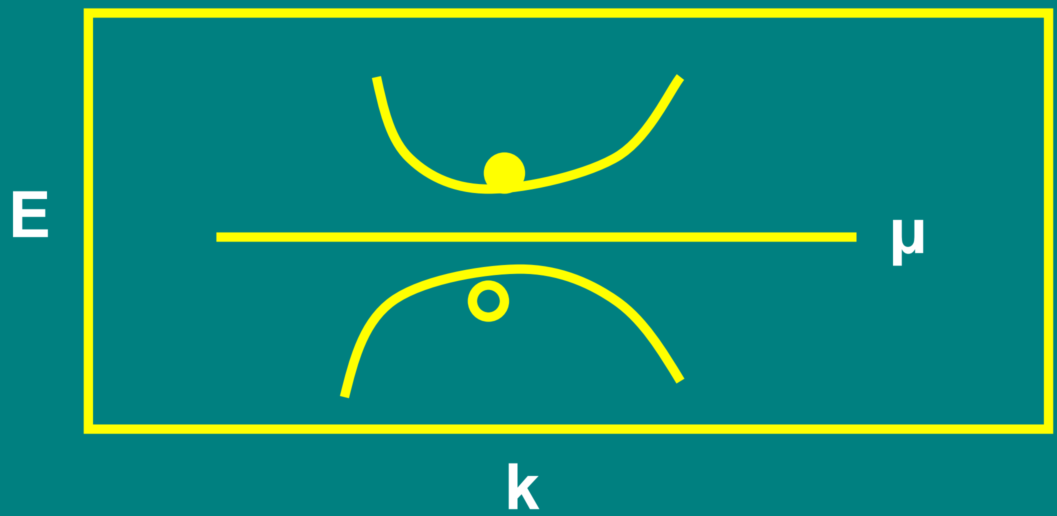

Only DMC

Bethe-Salpeter does not work!

Problems suitable for DMC: one or few particles in bosonic bathes.

Exciton

$$\hat{H}_0^{\text{par}} = \sum_{\mathbf{k}} \varepsilon_a(\mathbf{k}) a_{\mathbf{k}}^\dagger a_{\mathbf{k}} + \sum_{\mathbf{k}} \varepsilon_h(\mathbf{k}) h_{\mathbf{k}} h_{\mathbf{k}}^\dagger$$

$$\hat{H}_{\text{a-h}} = -N^{-1} \sum_{\mathbf{pkk'}} \mathcal{U}(\mathbf{p},\mathbf{k},\mathbf{k'}) a_{\mathbf{p+k}}^\dagger h_{\mathbf{p-k}}^\dagger h_{\mathbf{p-k'}} a_{\mathbf{p+k'}}$$

More realistic

Exciton-polaron

$$\hat{H}_{\text{par-bos}} = i \sum_{\kappa=1}^{Q} \sum_{\mathbf{k},\mathbf{q}} (b_{\mathbf{q},\kappa}^\dagger - b_{-\mathbf{q},\kappa}) \left[\gamma_{aa,\kappa}(\mathbf{k},\mathbf{q}) a_{\mathbf{k-q}}^\dagger a_{\mathbf{k}} + \gamma_{hh,\kappa}(\mathbf{k},\mathbf{q}) h_{\mathbf{k-q}}^\dagger h_{\mathbf{k}} + \gamma_{ah,\kappa}(\mathbf{k},\mathbf{q}) h_{\mathbf{k-q}}^\dagger a_{\mathbf{k}}\right] + h.c.$$

$$\hat{H}_{\text{bos}} = \sum_{\kappa=1}^{Q} \sum_{\mathbf{q}} \omega_{\mathbf{q},\kappa} b_{\mathbf{q},\kappa}^\dagger b_{\mathbf{q},\kappa}$$

Thermo-dynamic limit

Problems suitable for DMC: one or few particles in bosonic bathes.

Thermodynamic limit

Jahn-Teller and Pseudo-Jahn-Teller polarons

$$\hat{H}_0^{\mathrm{PJT}} = \sum_{\mathbf{k}} \sum_{i=1}^{T} \epsilon_i(\mathbf{k}) a_{i,\mathbf{k}}^{\dagger} a_{i,\mathbf{k}}$$

$$\hat{H}_{\text{par-bos}} = i \sum_{\kappa}^{Q} \sum_{\mathbf{k},\mathbf{q}} \sum_{i,j=1}^{T} \gamma_{ij,\kappa}(\mathbf{k},\mathbf{q}) (b_{\mathbf{q},\kappa}^{\dagger} - b_{-\mathbf{q},\kappa}) a_{i,\mathbf{k}-\mathbf{q}}^{\dagger} a_{j,\mathbf{k}} + h.c.$$

Decoherence of qubit: spin-boson Hamiltonian

$$\hat{H}_0 = 1/2\epsilon\left[c_1^\dagger c_1 - c_2^\dagger c_2\right] + \sum_\alpha \omega_\alpha b_\alpha^\dagger b_\alpha$$

$$\hat{H}_{int}^{(1)} = 1/2\Delta\left[c_1^\dagger c_2 + c_2^\dagger c_1\right]$$

$$\hat{H}_{int}^{(2)} = \sum_\alpha \sum_{\delta=1}^{2} \gamma_\alpha c_\delta^\dagger c_\delta \left[b_\alpha^\dagger + b_\alpha\right]$$

$J(\omega) \equiv \pi\sum_\alpha \gamma_\alpha^2 \delta(\omega - \omega_\alpha)$ can be approximated as $J(\omega) \sim \omega^s$

Advantages.

- No Trotter decomposition – no systematic errors
- Infinite systems – no finite scaling
- Infinite systems – exact momentum dependence
- Possibility to include damping
- No large PC memory is required

Physical properties under interest

Exciton: two-particle Green function

$$G_{\mathbf{k}}^{\mathbf{p}\mathbf{p}'}(\tau) = \langle \mathrm{vac} \mid a_{\mathbf{k}+\mathbf{p}'}(\tau) h_{\mathbf{k}-\mathbf{p}'}(\tau) h_{\mathbf{k}-\mathbf{p}}^{\dagger} a_{\mathbf{k}+\mathbf{p}}^{\dagger} \mid \mathrm{vac} \rangle$$

Jahn-Teller polaron: matrix Green function

$$G_{\mathbf{k},ij}(\tau) = \langle \mathrm{vac} \mid a_{i,\mathbf{k}}(\tau) a_{j,\mathbf{k}}^{\dagger} \mid \mathrm{vac} \rangle, \quad i,j = 1,2$$

Ordinary polaron: scalar green function

$$G_{\mathbf{k}}(\tau) = \langle \mathrm{vac} \mid a_{\mathbf{k}}(\tau) a_{\mathbf{k}}^{\dagger} \mid \mathrm{vac} \rangle$$

No simple connection to measurable properties!

Physical properties under interest: Lehmann function.

Lehmann spectral function (LSF)

$$L_{\mathbf{k}}(\omega) = \sum_{\nu} \delta(\omega - E_{\nu}(\mathbf{k}))\, |\langle \nu | a^{\dagger}_{\mathbf{k}} | \mathrm{vac} \rangle|^2$$

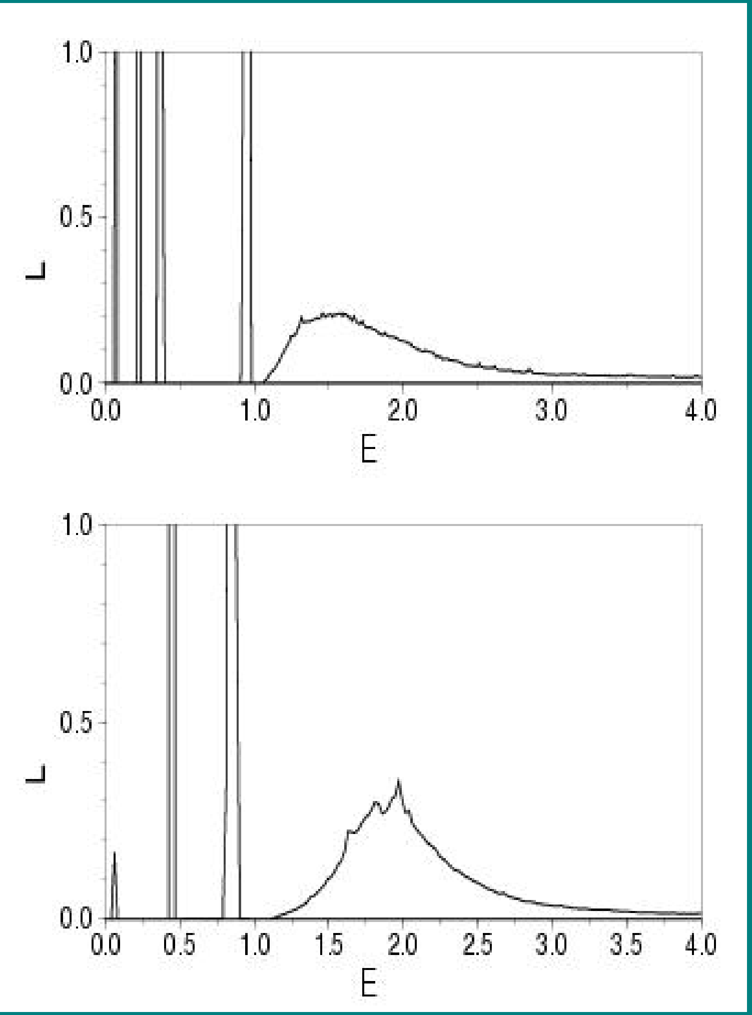

LSF has poles (sharp peaks) at the energies of stable (metastable) states. It is a measurable (in ARPES) quantity.

LSF can be determined from equation:

$$G_{\mathbf{k}}(\tau) = \int_0^{\infty} d\omega\, L_{\mathbf{k}}(\omega)\, e^{-\omega\tau}$$

Physical properties under interest: Lehmann function.

Lehmann spectral function (LSF)

$$L_{\mathbf{k}}(\omega) = \sum_{\nu} \delta(\omega - E_\nu(\mathbf{k}))\, |\langle \nu | a^\dagger_{\mathbf{k}} | \mathrm{vac} \rangle|^2$$

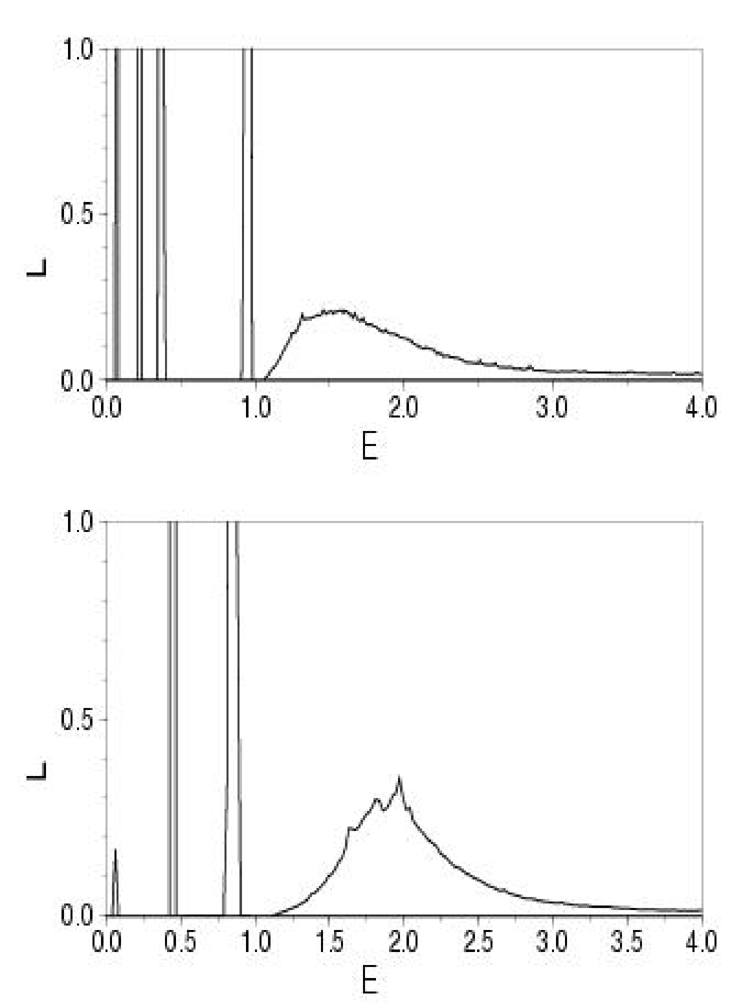

LSF can be determined from equation:

$$G_{\mathbf{k}}(\tau) = \int_0^\infty d\omega\, L_{\mathbf{k}}(\omega)\, e^{-\omega\tau}$$

Solving of this equation is
a notoriously difficult problem

$$L_{\mathbf{k}}(\omega) = \hat{\mathcal{F}}_\omega^{-1}\left[G_{\mathbf{k}}(\tau)\right]$$

Physical properties under interest: Excitonic absorption.

Such relation between imaginary-time function and spectral properties is rather general:

$$G_{\mathbf{k}}(\tau) = \int_0^\infty d\omega\, L_{\mathbf{k}}(\omega)\, e^{-\omega\tau}$$

Exciton: two-particle Green function

$$G_{\mathbf{k}}^{\mathbf{p}\mathbf{p}'}(\tau) = \langle \mathrm{vac} \mid a_{\mathbf{k}+\mathbf{p}'}(\tau) h_{\mathbf{k}-\mathbf{p}'}(\tau) h^{\dagger}_{\mathbf{k}-\mathbf{p}} a^{\dagger}_{\mathbf{k}+\mathbf{p}} \mid \mathrm{vac} \rangle$$

Light absorption is expressed as solution of the same equation

$$\mathcal{I}(\omega) = \hat{\mathcal{F}}_{\omega}^{-1} \left[\sum_{\mathbf{p}\mathbf{p}'} G_{\mathbf{k}=0}^{\mathbf{p}\mathbf{p}'}(\tau) \right]$$

Physical properties under interest: absorption by polaron.

Such relation between imaginary-time function and spectral properties is rather general:

$$G_{\mathbf{k}}(\tau) = \int_0^\infty d\omega \, L_{\mathbf{k}}(\omega) \, e^{-\omega\tau}$$

Current–current corelation function $\langle J_\beta(\tau) J_\delta \rangle$ is related to optical absorption by polarons by the same expression:

$$\sigma_{\beta\delta}(\omega) = \pi \hat{\mathcal{F}}_\omega^{-1} \left[\langle J_\beta(\tau) J_\delta \rangle \right] / \omega$$

About methods

1. Diagrammatic Monte Carlo

2. Analytic continuation

General rules to calculate Matsubara GF. Example: polaron

$$\hat{H}_0 = \sum_{\mathbf{k}} \epsilon(\mathbf{k}) a^\dagger_{\mathbf{k}} a_{\mathbf{k}} + \sum_{\mathbf{q}} \omega_{\mathbf{q}} b^\dagger_{\mathbf{q}} b_{\mathbf{q}}$$

$$\hat{H}_{\rm int} = \sum_{\mathbf{k},\mathbf{q}} V(\mathbf{k},\mathbf{q})(b^\dagger_{\mathbf{q}} - b_{-\mathbf{q}}) a^\dagger_{\mathbf{k}-\mathbf{q}} a_{\mathbf{k}} + h.c.$$

Feynman expansion:

$$G_{\mathbf{k}}(\tau) = \left\langle \mathrm{vac} \left| T_\tau \left[a_{\mathbf{k}}(\tau) a^\dagger_{\mathbf{k}}(0) \exp\left\{ -\int_0^\infty \hat{H}_{\rm int}(\tau') d\tau' \right\} \right] \right| \mathrm{vac} \right\rangle_{\rm con}$$

$$\hat{A}(\tau) = \exp[\tau(\hat{H}_{\rm par} + \hat{H}_{\rm ph})] \hat{A} \exp[-\tau(\hat{H}_{\rm par} + \hat{H}_{\rm ph})]$$

General rules to calculate Matsubara GF. Example: polaron

Feynman expansion:

$$G_{\mathbf{k}}(\tau) = \left\langle \text{vac} \left| T_\tau \left[a_{\mathbf{k}}(\tau) a^\dagger_{\mathbf{k}}(0) \exp\left\{ - \int_0^\infty \hat{H}_{\text{int}}(\tau') d\tau' \right\} \right] \right| \text{vac} \right\rangle_{\text{con}}$$

Infinite series of integrals with an ever increasing order:

$$G_{\mathbf{k}}(\tau) = \sum_{m=0,2,4\ldots}^{\infty} \sum_{\xi_m} \int dx'_1 \cdots dx'_m \, \mathcal{D}_m^{(\xi_m)}(\tau; \{x'_1, \ldots, x'_m\})$$

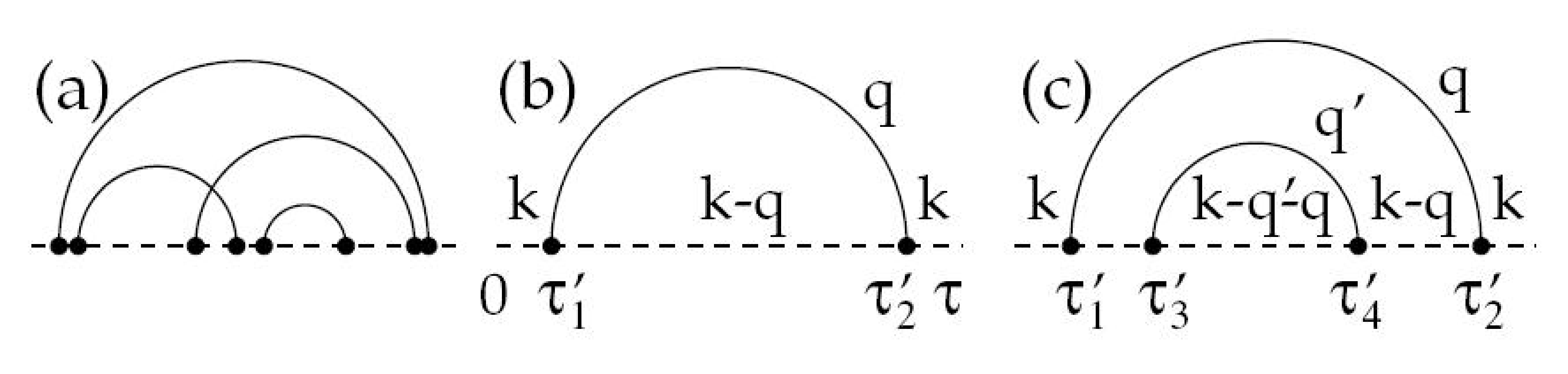

General rules to calculate Matsubara GF. Example: polaron

Weight?

Let us attribute weights D to terms of expansion. The weight is a factor of:

- Green function of bare particle $G^{(0)}(k,\tau)=\exp\{-\varepsilon(k)\tau\}$ is attributed to horizontal line.
- Green function of phonon $D^{(0)}(k,\tau)=\exp\{-\omega(k)\tau\}$ is attributed to phonon arch.
- $V(k,q)$ for each interaction vortex

$$G_{\mathbf{k}}(\tau) = \sum_{m=0,2,4\dots}^{\infty} \sum_{\xi_m} \int dx'_1 \cdots dx'_m \, \boxed{\mathcal{D}_m^{(\xi_m)}(\tau;\{x'_1,\dots,x'_m\})}$$

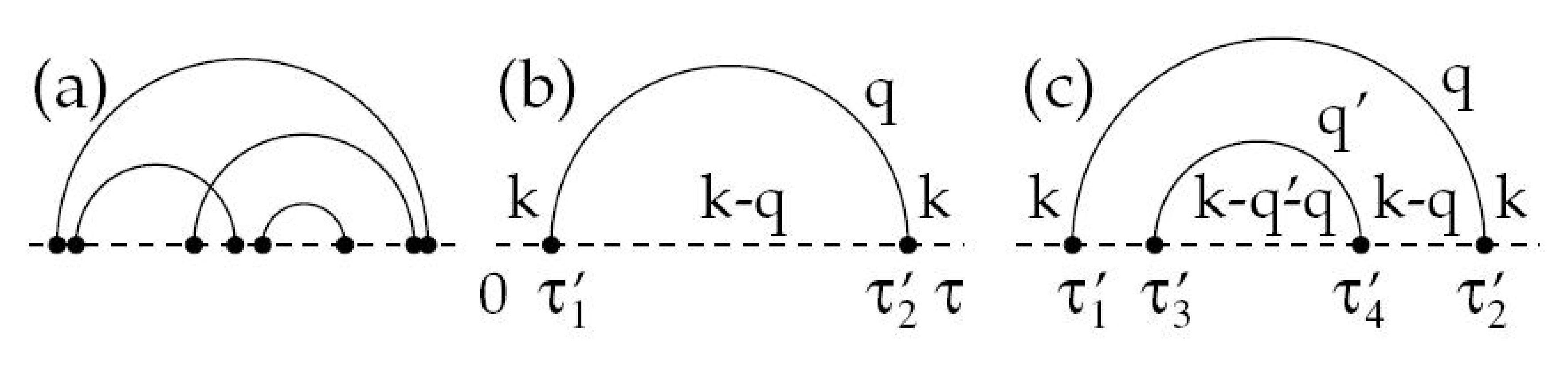

General rules to calculate Matsubara GF. Example: polaron

For example, the weight of Feynman diagram in Fig. (b) is:

$$\mathcal{D}_2(\tau; \{\tau_2', \tau_1', \mathbf{q}\}) =$$
$$|V(\mathbf{k}, \mathbf{q})|^2 \, D_{\mathbf{q}}^{(0)}(\tau_2' - \tau_1') G_{\mathbf{k}}^{(0)}(\tau_1') G_{\mathbf{k}-\mathbf{q}}^{(0)}(\tau_2' - \tau_1') G_{\mathbf{k}}^{(0)}(\tau - \tau_2')$$

$$G_{\mathbf{k}}(\tau) = \sum_{m=0,2,4\ldots}^{\infty} \sum_{\xi_m} \int dx_1' \cdots dx_m' \, \mathcal{D}_m^{(\xi_m)}(\tau; \{x_1', \ldots, x_m'\})$$

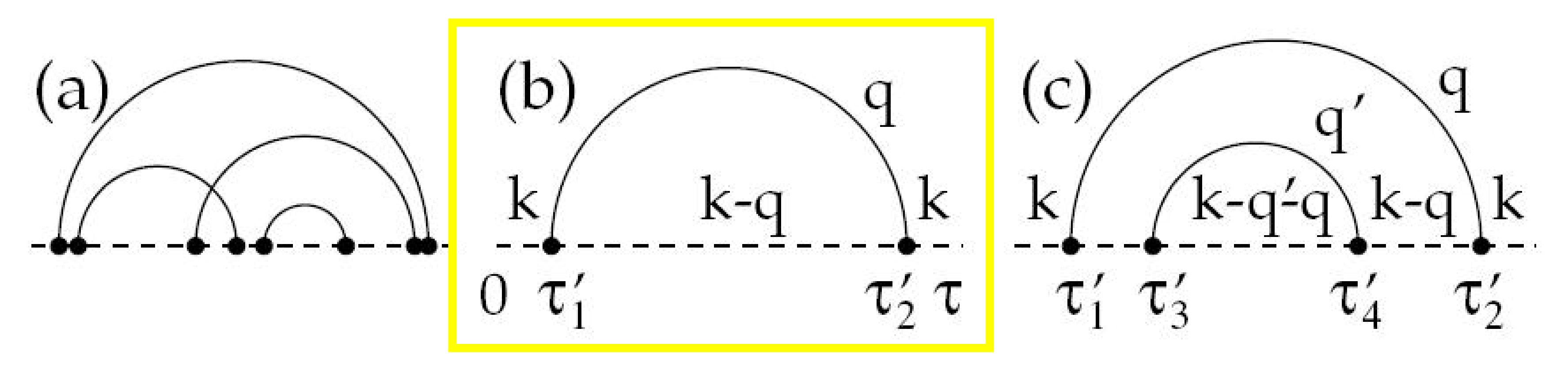

Exciton.

$$\hat{H}_0^{\text{par}} = \sum_{\mathbf{k}} \varepsilon_a(\mathbf{k}) a_{\mathbf{k}}^{\dagger} a_{\mathbf{k}} + \sum_{\mathbf{k}} \varepsilon_h(\mathbf{k}) h_{\mathbf{k}} h_{\mathbf{k}}^{\dagger}$$

$$\hat{H}_{\text{a-h}} = -N^{-1} \sum_{\mathbf{pkk'}} \mathcal{U}(\mathbf{p},\mathbf{k},\mathbf{k}') a_{\mathbf{p}+\mathbf{k}}^{\dagger} h_{\mathbf{p}-\mathbf{k}}^{\dagger} h_{\mathbf{p}-\mathbf{k}'} a_{\mathbf{p}+\mathbf{k}'}$$

Weight of the FD is the factor of interaction vortexes U and propagators of e-h pairs

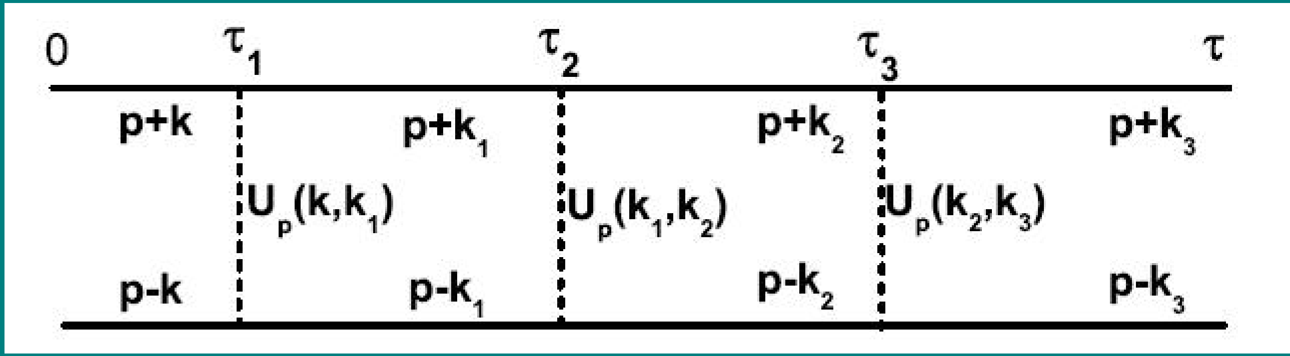

$$G_p(k, \tau_{i+1} - \tau_i) = \exp\left[-(\epsilon_p(k) - \mu)(\tau_{i+1} - \tau_i)\ .\right]$$

$$\epsilon_{\mathbf{p}}(\mathbf{k}) = \varepsilon_c(\mathbf{p}+\mathbf{k}) - \varepsilon_v(\mathbf{p}-\mathbf{k})$$

Exciton problem: E. A. Burovski et.al., Phys. Rev. Lett. vol. 87, 186402 (2001).

Phonons

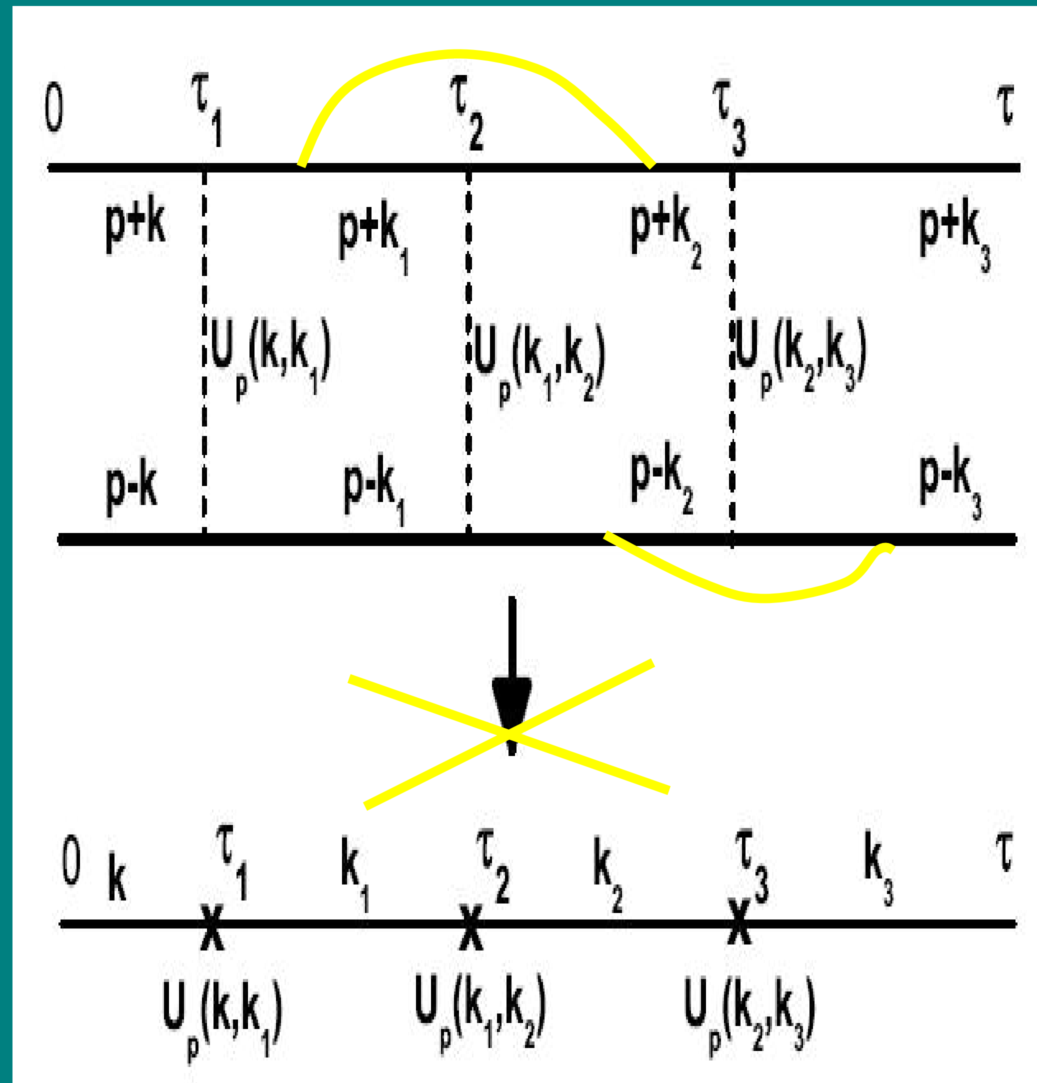

Ill-defined objects: auxiliary interactions

Generally, dispersion relation Є(k) in realistic systems is ill-defined. One can speak of Lehman function (LF) $L_k(\omega)$, which is normalized to unity probability to find QP with momentum k at the energy ω.

$$L_{\mathbf{k}}(\omega) = \sum_{\nu} \delta(\omega - E_{\nu}(\mathbf{k})) \, |\langle \nu | a_{\mathbf{k}}^{\dagger} | \mathrm{vac} \rangle|^2$$

$$\int_0^{+\infty} d\omega L_{\mathbf{k}}(\omega) = 1$$

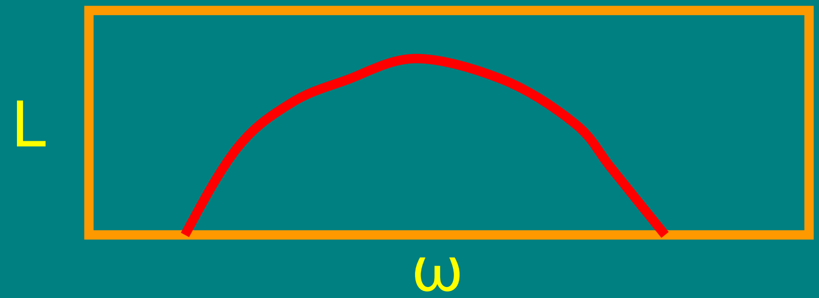

Only for non-interacting system the LF reduces to delta-function and, thus, sets up dispersion relation ω=Є(k).

$$L_{\mathbf{k}}^{\mathrm{NONINT}}(\omega) = \delta(\omega - \epsilon(\mathbf{k}))$$

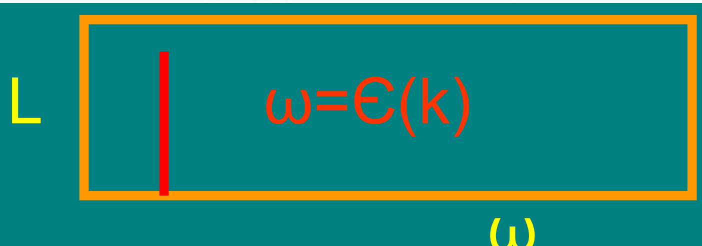

Ill-defined objects: auxiliary interactions

Generally, dispersion relation Є(k) in realistic systems is ill-defined. One can speak of Lehman function (LF) $L_k(\omega)$, which is normalized to unity probability to find QP with momentum k at the energy ω.

$$L_{\mathbf{k}}(\omega) = \sum_{\nu} \delta(\omega - E_{\nu}(\mathbf{k}))\, |\langle \nu | a^{\dagger}_{\mathbf{k}} | \mathrm{vac} \rangle|^2$$

$$\int_0^{+\infty} d\omega L_{\mathbf{k}}(\omega) = 1$$

Neither rules nor strategy is changed when there is a damping of QP or bosonic bath

Only for non-interacting system the LF reduces to delta-function and, thus, sets up dispersion relation ω=Є(k).

$$L^{\mathrm{NONINT}}_{\mathbf{k}}(\omega) = \delta(\omega - \epsilon(\mathbf{k}))$$

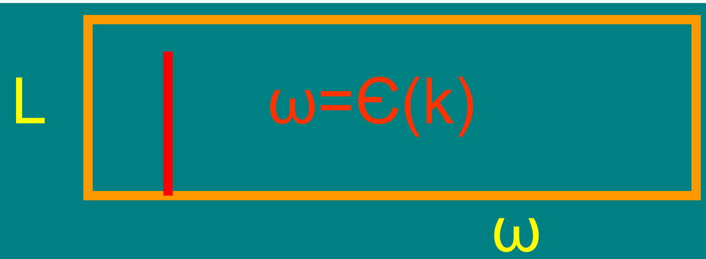

Ill-defined objects: auxiliary interactions

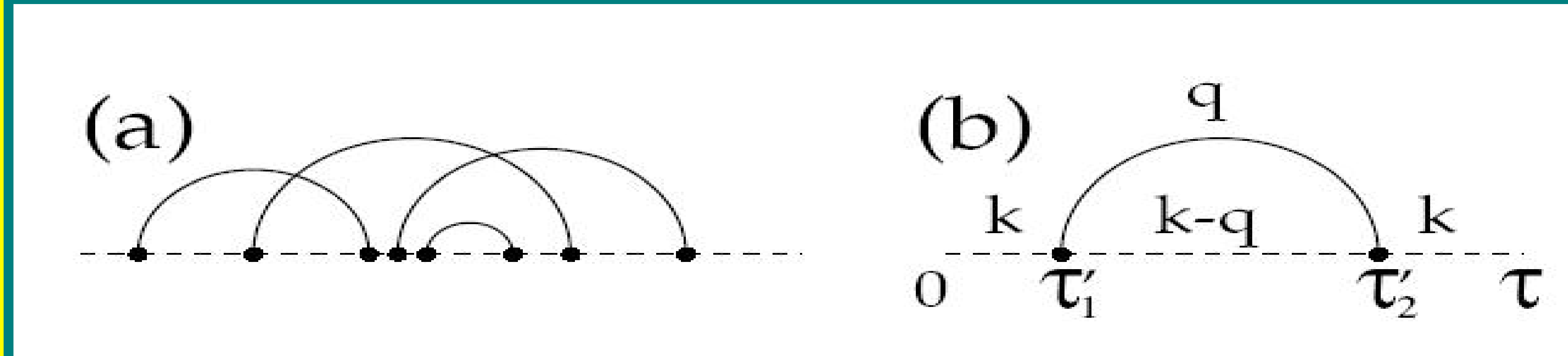

Neither rules nor strategy is changed when there is a damping of QP or bosonic bath

Green function of bare particle $G^{(0)}(k,\tau)=\exp\{-\varepsilon(k)\tau\}$ is attributed to horizontal line.

- Green function of phonon $D^{(0)}(k,\tau)=\exp\{-\omega(k)\tau\}$ is attributed to phonon arch.
- V(k,q) for each interaction vortex

Ill-defined objects: auxiliary interactions

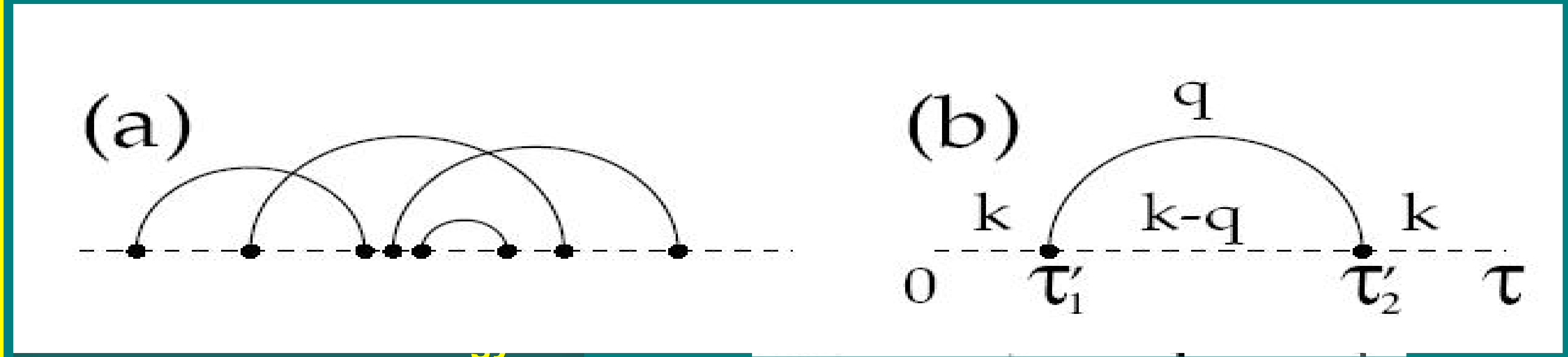

Neither rules nor strategy is changed when there is a damping of QP or bosonic bath

$$\tilde{G}^{(0)}_{\mathbf{k}}(\tau) = \frac{1}{\pi}\int_{-\infty}^{\infty} d\omega e^{-\omega\tau} \frac{Im\Sigma_{\mathrm{ret}}(\mathbf{k},\omega)}{[\omega - \epsilon(\mathbf{k}) - Re\Sigma_{\mathrm{ret}}(\mathbf{k},\omega)]^2 + [Im\Sigma_{\mathrm{ret}}(\mathbf{k},\omega]^2}$$

Procedure of Diagrammatic Monte Carlo ends up with statistics of external variable τ, which converges to exact answer

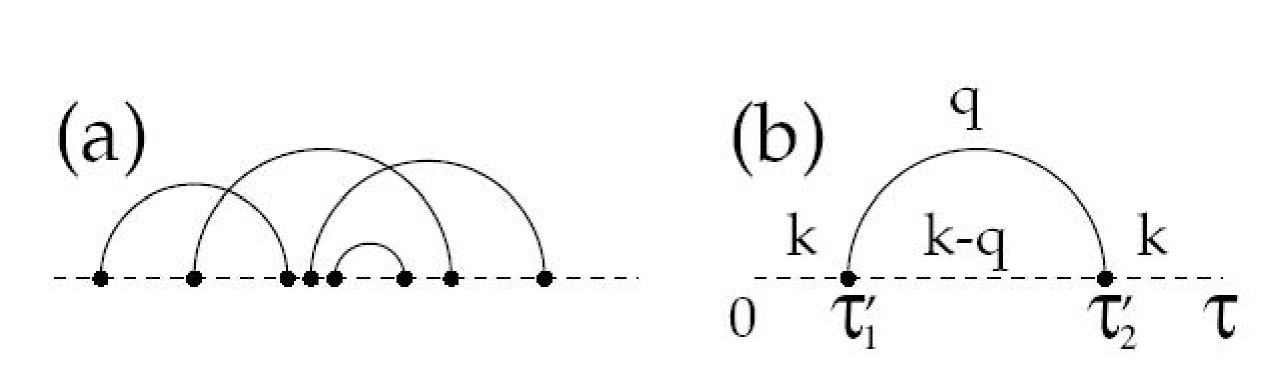

The series should be sign definite to avoid sign problem and assure fast convergency.
However, if it is not the case (e.g. for optical conductivity in t-J model, k-dependence of interaction vortex, etc …) one needs to accumulate very large statistics.

It is clear that Matsubara representation is necessary!

Method of analytic continuation

$$G_k(\tau) = \int^{\infty} L_k(\omega)\exp(-\omega\tau)\, d\omega$$

- LSF can be obtained from inverting of integral equation.
- This equation is the so called "ill defined problem"

Main difficulty with ill defined problems is the "saw tooth noise" instability!!!

If solution is searched by naïve minimization of the deviation

$$D = \int d\tau\, [G(\tau) - \hat{G}(\tau)] ,$$

where $\hat{G}(\tau)$ is obtained from approximate solution $\acute{L}(\omega)$, fluctuations of approximate solution are larger than the LSF itself!!!!

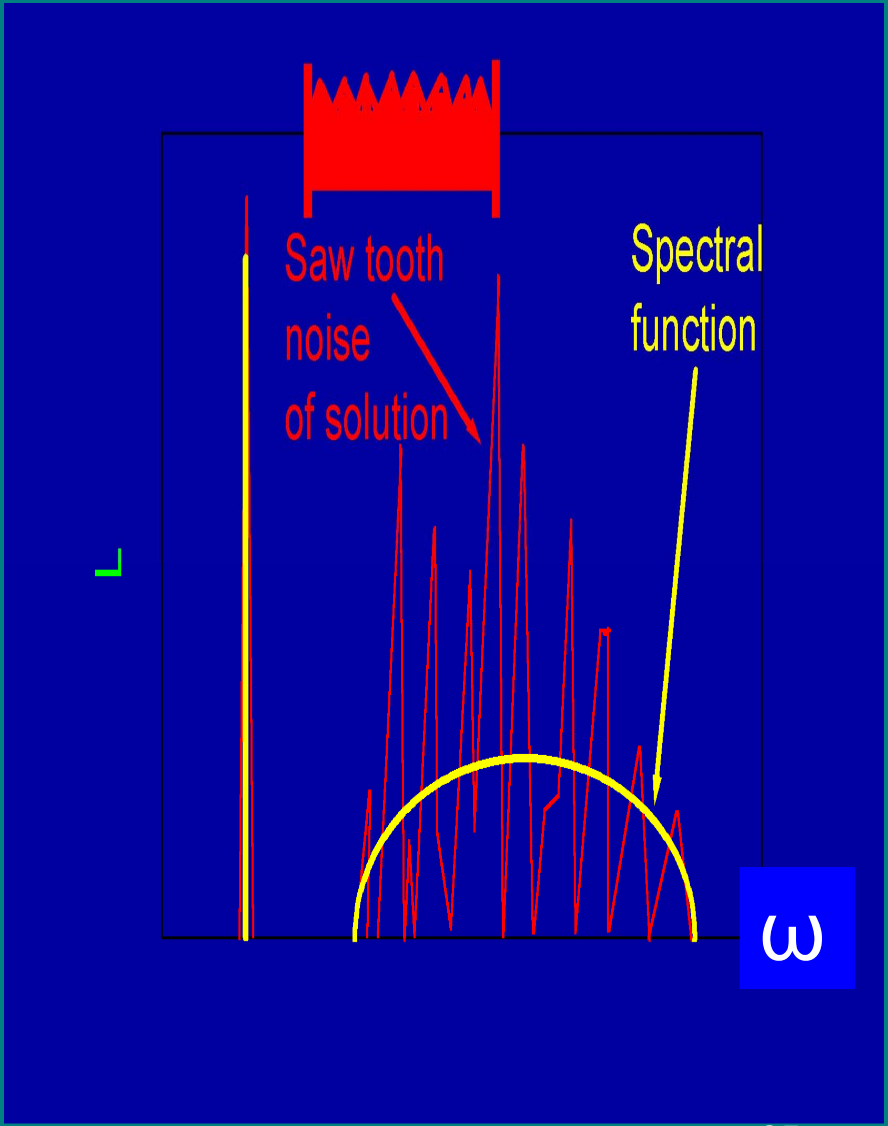

Standard regularization method to fight with saw tooth noise. (used in popular Maximal Entropy method too)

$$G_k(\tau) = \int^{\infty} L_k(\omega)\, \exp(-\omega\tau)\, d\omega$$

$$+ F[\, L,\, dL / d\omega,\, d^2L / d\omega^2 \,]$$

A nonlinear functional F, which suppresses large derivatives of solution L is added to linear equation. This suppresses saw tooth noise.

However, typical LSF of particle is a sharp peak and continuum with sharp edge. Hence, regularization procedure destroys both sharp peaks and sharp edges.

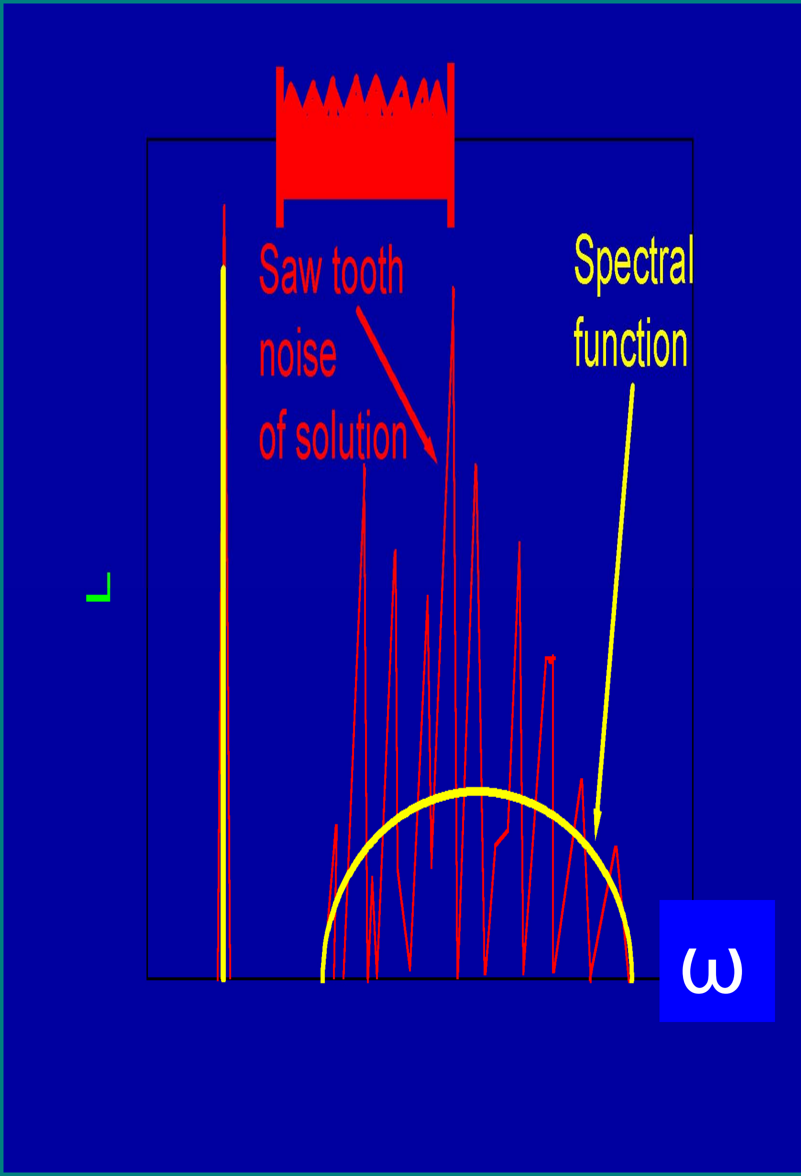

Standard regularization method to fight with saw tooth noise. (used in popular Maximal Entropy method too)

$$G_k(\tau) = \int^{\infty} L_k(\omega)\, d\omega$$

$$+ F[\, L,\ dL / d\omega,\ d^2L / d\omega^2\,]$$

A nonlinear functional F, which suppresses large derivatives of solution L is added to linear equation. This suppresses saw tooth noise.

However, typical LSF of particle is a sharp peak and continuum with sharp edge. Hence, regularization procedure destroys both sharp peaks and sharp edges.

How to defeat saw tooth noise without regularization?

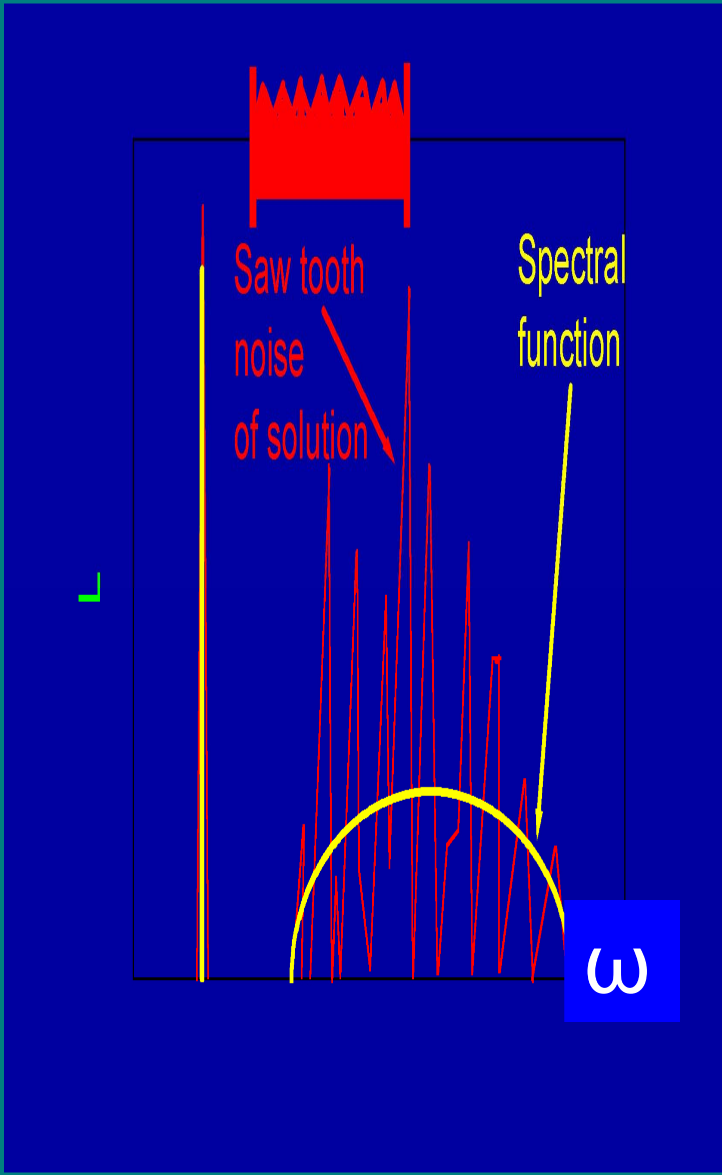

Stochastic Optimization method.

- Particular solution $L^{(i)}(\omega)$ for LSF is presented as a sum of a number N of rectangles with some width, height and center.

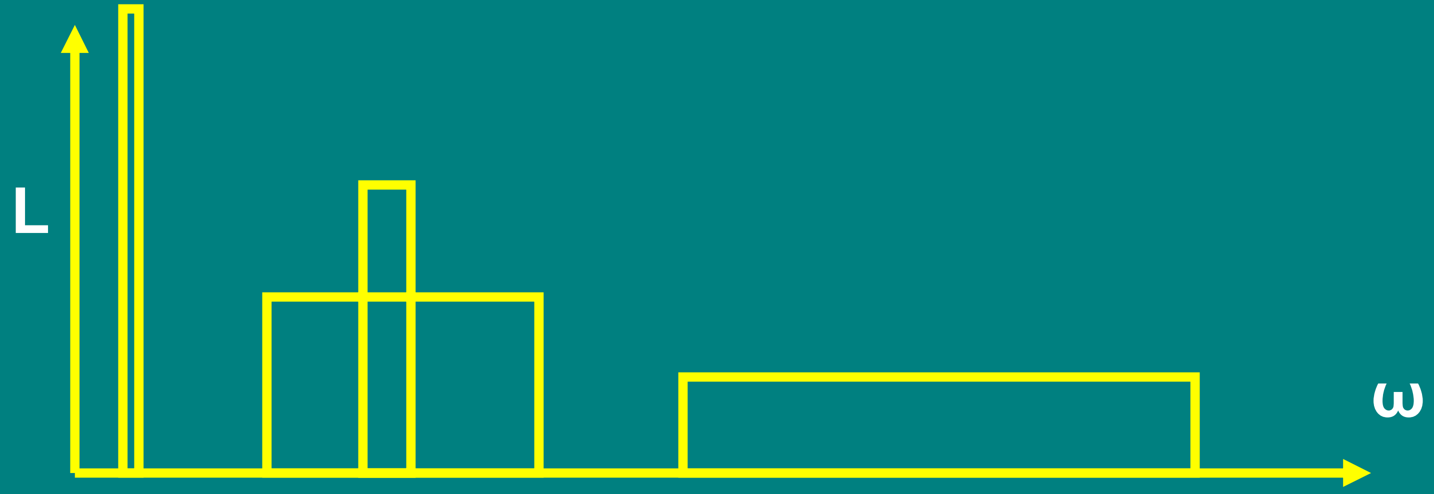

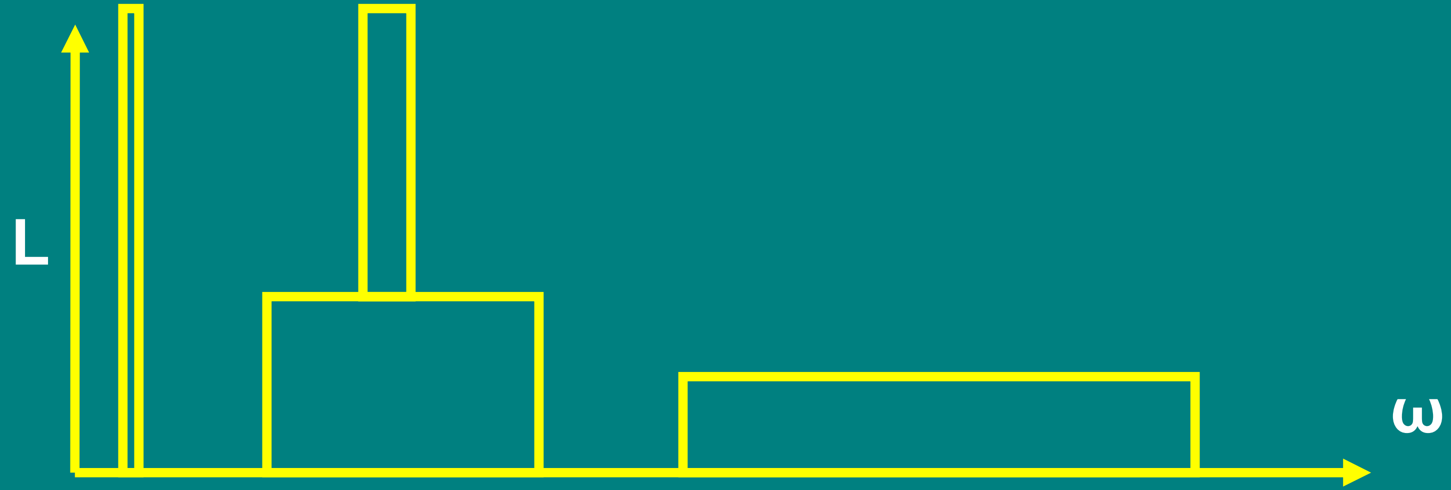

Stochastic Optimization method.

- Particular solution $L^{(i)}(\omega)$ for LSF is presented as a sum of a number N of rectangles with some width, height and center.
- Initial configuration of rectangles is created by random number generator (i.e. number N and all parameters of of rectangles are randomly generated).

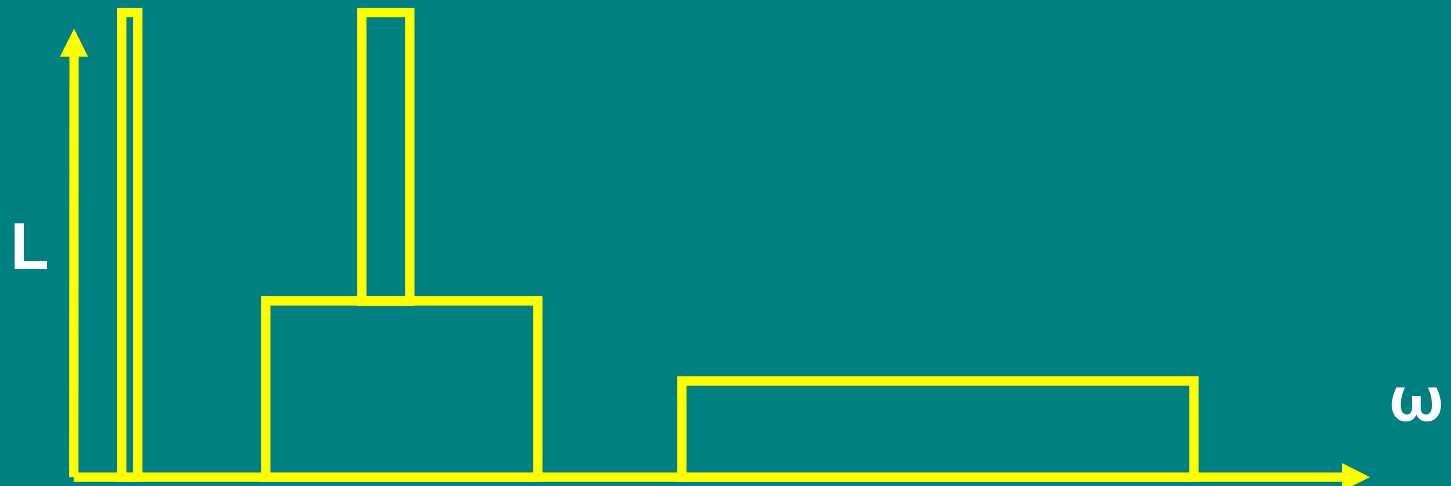

Stochastic Optimization method.

- Particular solution $L^{(i)}(\omega)$ for LSF is presented as a sum of a number N of rectangles with some width, height and center.
- Initial configuration of rectangles is created by random number generator (i.e. number N and all parameters of of rectangles are randomly generated).
- Each particular solution $L^{(i)}(\omega)$ is obtained by a naïve method without regularization (though, varying number N).

Deviation measure for configuration:

$$D[\tilde{L}_{\mathbf{k}}(\omega)] = \int_0^{\tau_{\max}} \left| G_{\mathbf{k}}(\tau) - \tilde{G}_{\mathbf{k}}(\tau) \right| G_{\mathbf{k}}^{-1}(\tau) d\tau$$

$$\widetilde{G}_{\mathbf{k}}(\tau) = \int_0^{\infty} d\omega \, \widetilde{L}_{\mathbf{k}}(\omega) \, e^{-\omega\tau}$$

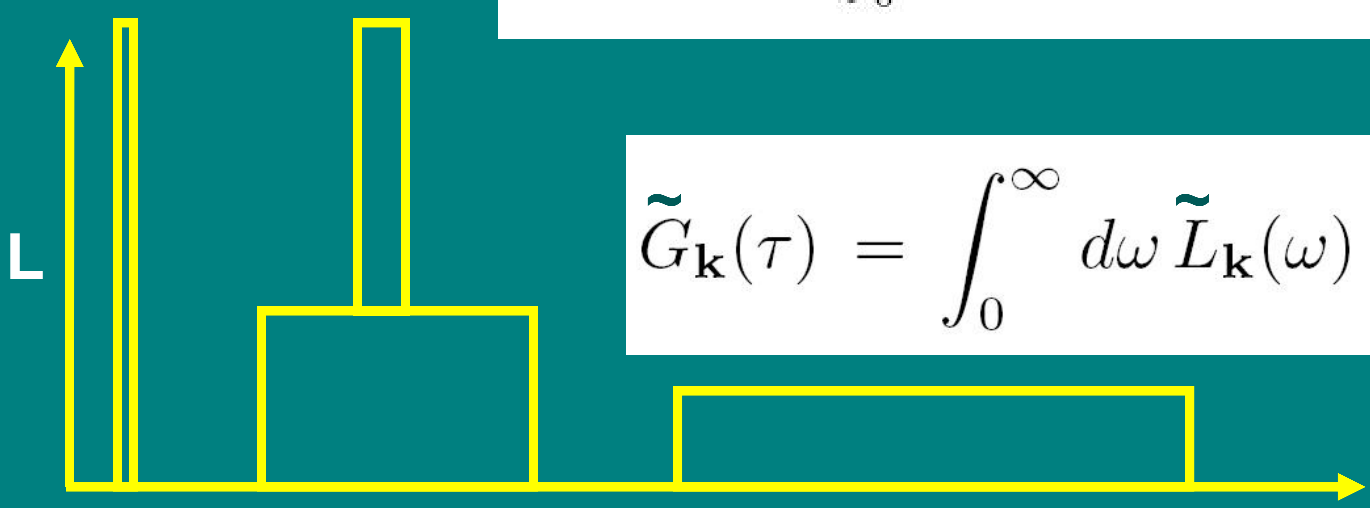

Stochastic Optimization method: update procedures.

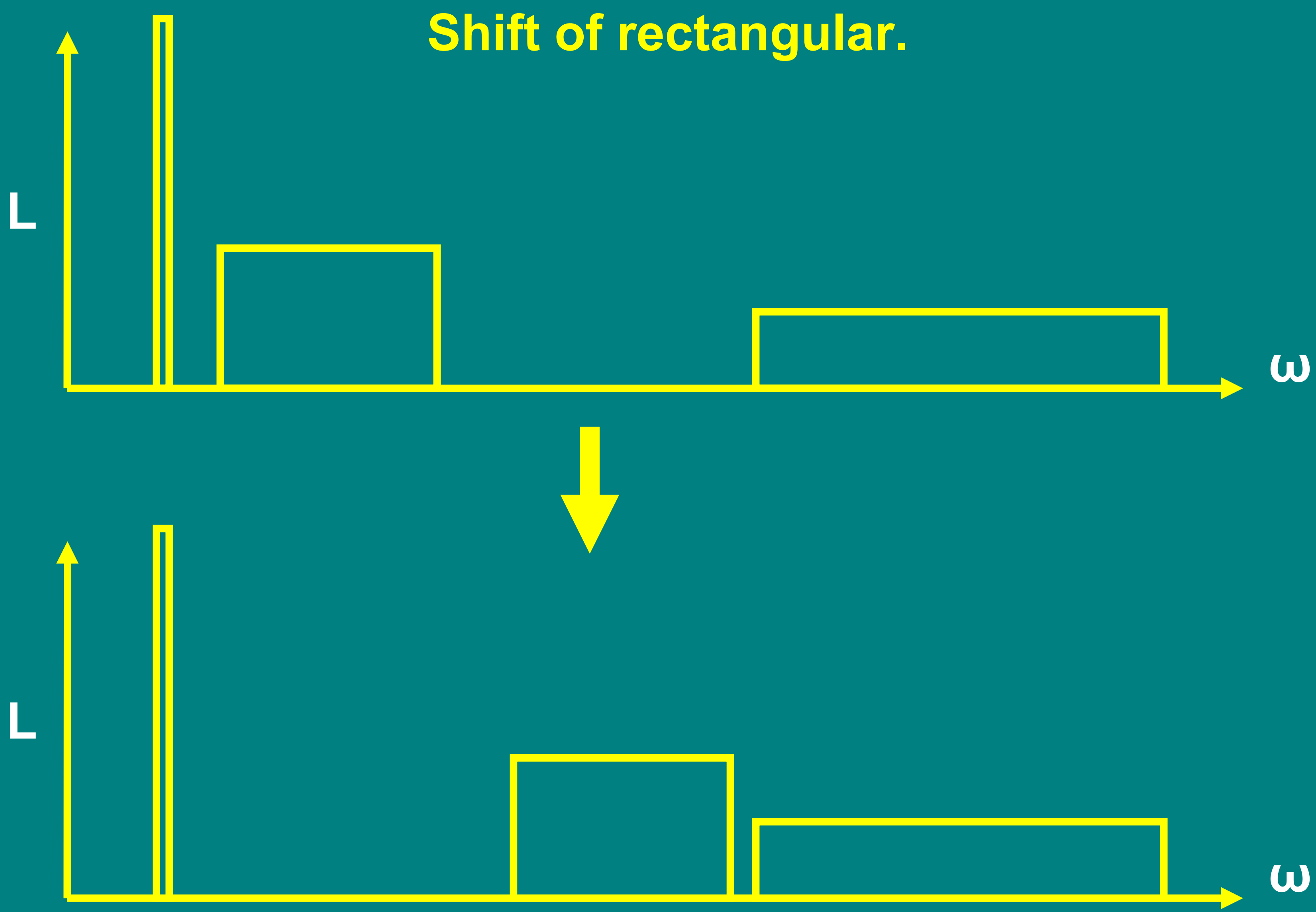

Stochastic Optimization method: update procedures.

Change of height of rectangular with fixed Z-factor.

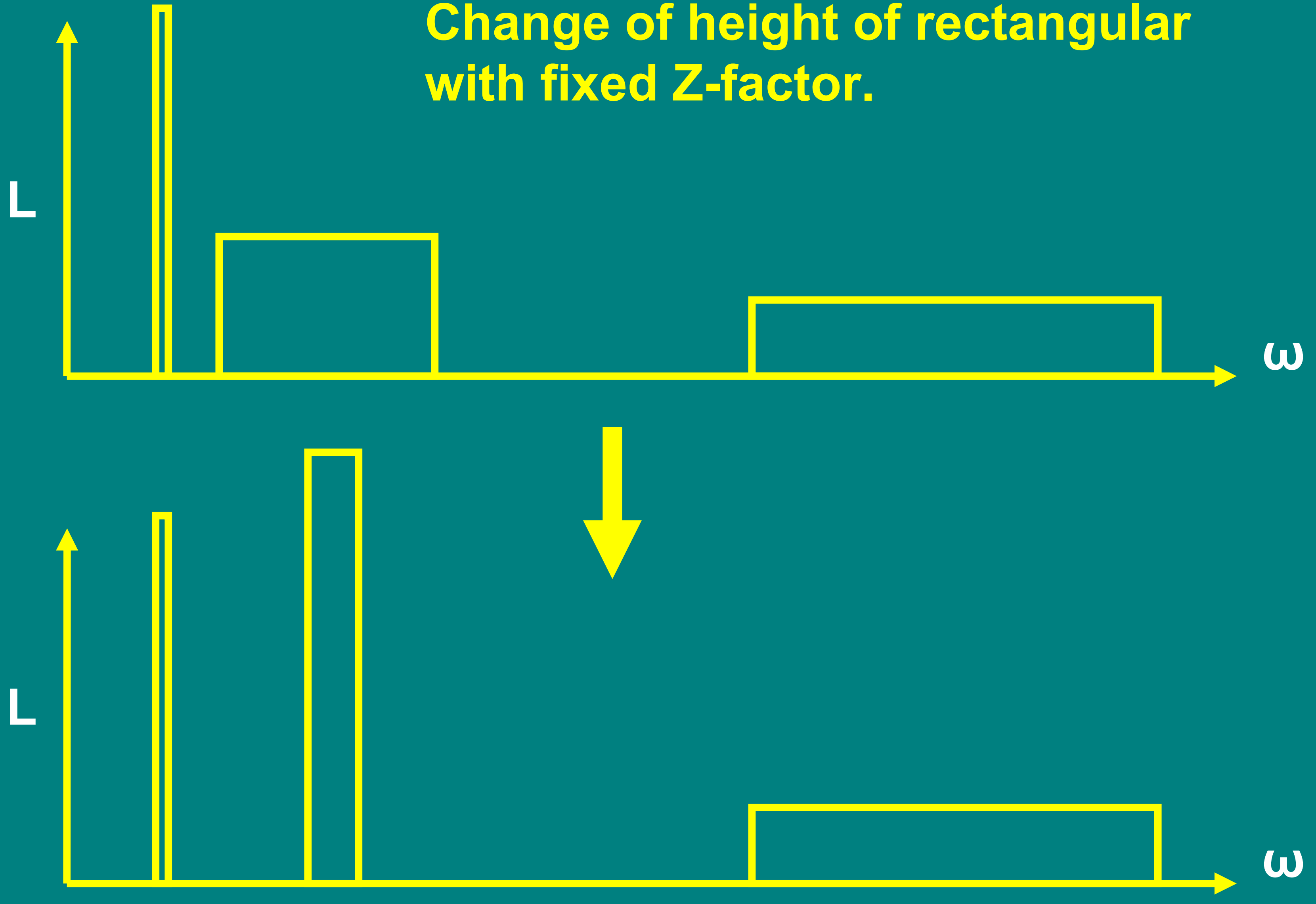

Stochastic Optimization method: update procedures.

Split of rectangular.

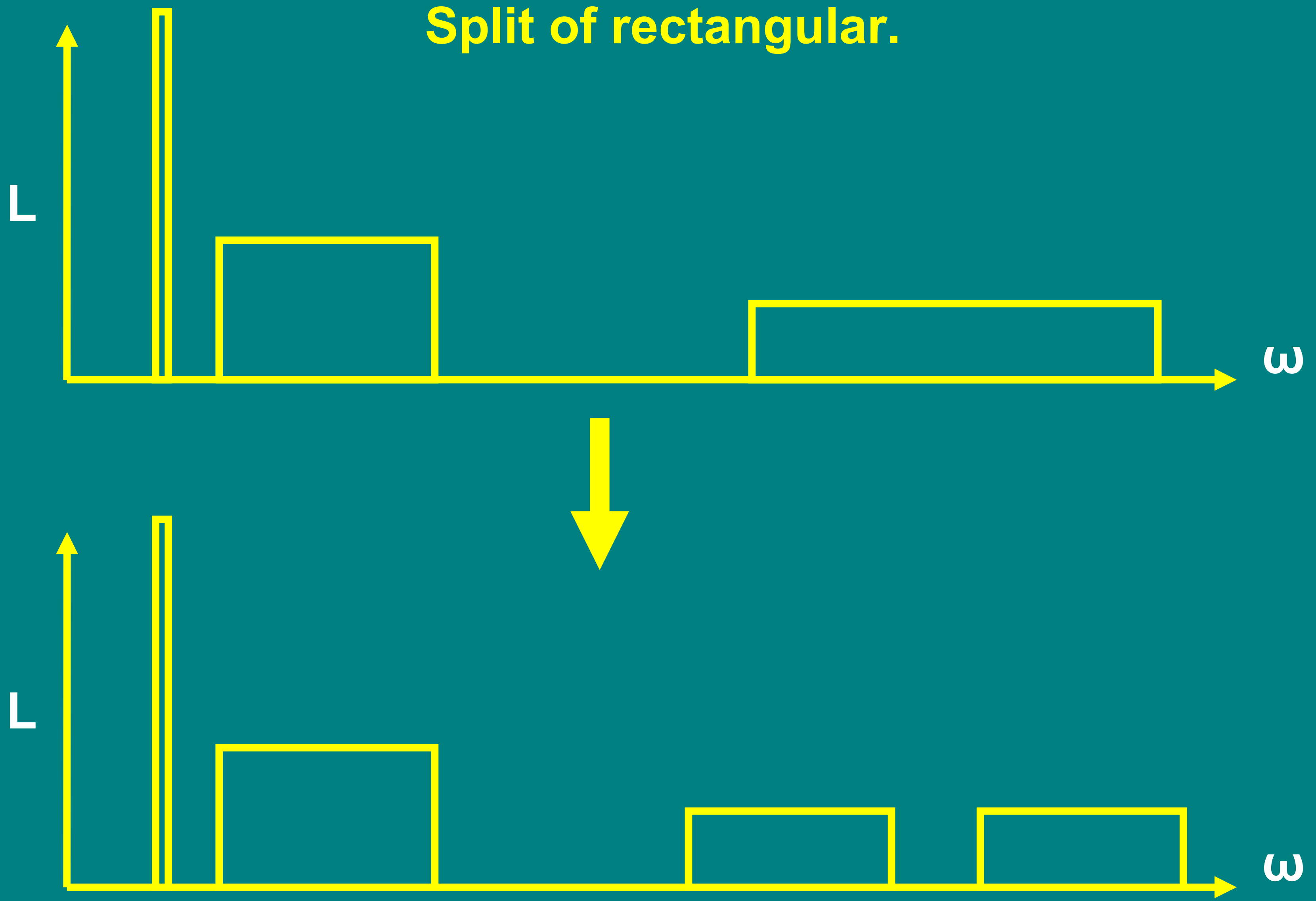

Stochastic Optimization method: update procedures.

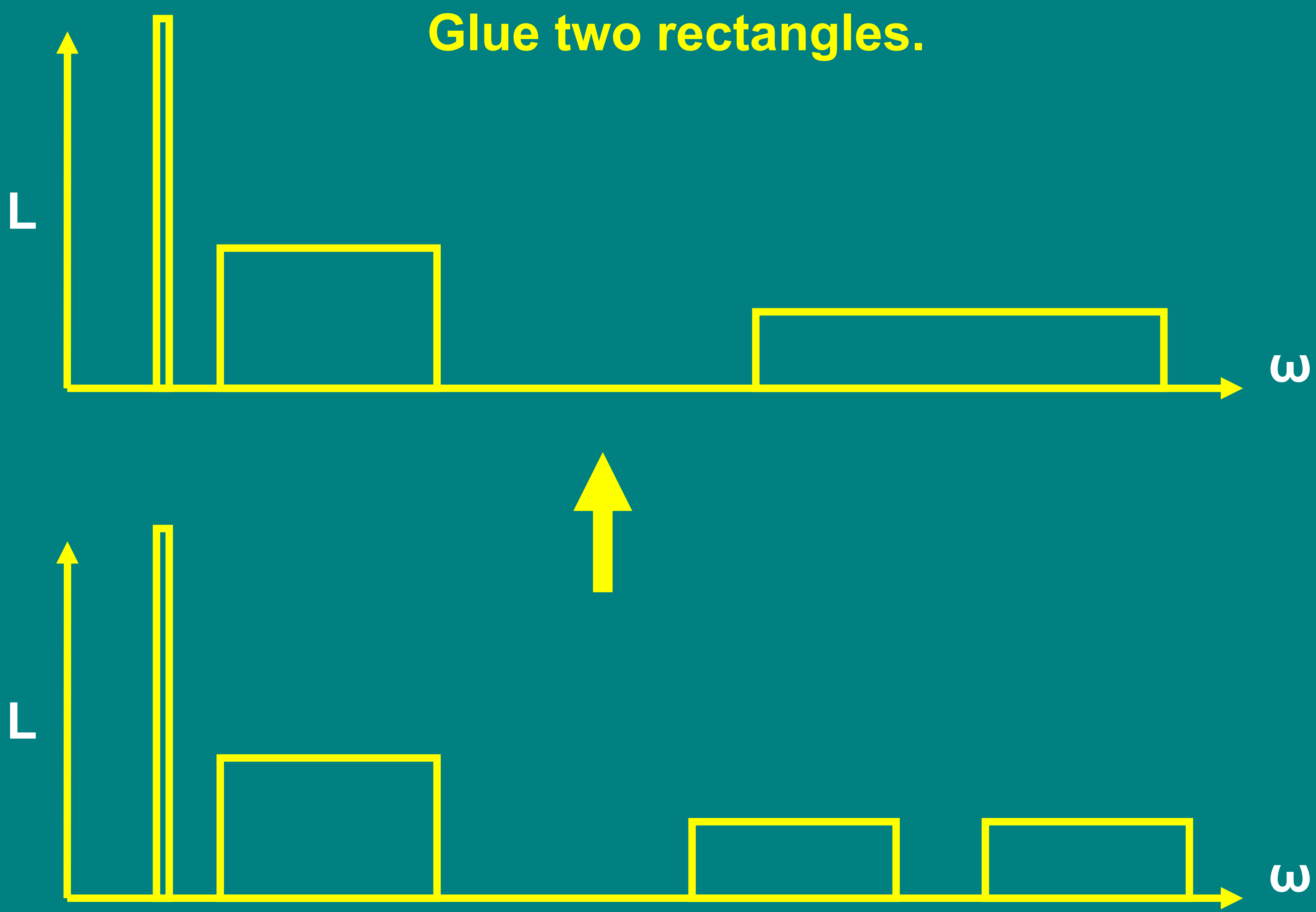

Stochastic Optimization method: update procedures.

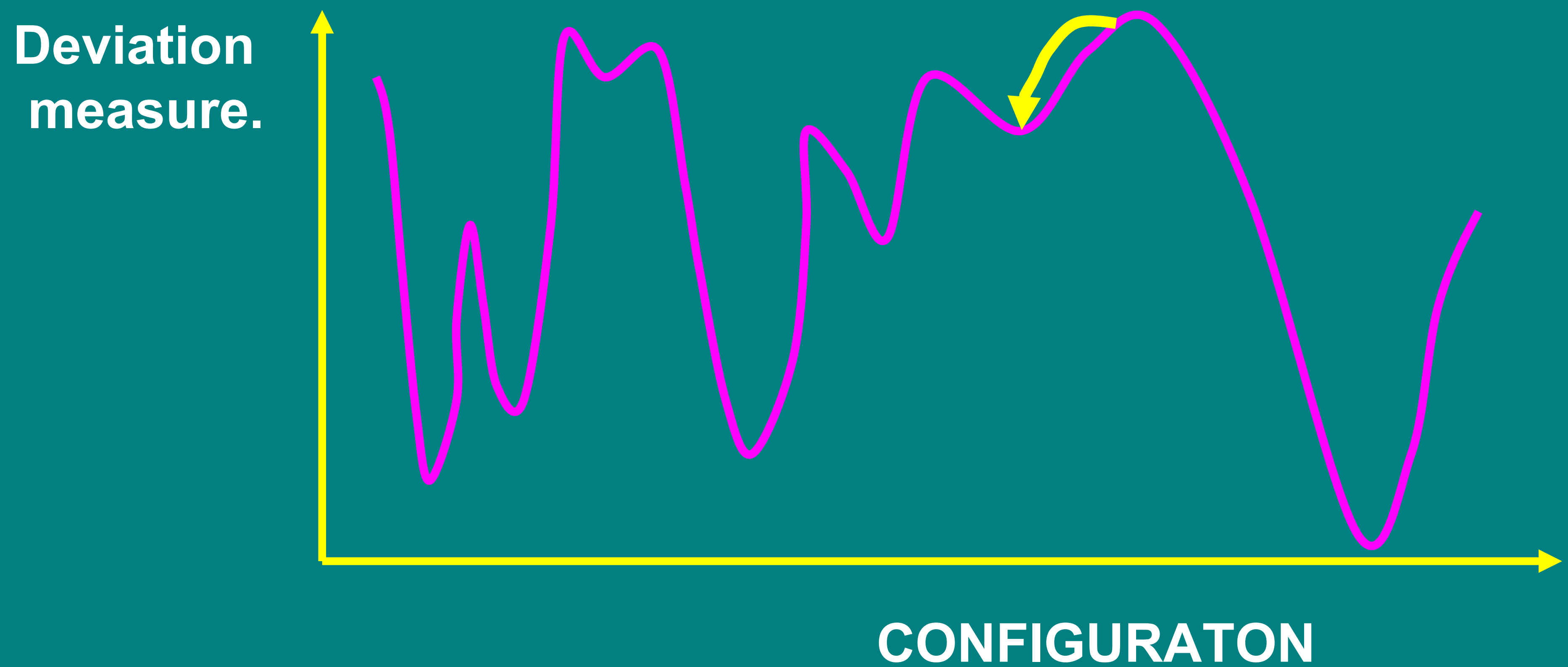

Accept only updates which decrease the deviation measure

WRONG STRATEGY

Stochastic Optimization method: update procedures.

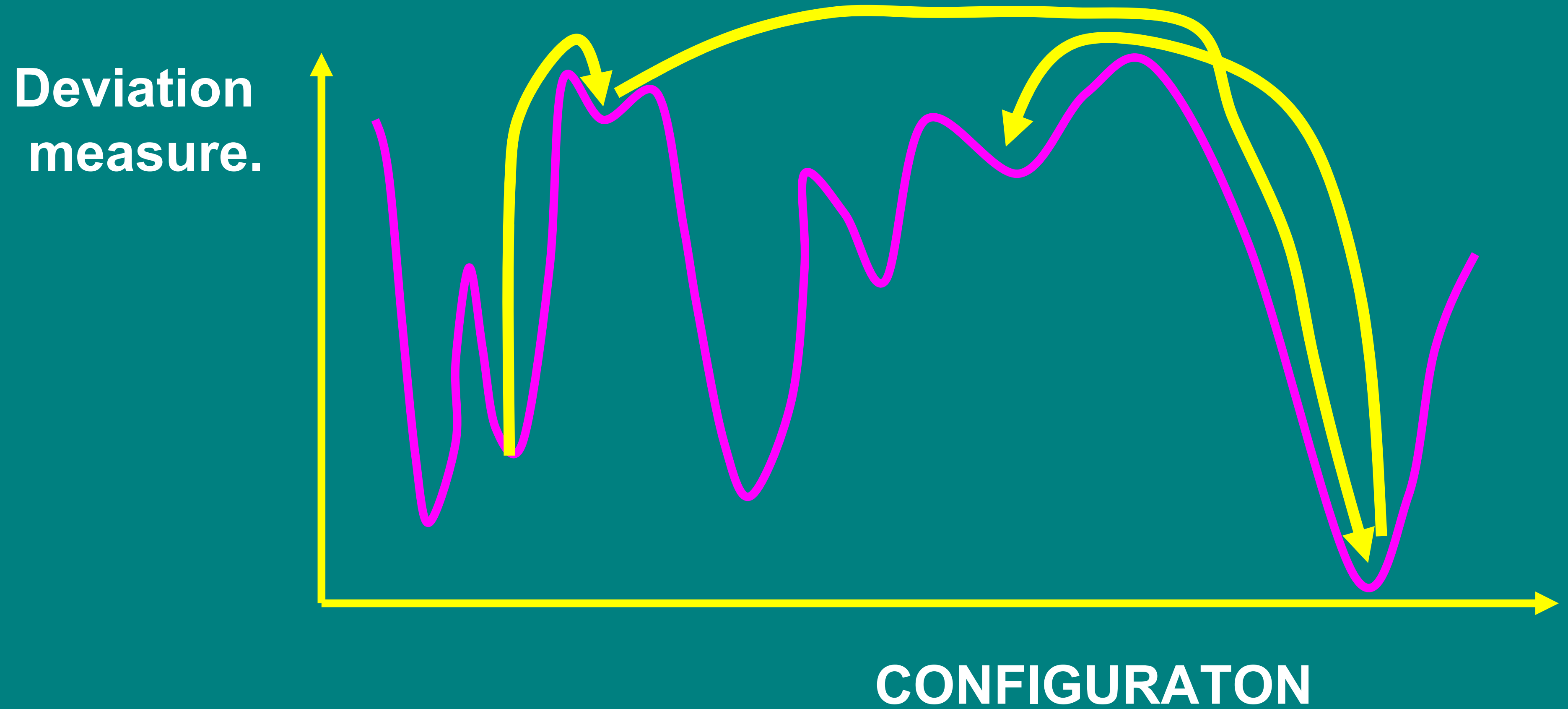

Always accept with some probability some updates which decrease the deviation measure

WRONG STRATEGY

Stochastic Optimization method: update procedures.

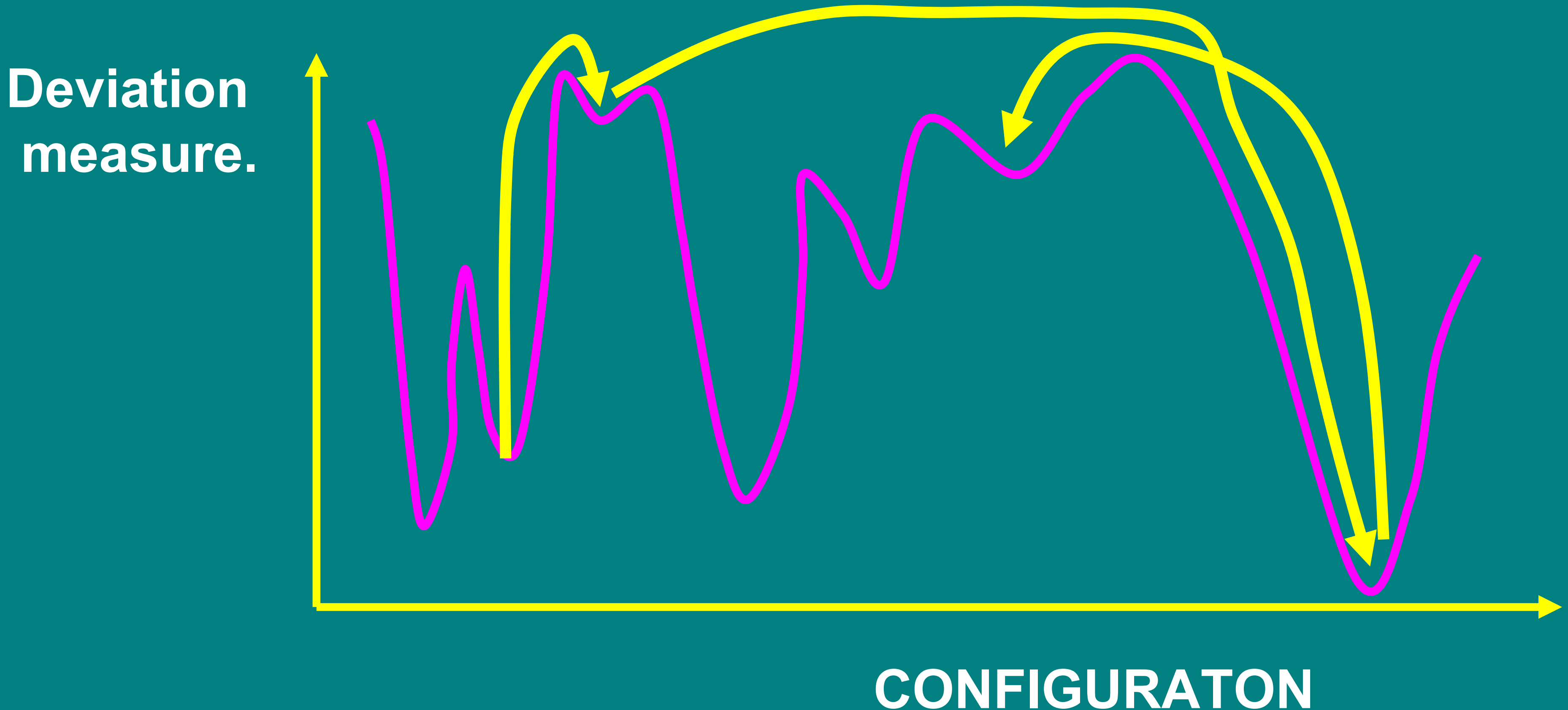

Shake-off two-step strategy:

Step 1: Increase of deviation measure is allowed during M steps with high probability

Step 2: Only decrease of deviation measure is allowed during last K steps.

Stochastic Optimization method: update procedures.

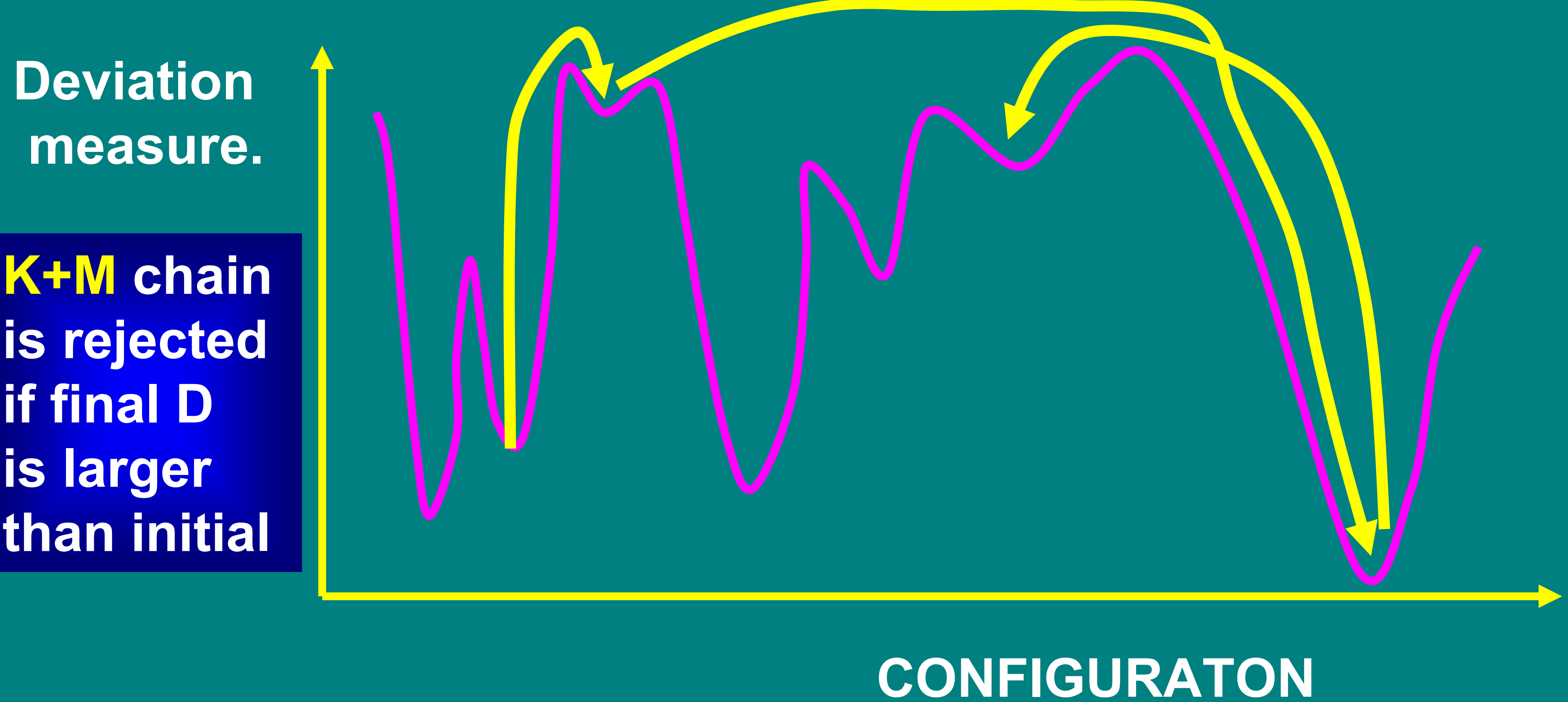

K+M chain is rejected if final D is larger than initial

Shake-off two-step strategy:

Step 1: Increase of deviation measure is allowed during M steps with high probability

Step 2: Only decrease of deviation measure is allowed during last K steps.

Stochastic Optimization method: update procedures.

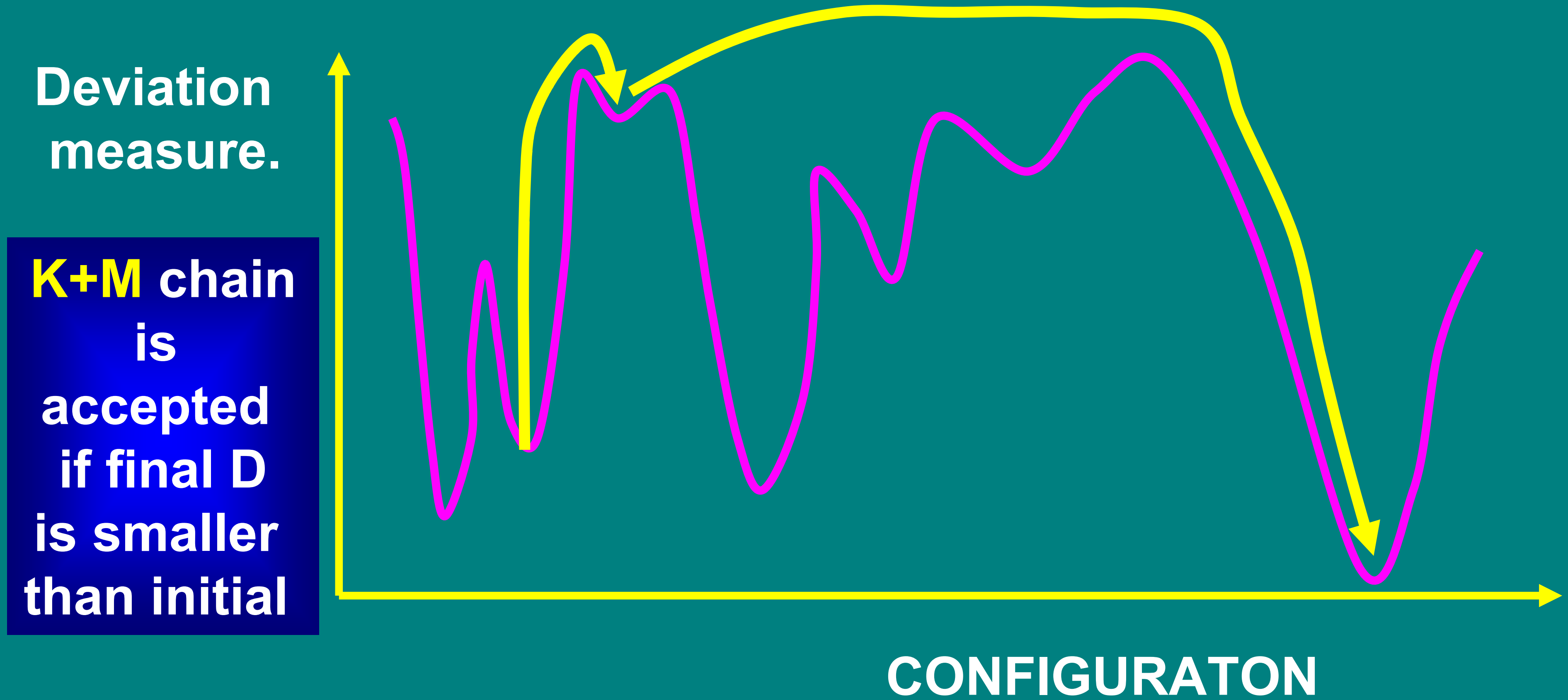

Shake-off two-step strategy:

Step 1: Increase of deviation measure is allowed during M steps with high probability

Step 2: Only decrease of deviation measure is allowed during last K steps.

Stochastic Optimization method.

- Particular solution $L^{(i)}(\omega)$ for LSF is presented as a sum of a number N of rectangles with some width, height and center.
- Initial configuration of rectangles is created by random number generator (i.e. number N and all parameters of of rectangles are randomly generated).
- Each particular solution $L^{(i)}(\omega)$ is obtained by a naïve method without regularization (though, varying number N).

- Final solution is obtained after M steps of such procedure

$$L(\omega) = M^{-1} \sum_i L^{(i)}(\omega)$$

- Each particular solution has saw tooth noise
- Final averaged solution $L(\omega)$ has no saw tooth noise though not regularized with sharp peaks/edges!!!!

Self-averaging of the saw-tooth noise.

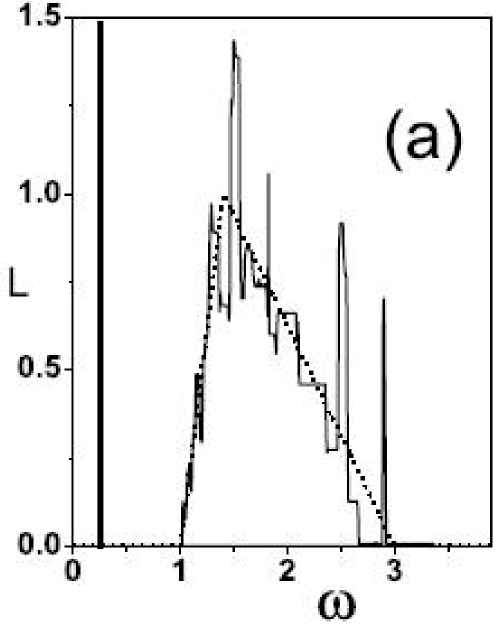

Fig. 7. Comparison of the actual spectral function (dashed line) with the results of spectral analysis after averaging over (a) $M = 4$, (b) $M = 28$, and (c) $M = 500$ particular solutions.

Self-averaging of the saw-tooth noise.

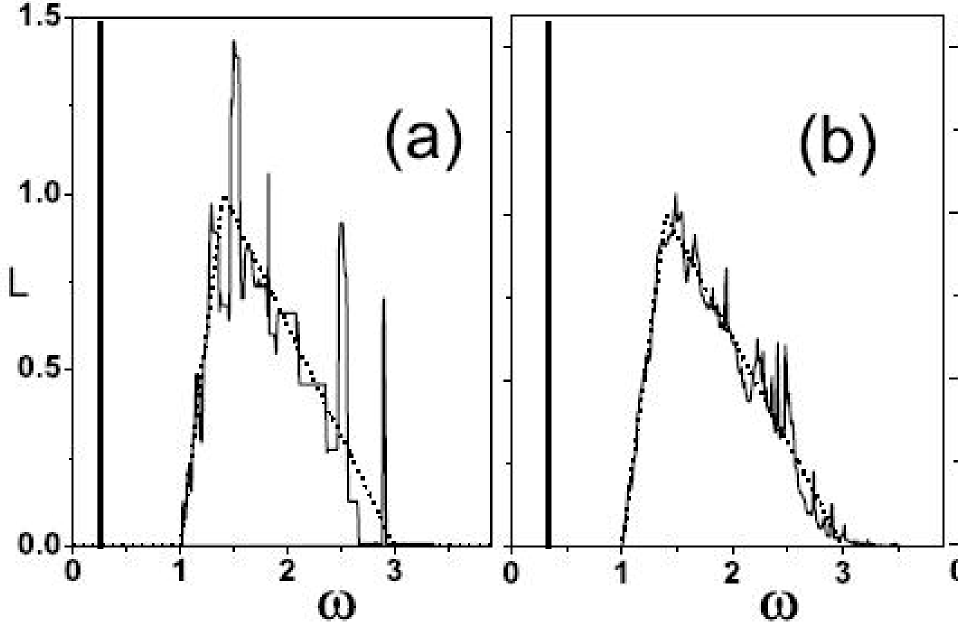

Fig. 7. Comparison of the actual spectral function (dashed line) with the results of spectral analysis after averaging over (a) $M = 4$, (b) $M = 28$, and (c) $M = 500$ particular solutions.

Self-averaging of the saw-tooth noise.

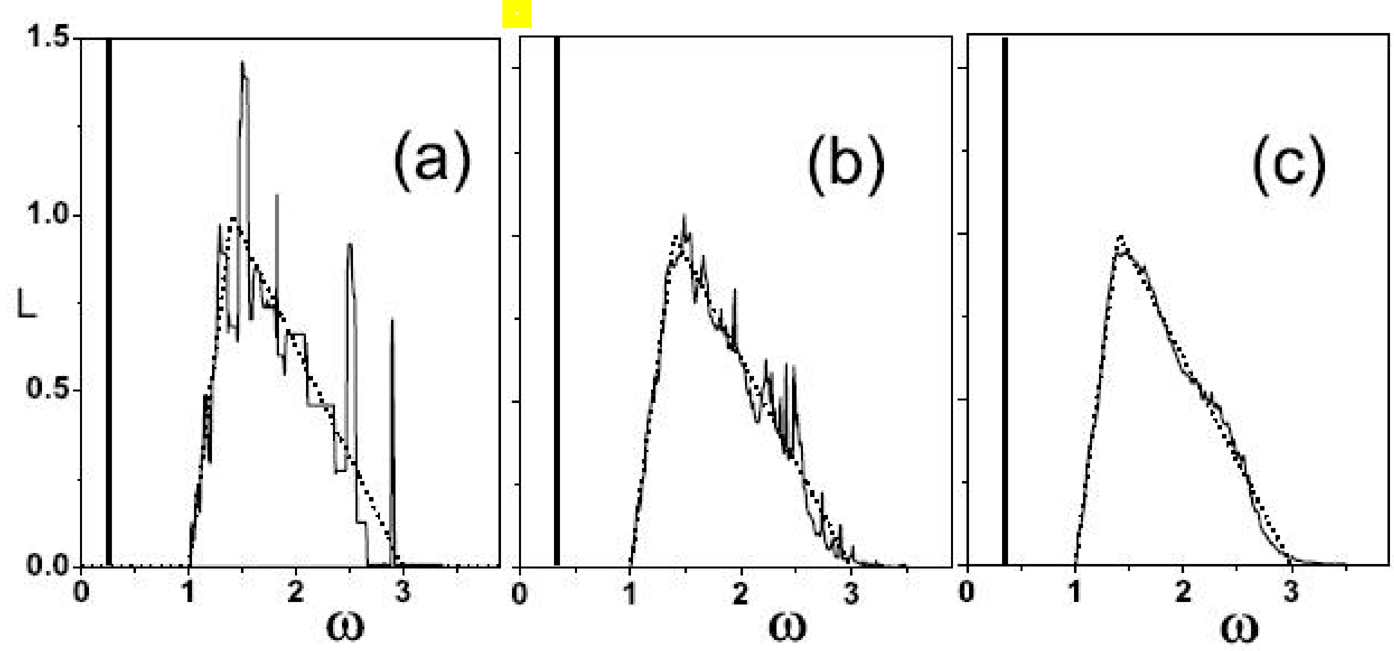

Fig. 7. Comparison of the actual spectral function (dashed line) with the results of spectral analysis after averaging over (a) $M = 4$, (b) $M = 28$, and (c) $M = 500$ particular solutions.

Test for Stochastic Optimization method

Lehman function for test has:

- Sharp δ-function with weight Z=0.05.
- Micro-gap to continuum with size δω=0.01
- Wide smooth incoherent continuum spread over δω=2

Such example of LSF is impossible to recover by any regularization procedure (including MEM). Though, Stochastic Optimization method is successful.

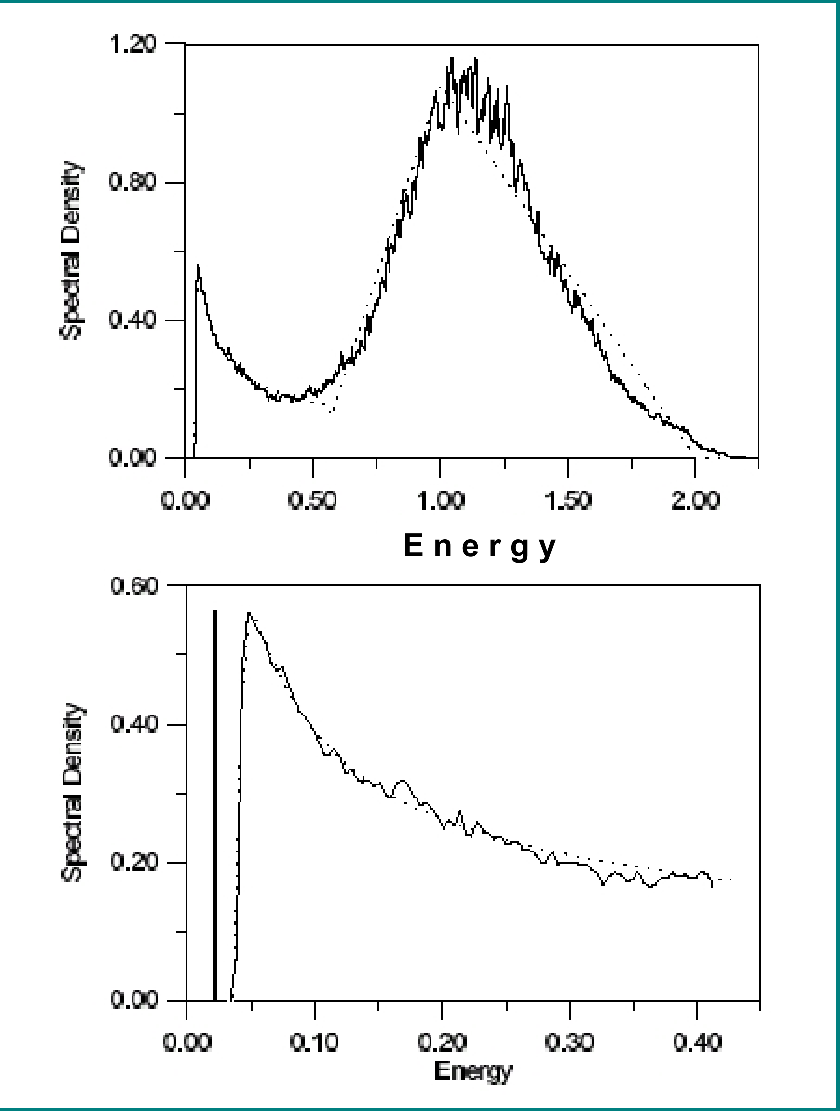

PHYSICAL REVIEW B **76**, 035115 (2007)

Analytical continuation of spectral data from imaginary time axis to real frequency axis using statistical sampling

K. Vafayi and O. Gunnarsson
Max-Planck-Institut für Festkörperforschung, D-70506 Stuttgart, Germany
(Received 27 February 2007; revised manuscript received 2 May 2007; published 19 July 2007)

We present a method for performing analytical continuation of spectral data from imaginary time to real frequencies based on a statistical sampling method. Compared with the maximum entropy method (MEM), an advantage is that no default model needs to be introduced. For the problems studied here, the statistical sampling method gives comparable or slightly better results than MEM using quite accurate default models.

DOI: 10.1103/PhysRevB.76.035115 PACS number(s): 72.15.Eb, 02.70.Ss

ity in Eq. (7) as a weight function. Comparing with the maximum entropy method (MEM), an advantage is that there is no need to provide a default model, which influences the MEM results if the method is close to its limit of applicability. For the problems considered here, the statistical sampling method gives comparable or slightly better results than MEM using default models close to the exact result. The

References

Method DMC, SOM for analytic continuation and Frohlich polaron:
A. S. Mishchenko et. al., Phys. Rev B, vol. 62, 6317 (2000)

Pseudo-Jahn-Teller polaron:
A. S. Mishchenko and N. Nagaosa, Phys. Rev. Lett., vol. 86, 4624 (2001)

Exciton:
E. A. Burovskii et. al., Phys. Rev. Lett., vol. 87, 186402 (2001)

Optical conductivity of polaron:
A. S. Mishchenko et. al., Phys. Rev. Lett., vol. 91, 236401 (2003)

ARPES in t-J-Holstein model:
A. S. Mishchenko and N. Nagaosa, Phys. Rev. Lett., vol. 93, 036402 (2004)

Role of adiabatic processes in optical conductivity:
G. de Filippis et. al., Phys. Rev. Lett., vol. 96, 136405 (2006)

Reviews:
A. S. Mishchenko, Phys-Usp, vol. 48, 887 (2005).

A. S. Mishchenko and N. Nagaosa, J. Phys. Soc. J., vol. 75, 011003 (2006).

A. S. Mishchenko and N. Nagaosa, Polarons, Springer, ed. by Alexandrov

Franck-Condon principle. Is it good for optical spectroscopy?

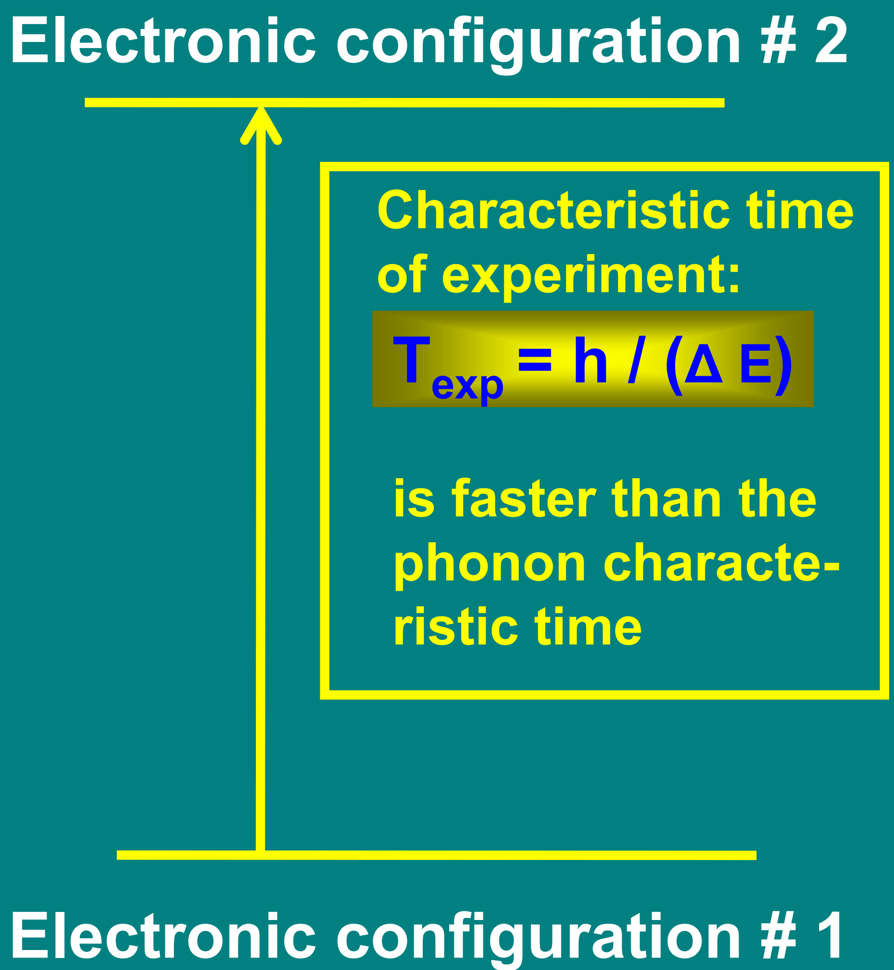

Optical conductiviry of polaron:

#1 = #2

FC principle is invalid?

Lehman function of Frohlich polaron - weak coupling

$$\hat{H}_{\text{par-bos}} = i \sum_{\kappa}^{Q} \sum_{\mathbf{k},\mathbf{q}} \sum_{i,j=1}^{T} \gamma_{ij,\kappa}(\mathbf{k},\mathbf{q})(b^{\dagger}_{\mathbf{q},\kappa} - b_{-\mathbf{q},\kappa}) a^{\dagger}_{i,\mathbf{k}-\mathbf{q}} a_{j,\mathbf{k}} + h.c.$$

Coupling vortex: γ(k,q) = a/q

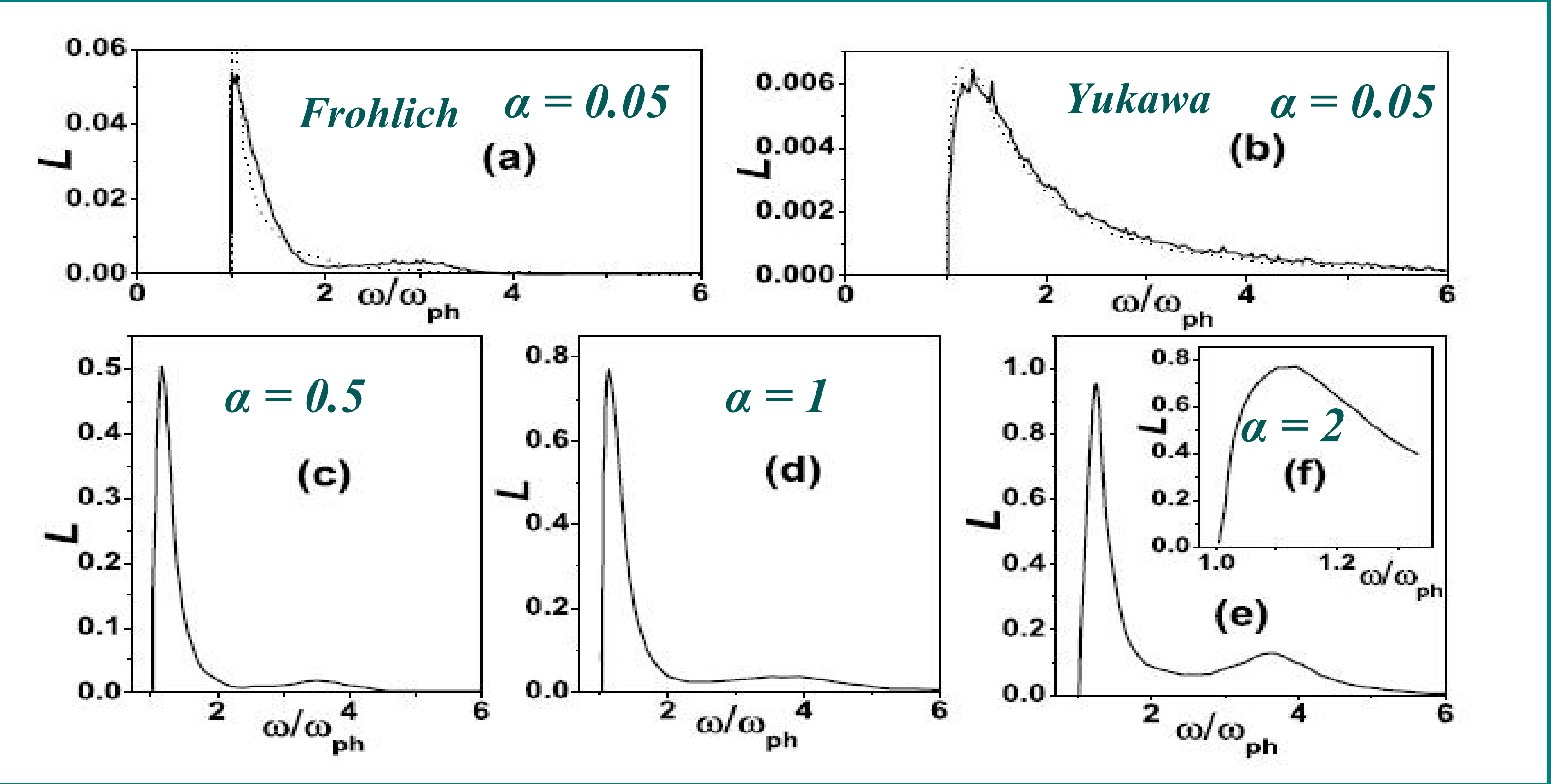

Lehman function of Frohlich polaron - intermediate and strong coupling

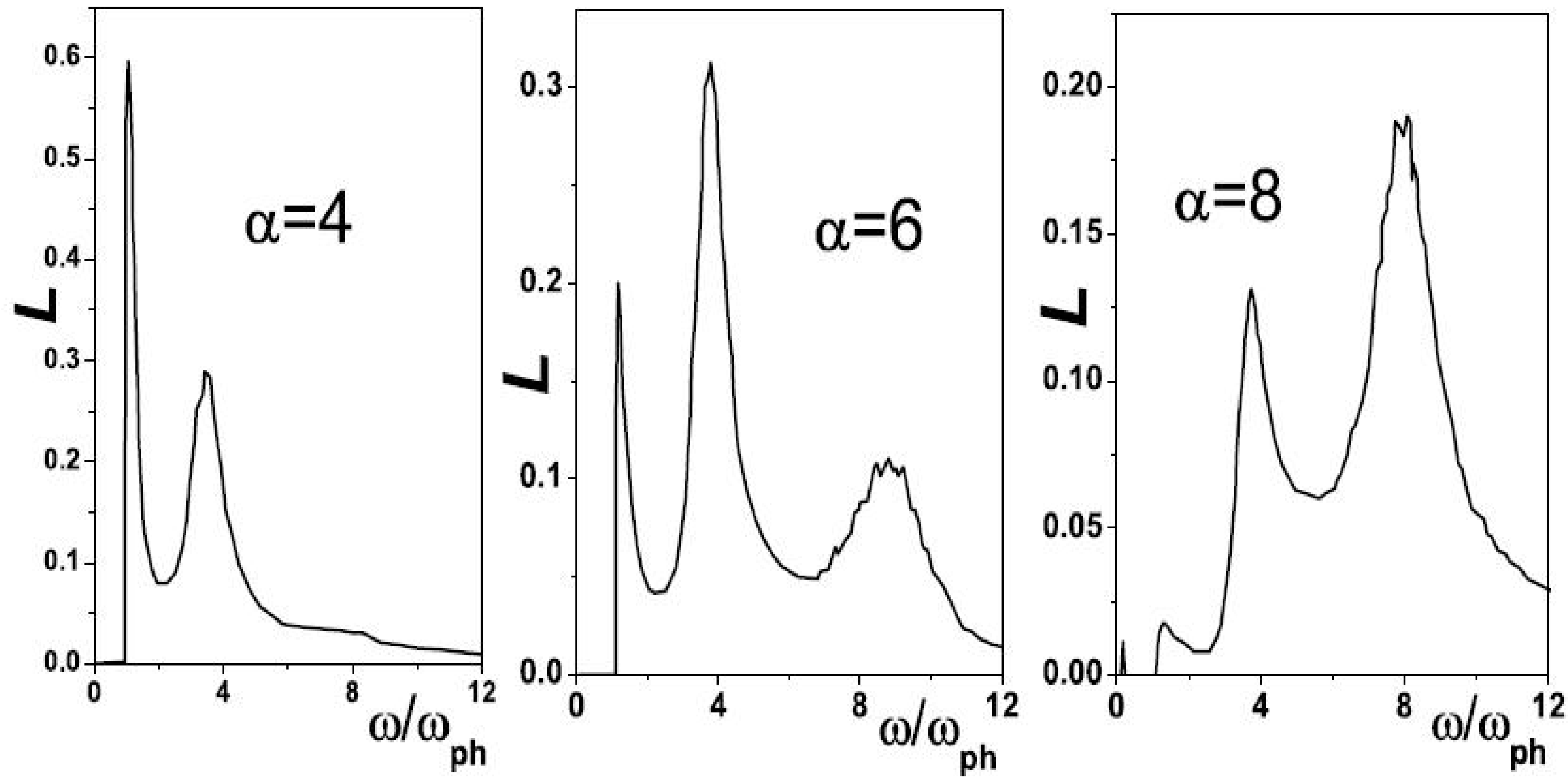

Optical conductivity of Froclich polaron

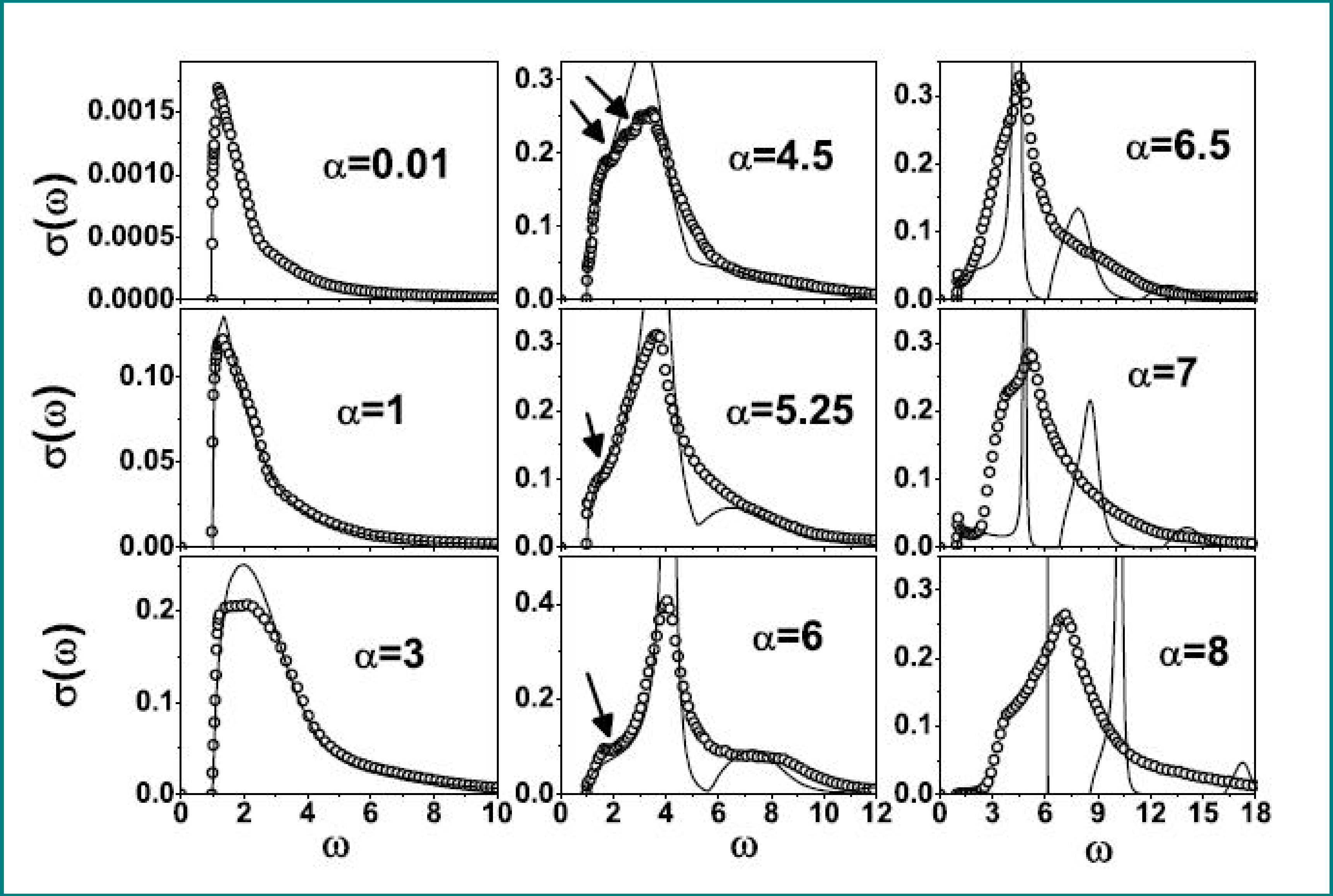

ASM, N. Nagaosa, N.V. Prokof'ev, A. Sakamoto, and B.V. Svistunov, PRL, v. 91, 236401, (2003)

Optical conductivity of Froclich polaron

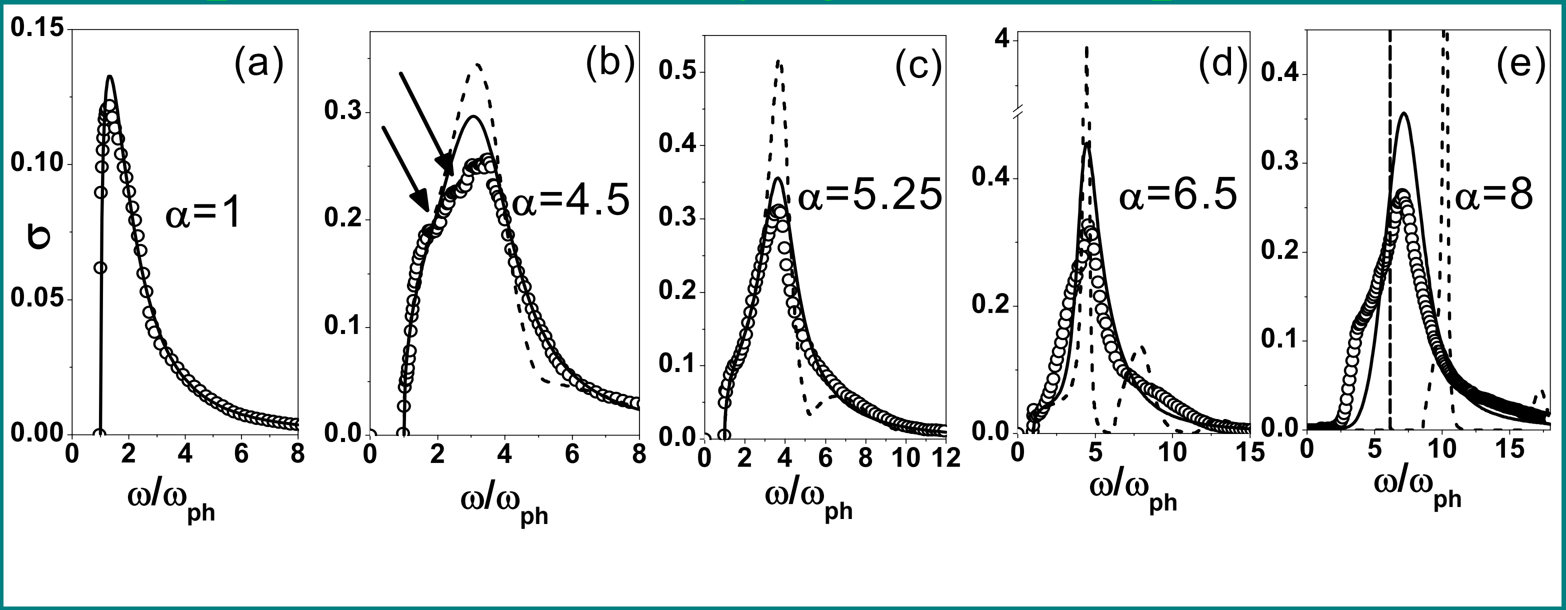

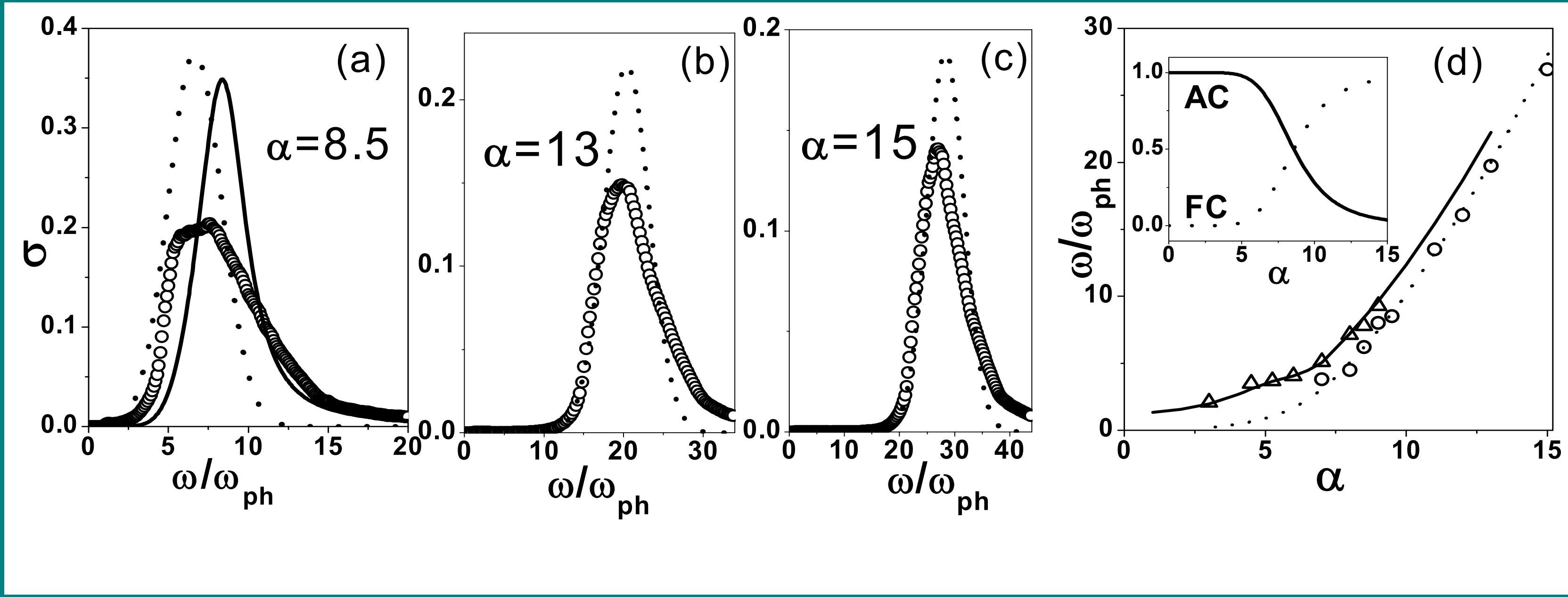

G. De Filippis, V. Cataudella, ASM, C.A. Perroni, J.T. Devreese, PRL, v. 96, 136405, (2006)

Times hierarchy in measurements process

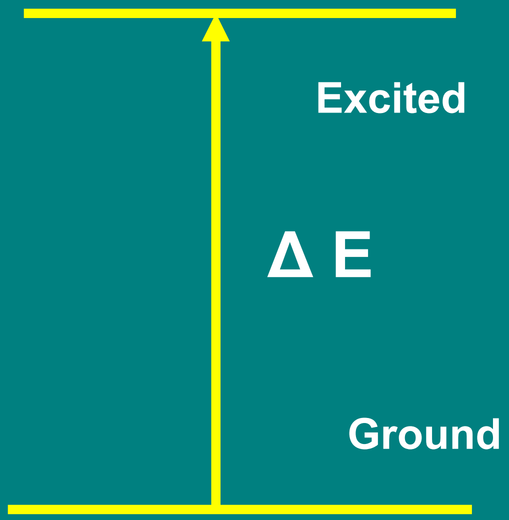

Characteristic time of experiment:

$T_{exp} = h / (\Delta E)$

Characteristic time of system: Interconfigurational mixing τ_{ic}

Adiabatic regime:

All subsystems of system are adjusted (e.g. electronic and lattice) during the measurement event

$$\tau_{exp} >> \tau_{ic}$$

a) static measurement (static susceptibility)

b) Slow measurement (infrared optical response)

Franck-Condon regime:

No time to adjust all subsystems (e.g. electronic and lattice) during the measurement event

$$\tau_{exp} << \tau_{ic}$$

(ARPES, high-energy optics)

Nonadiabatic mixing

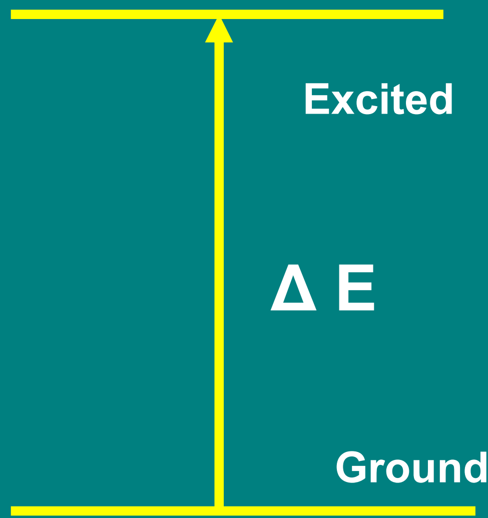

$$\Psi_{GR}(r,Q) = \sum_e \sum_\beta \xi^{GR}_{e\beta}\, \chi_{e\beta}(Q)\, \varphi_e(r,Q)$$

$$\Psi_{EX}(r,Q) = \sum_e \sum_\beta \xi^{EX}_{e\beta}\, \chi_{e\beta}(Q)\, \varphi_e(r,Q)$$

Maximal mixing between ground and excited state:

$\xi^{EX}_{gr} = 2^{-1/2}$; $\xi^{GR}_{ex} = 2^{-1/2}$

$$(E-E_{e\beta})\, \xi_{e\beta} = \sum_l \sum_\mu D\, \xi_{l\mu}$$

D – nonadiabatic operator

Measure for adiabatically connected processes:

$I_{AC} = 2\, \xi^{EX}_{gr}\, \xi^{GR}_{ex}$

Interconfigurational mixing time:

$\tau_{ic} = 1 / \langle D_{GR\rightarrow EX} \rangle$

Measure for Franck-Condon processes:

$I_{AC} = 1 - I_{FC}$

Nonadiabatic mixing

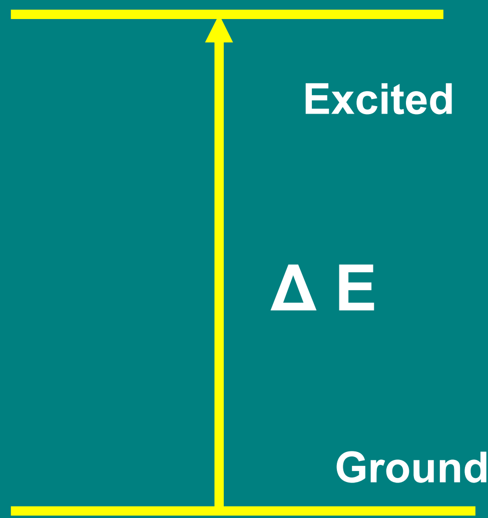

K.A.Kikoin and A.S.Mishchenko, Sov.Phys.JETP, vol. 77, 828 (1993).

$$D = (M/\Delta E)\, n_\beta^{1/2} + (M/\Delta E)^2$$

$$M \sim \alpha^{1/2} \,;\; n_\beta \sim \Delta E \,;\; \Delta E \sim \alpha^2$$

Maximal mixing between ground and excited state:

$$\xi^{EX}{}_{gr} = 2^{-1/2} \,;\; \xi^{GR}{}_{ex} = 2^{-1/2}$$

Measure for adiabatically connected processes:

$$I_{AC} = 2\, \xi^{EX}{}_{gr}\, \xi^{GR}{}_{ex}$$

Measure for Franck-Condon processes:

$$I_{AC} = 1 - I_{FC}$$

$$I_{FC} = [\, 1 + 4\, (\, \tau_{exp} / \tau_{ic}\,)^2\,]^{-1}$$

$$\tau_{ic} = 1 / \langle D_{GR\rightarrow EX} \rangle$$

$$T_{exp} = 1 / (\Delta E)$$

Nonadiabatic mixing

$$I_{FC} = [\ 1 + 4\ (\ \tau_{exp}\ /\ \tau_{ic}\ )^2\ ]^{-1}$$

$$\tau_{ic} = 1\ /\ \langle D_{GR\rightarrow EX} \rangle$$

$$T_{exp} = 1\ /\ (\Delta\ E)$$

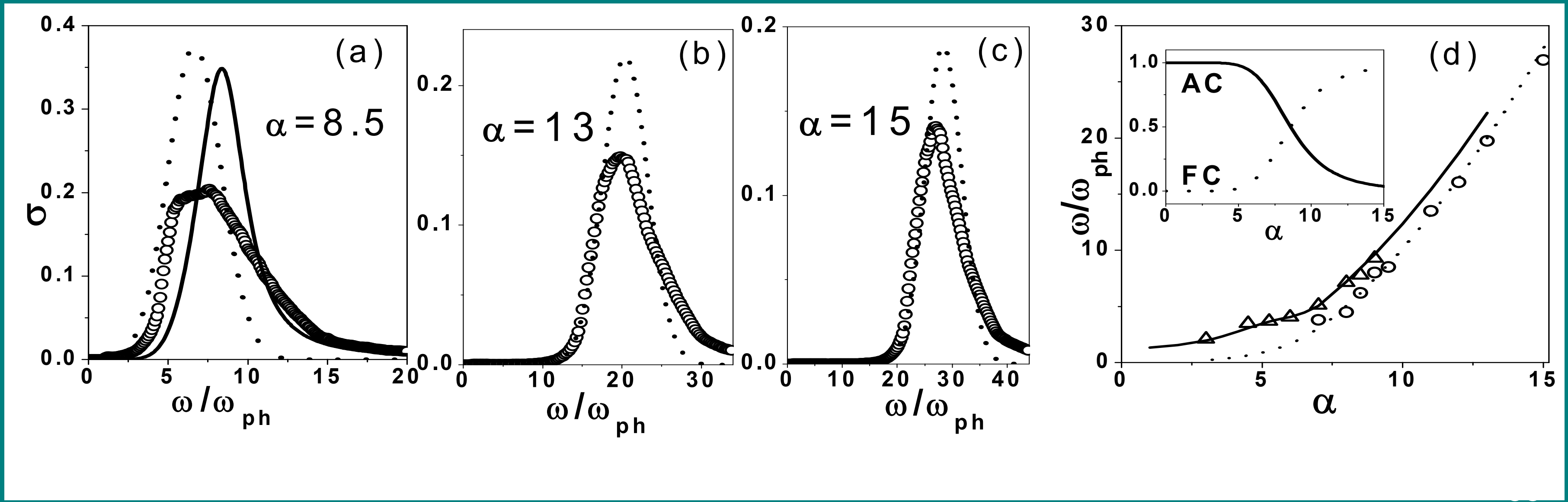

Problems of theoretical description of ARPES spectra in $Sr_2CuO_2Cl_2$ and $Ca_{2-x}Na_xCuO_2Cl_2$

Theoretical results for undoped insulators:

1. Lehman spectral function at all momenta has a **sharp** quasiprticle peak
2. Sharp quasiparticle peak has dispersion with the banwidth of the order of exchange constant J.

Experimental results:

1. ARPES data at all momenta demonstrate a very **broad** quasiparticle peak in the low energy part with incoherent continuum at high energies.
2. The dispersion of broad quasiparticle peak coincides with prediction of extended t-J model (t-t'-t''-J model).

Complete success of theory in explanation of dispersion and Complete failure of theory in explanation of linewidth.

Main problem is the LINE SHAPE

Theory

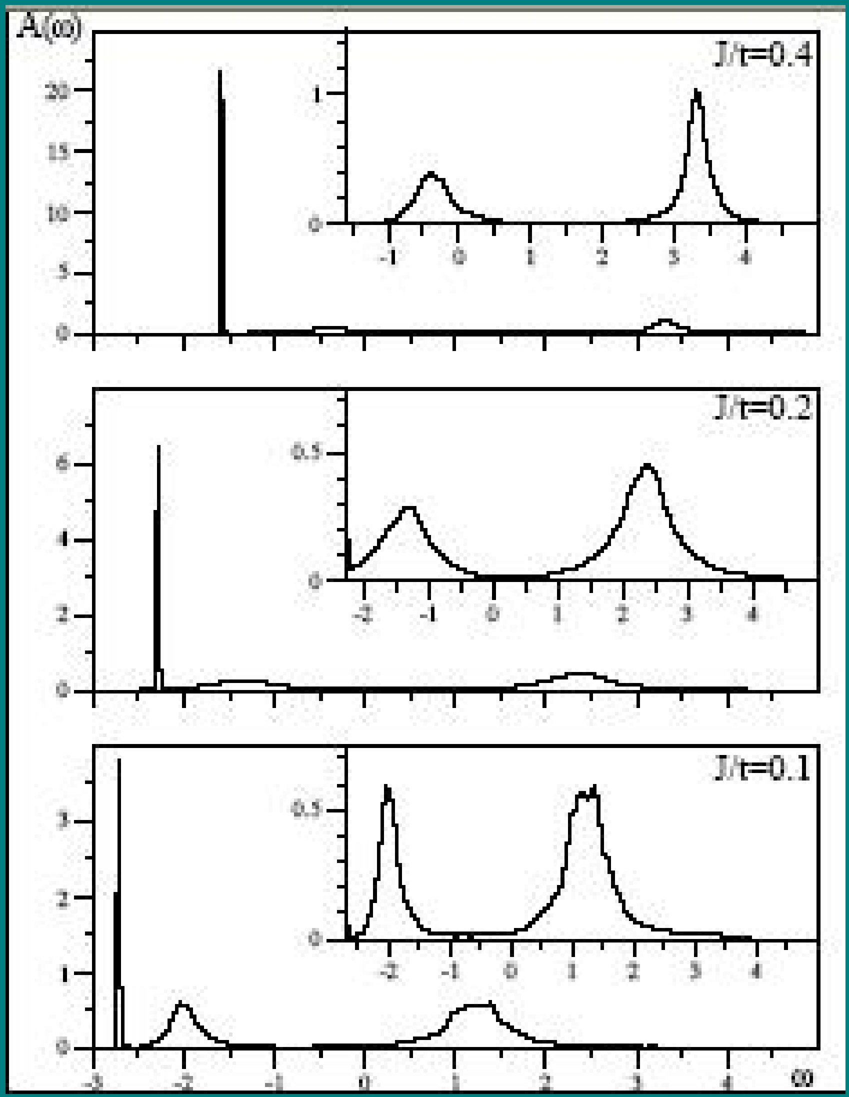

A.S. Mishchenko, B.V. Svistunov, N.V. Prokof'ev, PRB, vol. 64, 033101 (2001)

Experiment

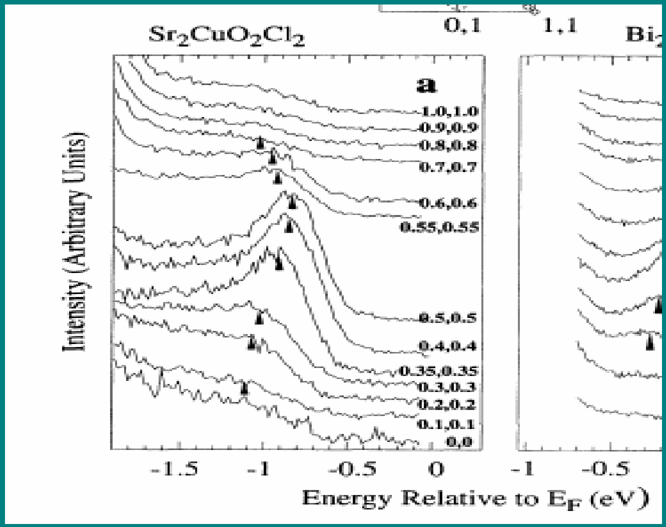

Wells et al, PRL (1995)

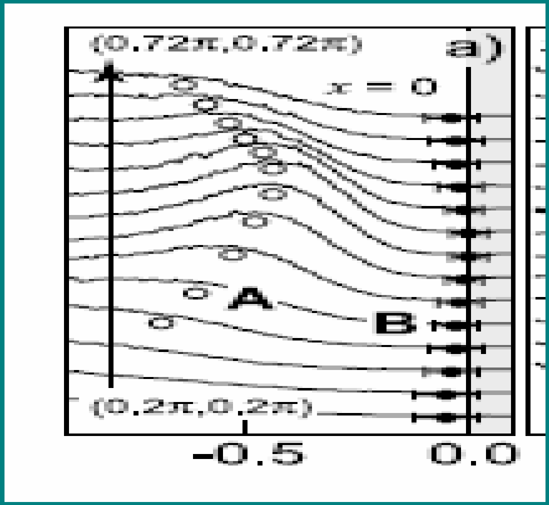

K. M. Shen et al, PRL (2004)

Spin-wave approximation in momentum representation for single hole in t-t'-t"-J model interacting with phonons

Hole with dispersion ε(k) in magnon and phonon bathes

$$H^{(0)}_{tt't''\text{-}J} = \Sigma_k \varepsilon(k)\, h_k^+ h_k + \Sigma_k \upsilon(k)\, \alpha_k^+ \alpha_k + \Sigma_k \omega_{ph}\, b_k^+ b_k$$

Scattering on magnons: $H_{h\text{-}m} = N^{-1} \Sigma_{k,q} M_{k,q} [\, h_k^+ h_{k-q}\, \alpha_q + h.c.]$

Scattering on phonons: $H_{h\text{-}ph} = N^{-1} \Sigma_{k,q}\, \gamma\, [\, h_k^+ h_{k-q}\, b_q + h.c.]$

Dimensionless EPI constants: $\lambda = \gamma^2 / 4t\omega_{ph}$

Feynman expansion which is sufficient for problem of one hole in t-J model coupled to phonons.

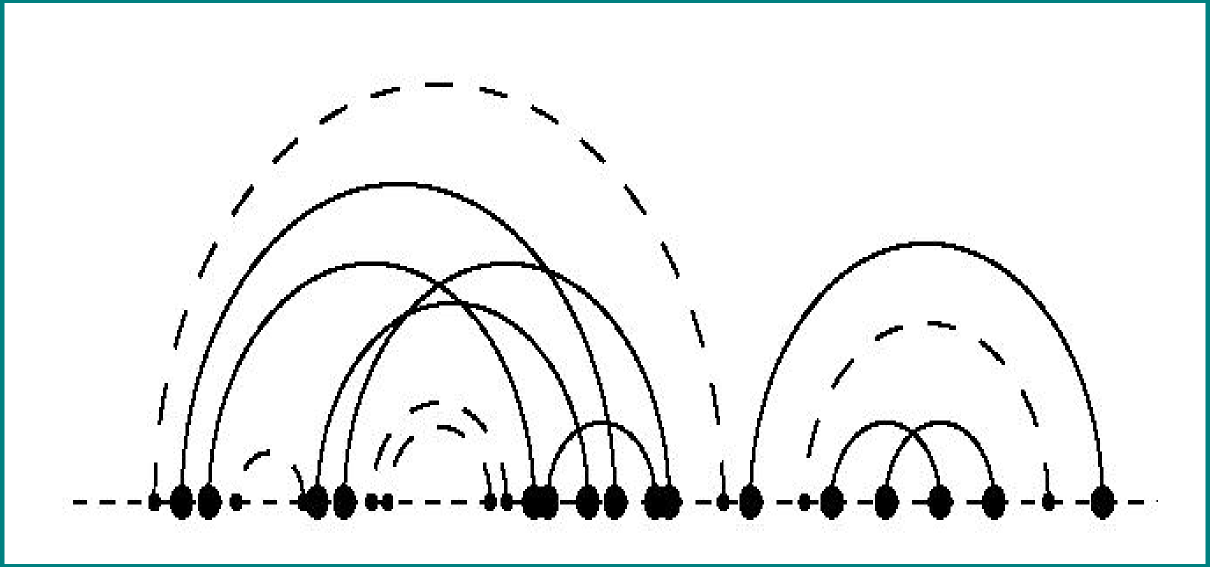

1. Intercrossing of phonon propagators is taken into account.

2. Magnon-magnon vertex corrections are neglected because coupling of the hole to magnons is weak.

This expansion can be summed by numerically exact Diagrammatic Monte Carlo method where all Feynman graphs are generated by Monte Carlo and summed up without systematic errors.

1. A.S.Mishchenko, N.V.Prokof'ev, A.Sakamoto, and B.V.Svistunov, Phys.Rev. B, vol.62, 6317 (2000).
2. A.S.Mishchenko and N.Nagaosa, Phys.Rev.Lett., vol.86, 4624 (2001).
3. E.A.Burovski, A.S.Mishchenko, N.V.Prokof'ev and B.V.Svistunov, Phys.Rev.Lett., vol.87, 186402 (2001) .
4. A.S.Mishchenko, N.Nagaosa, N.V.Prokof'ev, A.Sakamoto, and B.V.Svistunov, Phys.Rev.Lett., vol.91, 236401 (2003).

Demonstration of the importance of phonon-phonon vertex corrections

Ordinary 2D Holstein model

Near neighbour hopping of hole

$$H^{(0)}_{t-J} = \Sigma_k \varepsilon_\kappa h^+_k h_k \; ; \quad \varepsilon_k = 2t\, \Sigma_{i=x,y} \cos(k_i)$$

Scattering of the hole by phonons

$$H_{e-ph} = \Omega \Sigma b^+_k b_k + N^{-1}\gamma\, \Sigma_{k,q} [\, h^+_k h_{k-q} b_q + h.c.]$$

For polaron problem DMC method is able to sum up Feynman graphs exactly:
(a) The whole sequence
(b) In non-crossing approximation

$t=1$, $\Omega=0.1$
Dimensionless constant
$g=\gamma^2/(8t\Omega)$

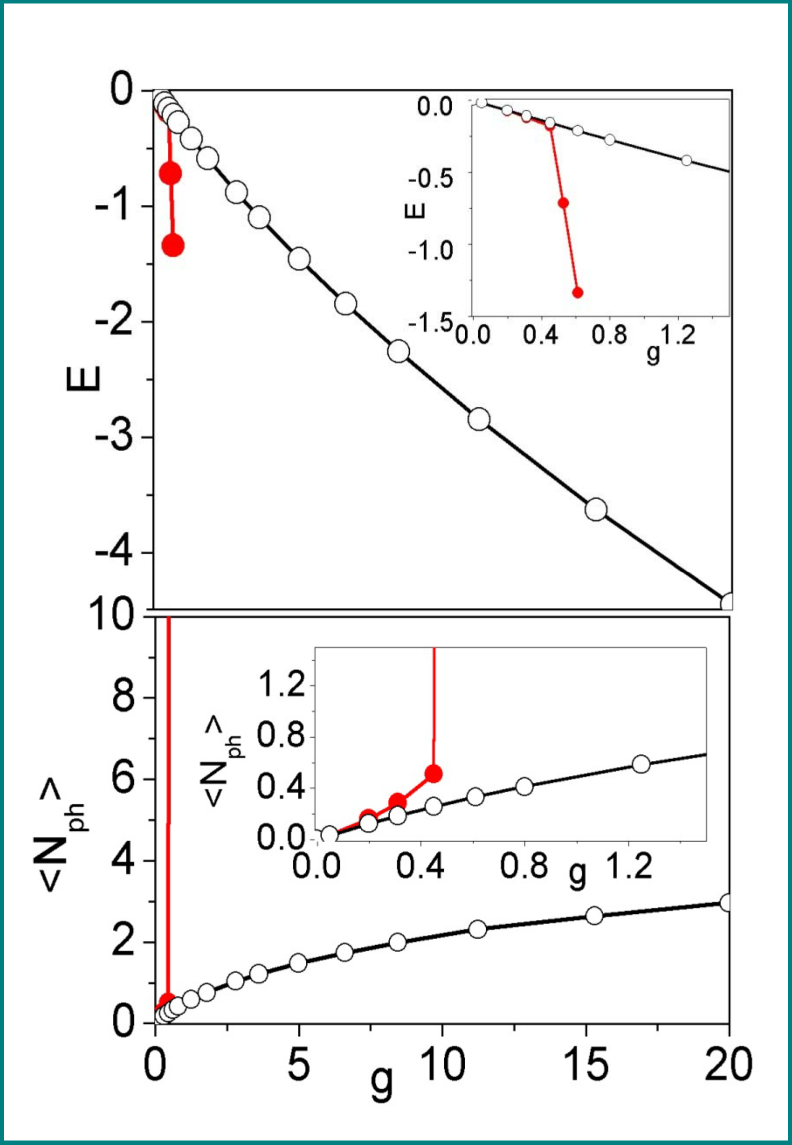

Transition into strong coupling regime:

(a) Occurs at λ=1 in exact summation

(b) Newer occurs in NCA (λ<60)

Dependence of ARPES spectrum in ground state S on the interaction constant g

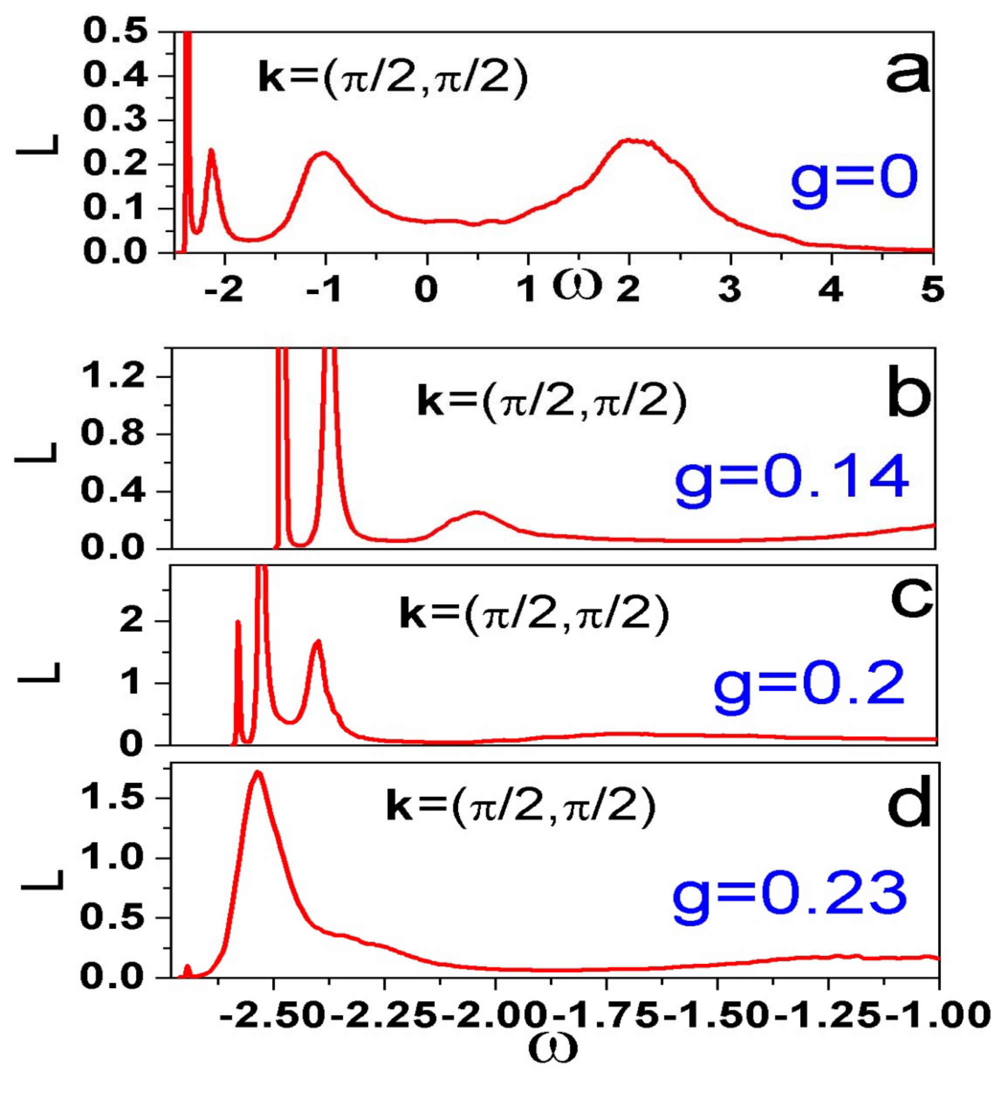

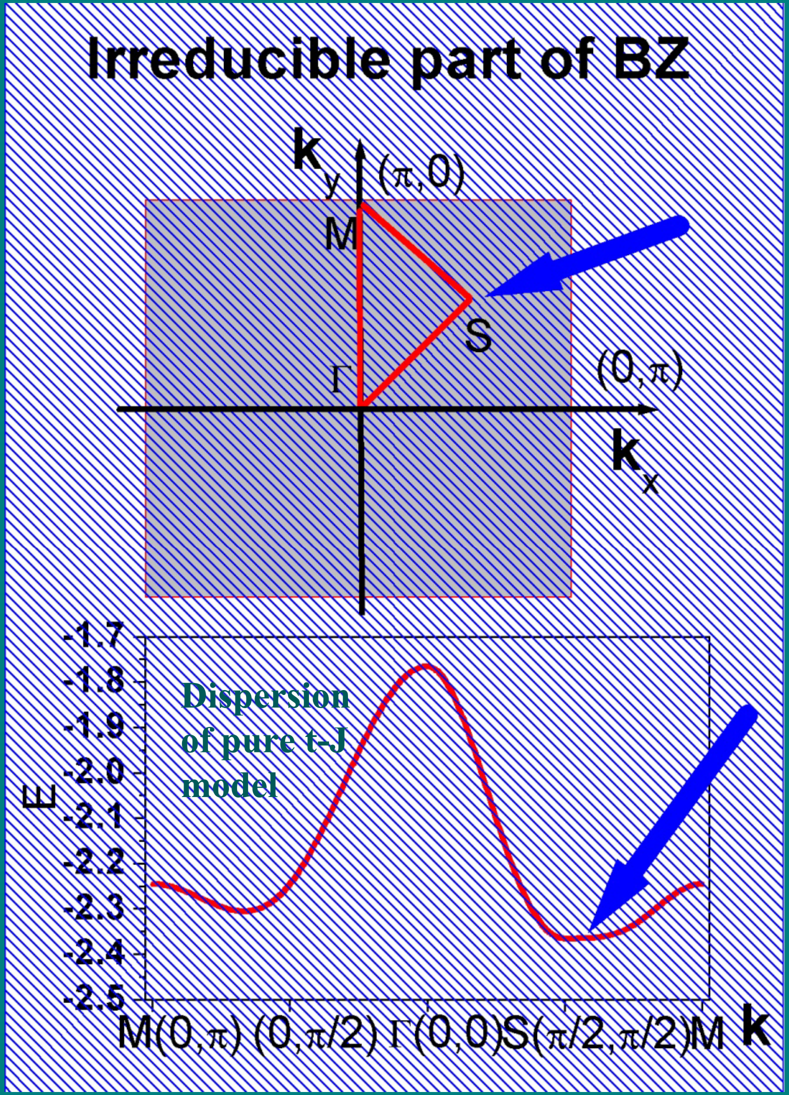

Dispersion of the broad peak in strong coupling regime

g=0.23

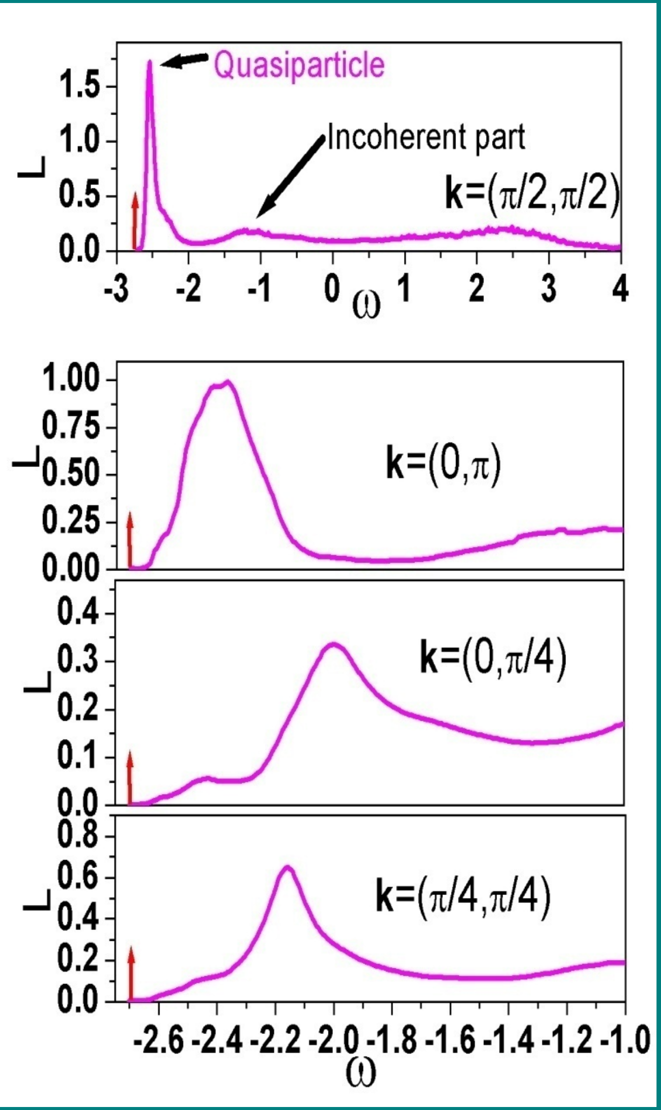

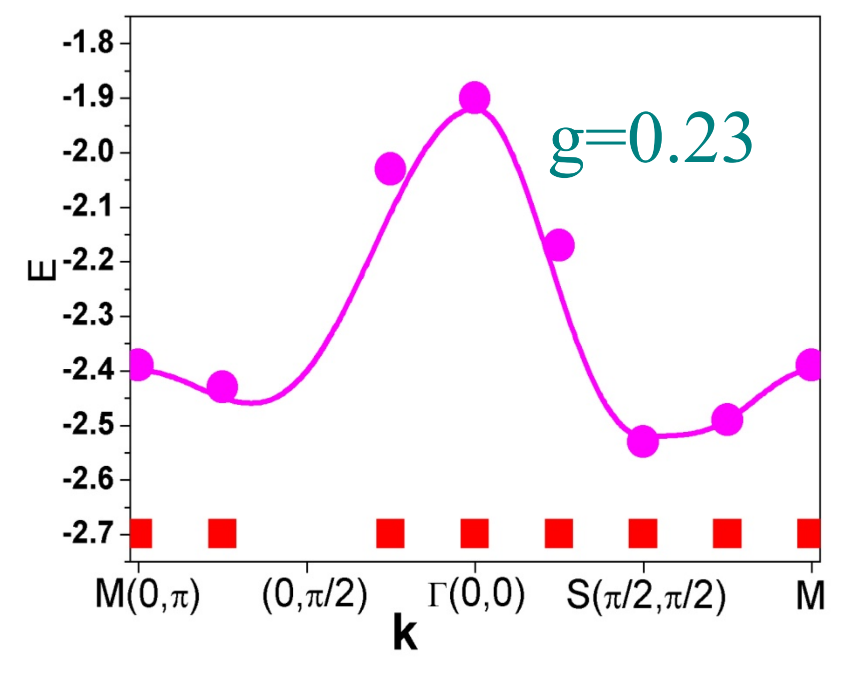

<u>Great surprise</u>: the dispersion of broad peak is <u>*exactly*</u> the same as that of pure t-J model.

Dispersion of the broad peak in strong coupling regime

g=0.2

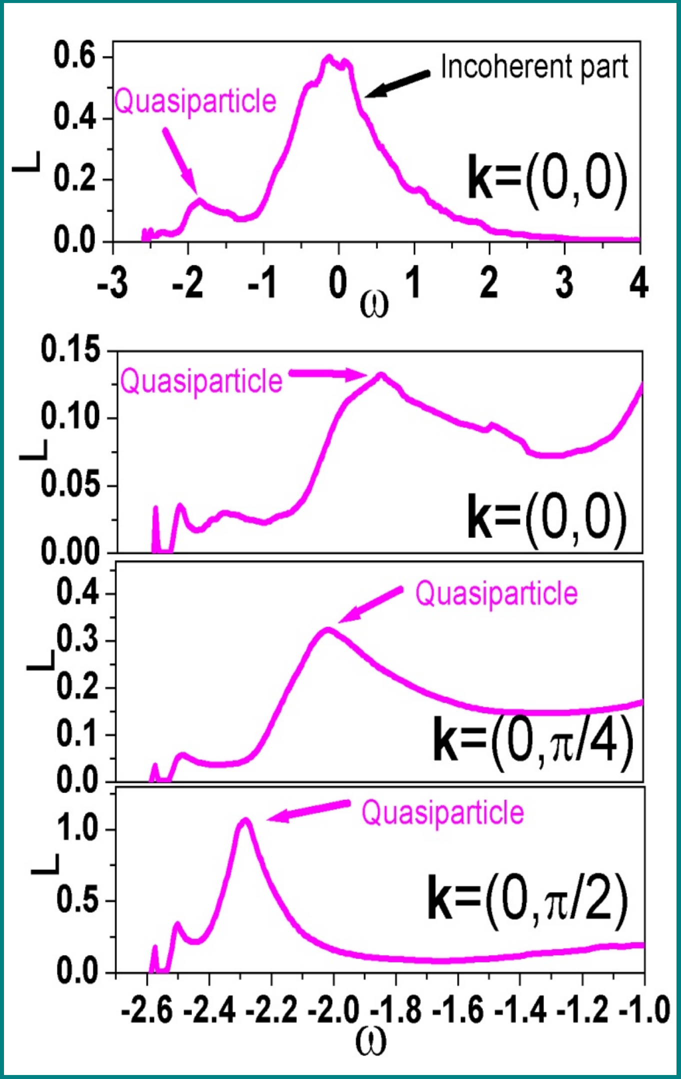

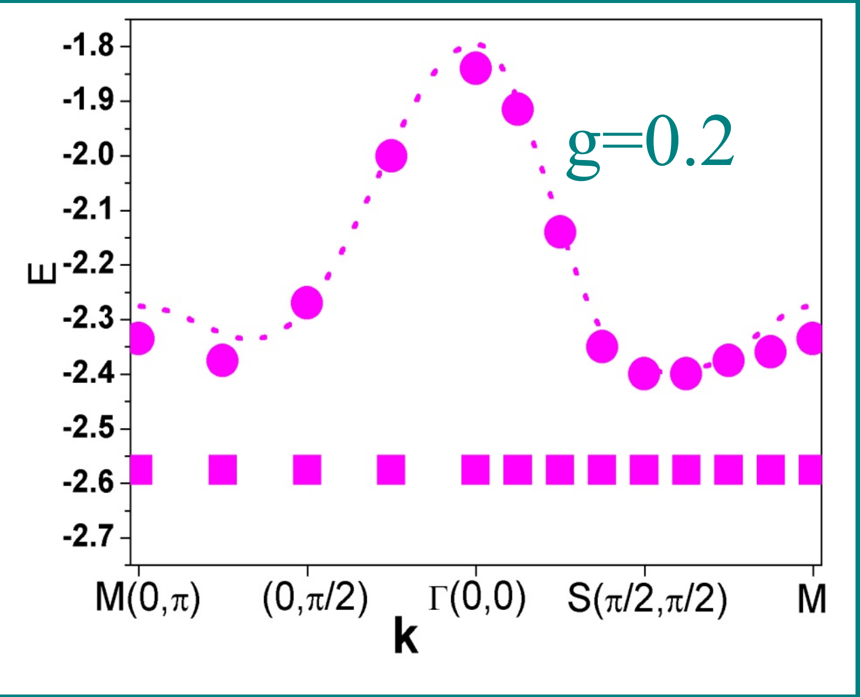

Similar dispersion of broad peak in strong coupling regime and that of pure t-J model is the general feature of strong coupling regime

ASM and N. Nagaosa, PRL, v. 93, 036402, (2004)

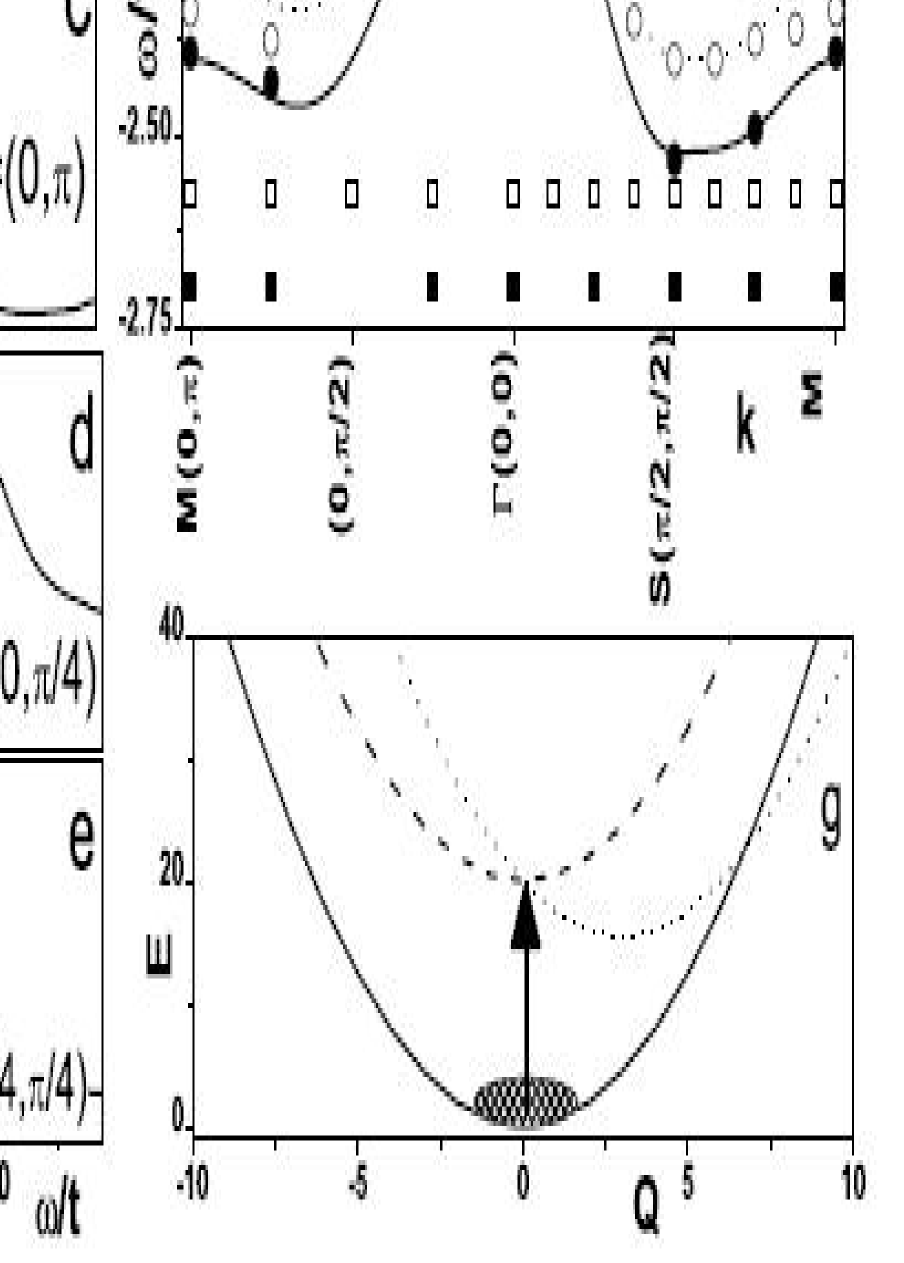

O. Rosch
and
O. Gunnarsson
Europhys. J. B
v. 43, 11 (2005)

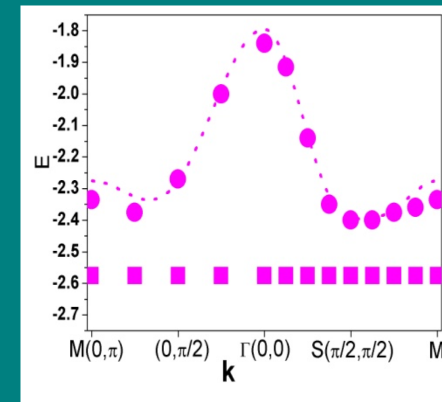

$E_{low} = Q^2/2$

$E_{up} = D + Q^2/2 - \lambda Q$

$E_{up} = D + (Q-\lambda)^2/2 - \lambda^2/2$

Q = 0 !!!!!!!!

Theoretical predictions are consistent with experiment

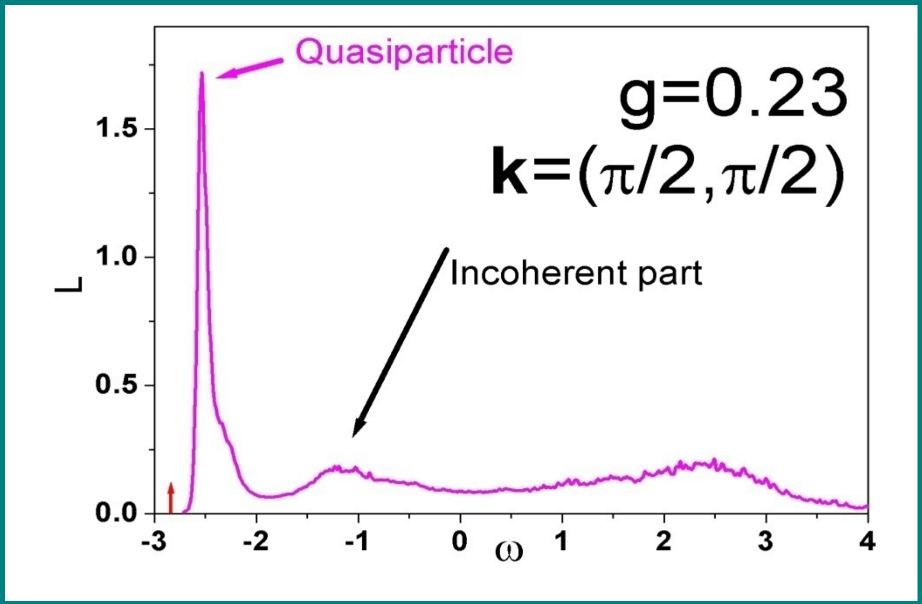

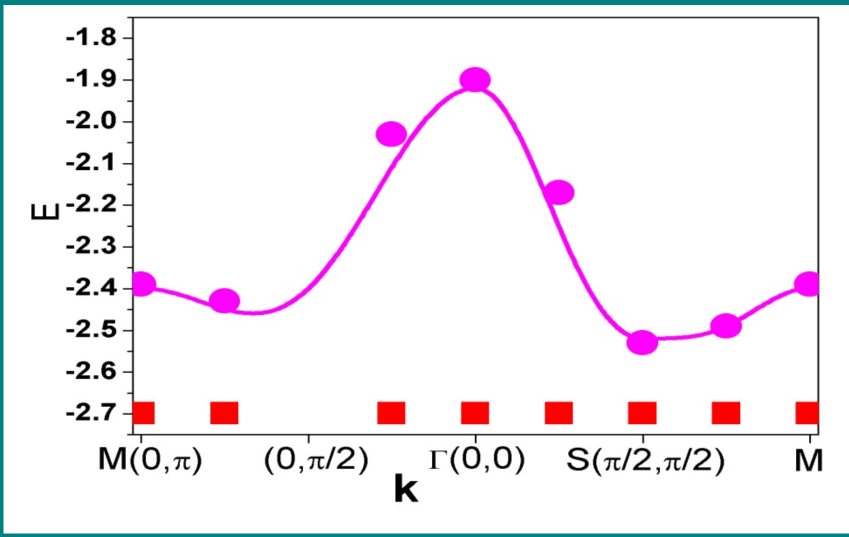

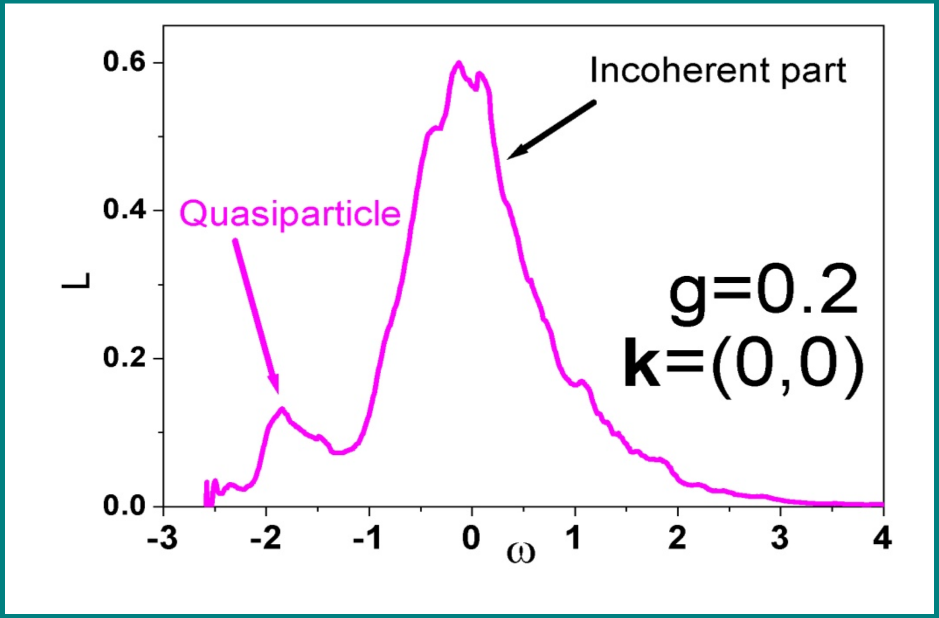

1. Broad quasiparticle has dispersion like in pure t-J model.
2. Weights of broad peaks are the same as in pure t-J model .
3. Nondispersive peak of ground state has small weight and can not be seen in ARPES.

Theoretical predictions are consistent with experiment

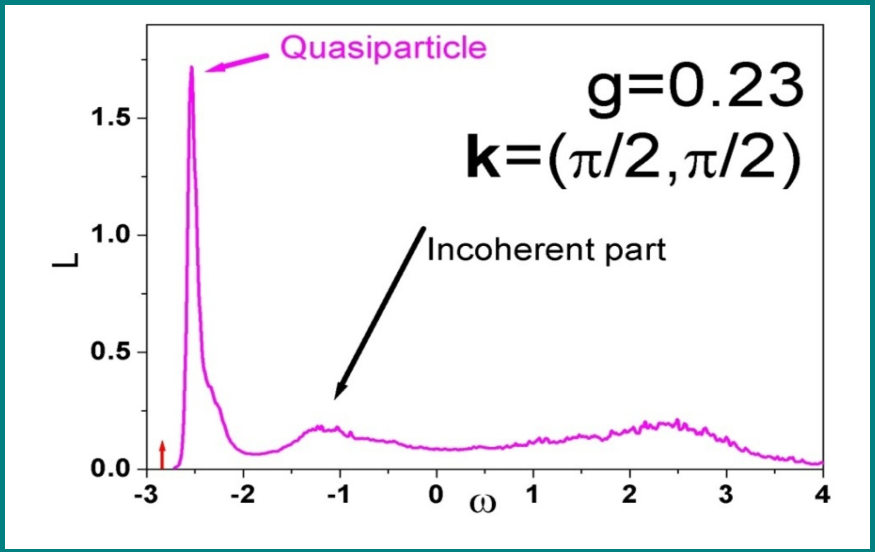

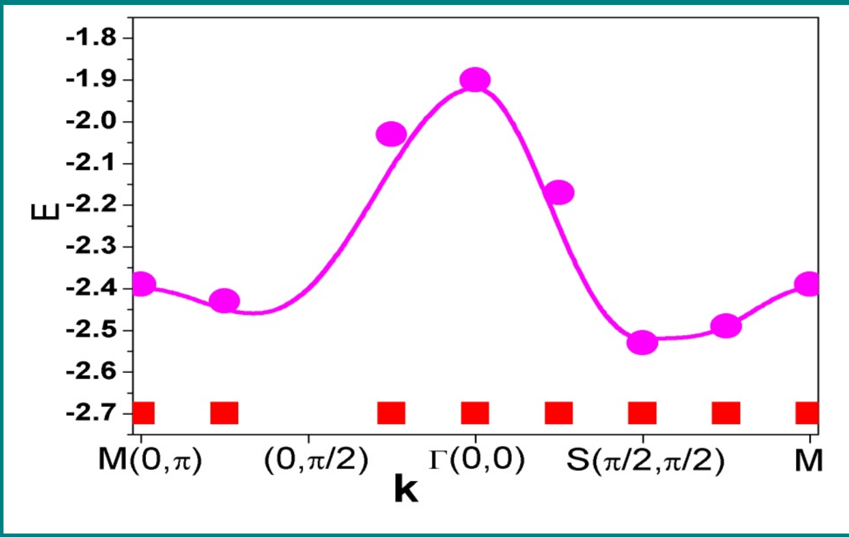

K M Shen et al, PRL, 2004

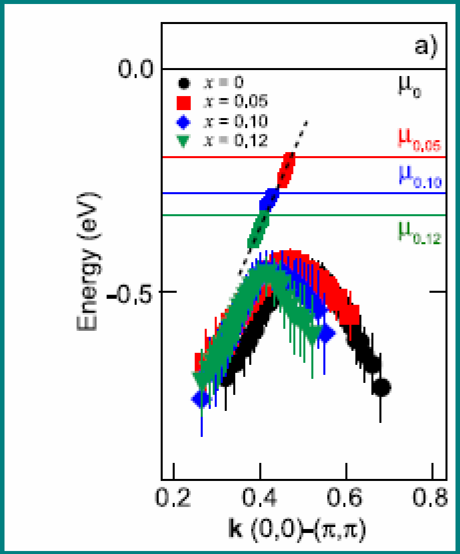

Chemical potential must be separated from the "fake" quasiparticle?

Linewidth ratio $W(x,x)/W(\pi/2,\pi/2)$ exactly reproduces experiment

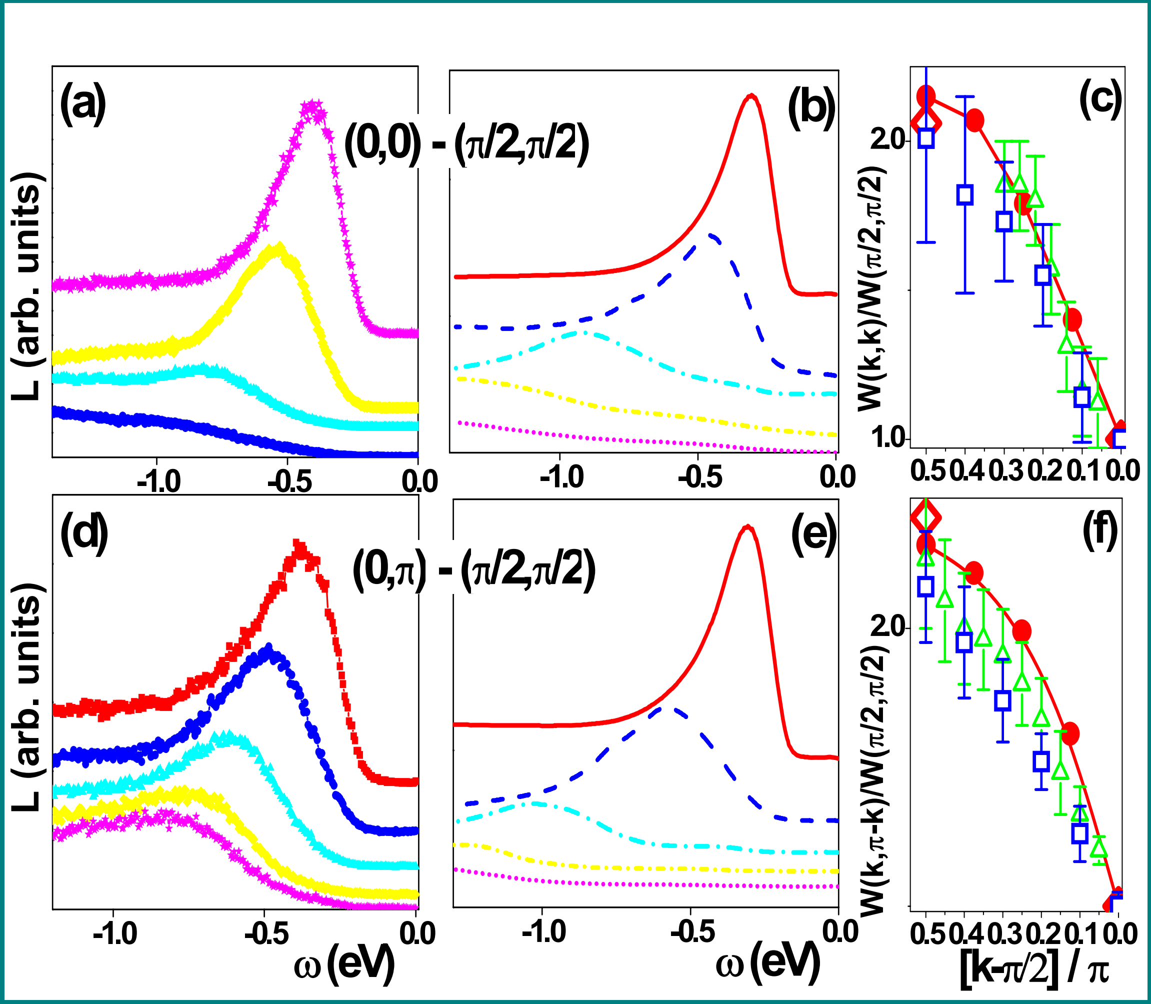

The ratio
$W(x,x)$ / $W(\pi/2,\pi/2)$
is universal
in theory
for any λ in
strong coupling
regime
(λ=0.7,1.0)
and universal
in experiment
for different
compounds
$(Sr,Ca)_2CuO_2Cl_2$

Doping dependence of the effective one-particle e-ph coupling

1. Spectral function measured by ARPES is the one-particle property of many-particle system.

2. Presence of other particles reduces the effective electron-phonon coupling which is seen by one particle.

3. Assuming mean-field like suppression of effective one-particle coupling we try to determine the doping dependence of effective electron-phonon coupling.

EDC and MDC Dispersion of LSCO: experiment

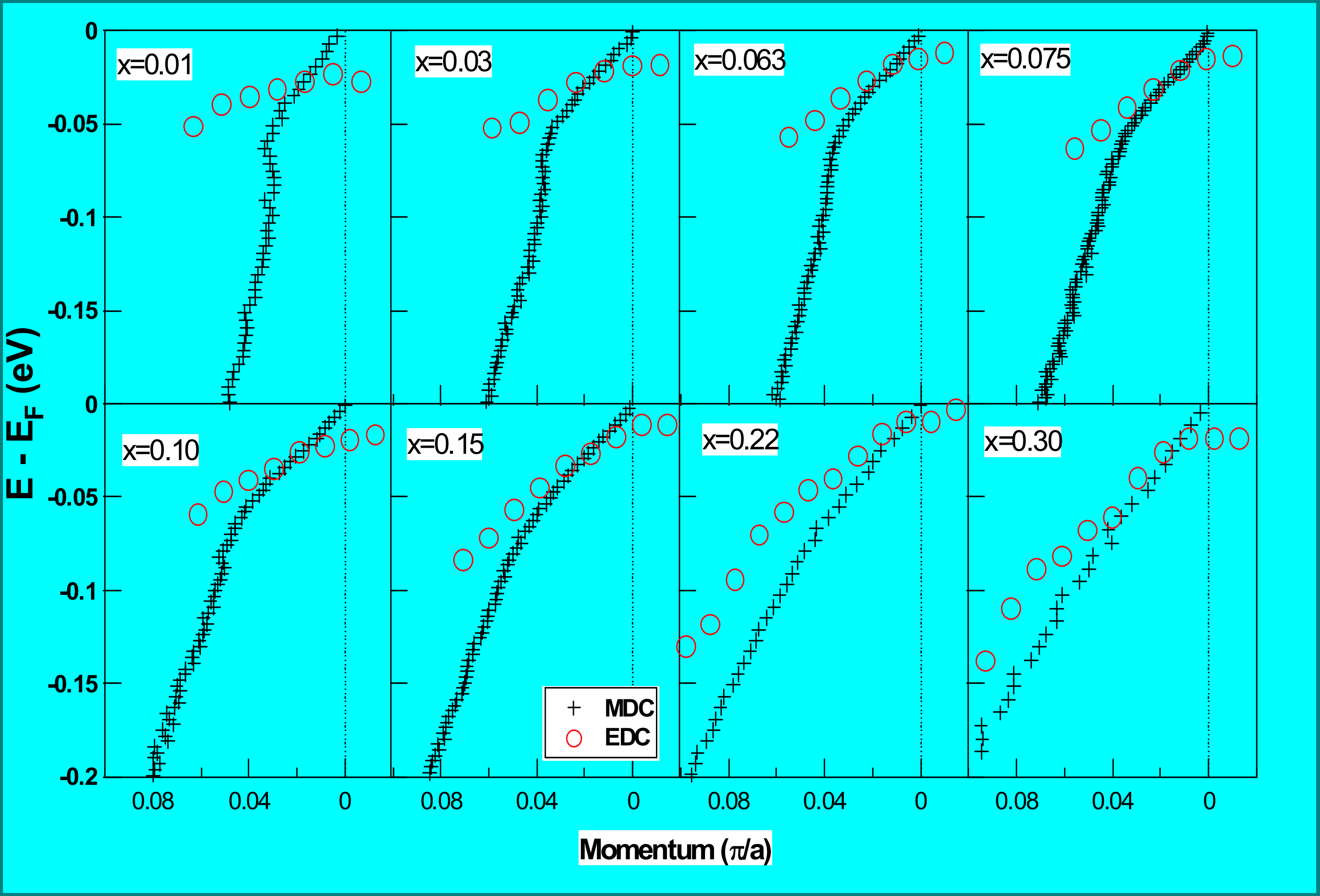

Theoretical data: theory or experiment?

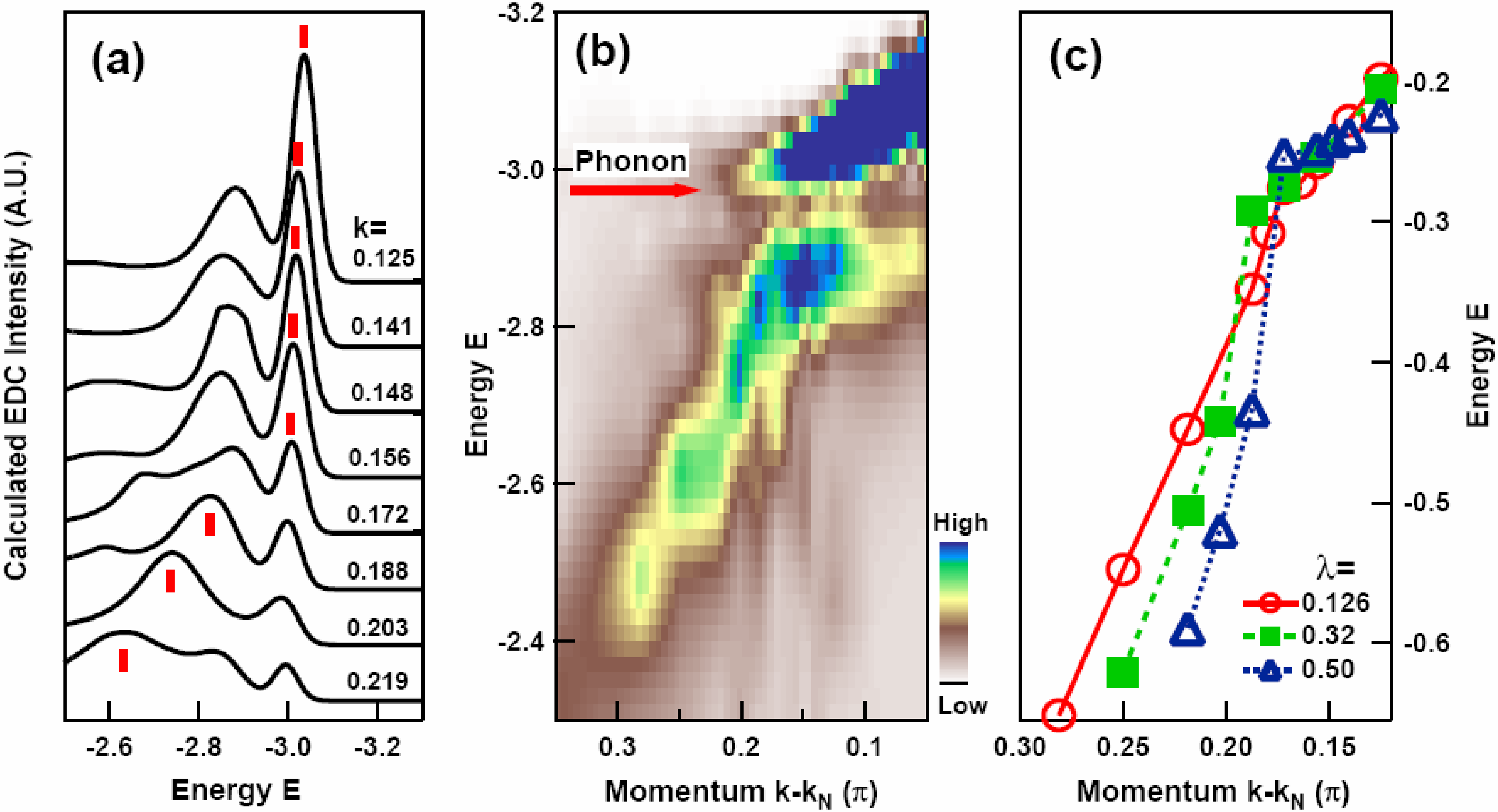

EDC and MDC Dispersion of LSCO

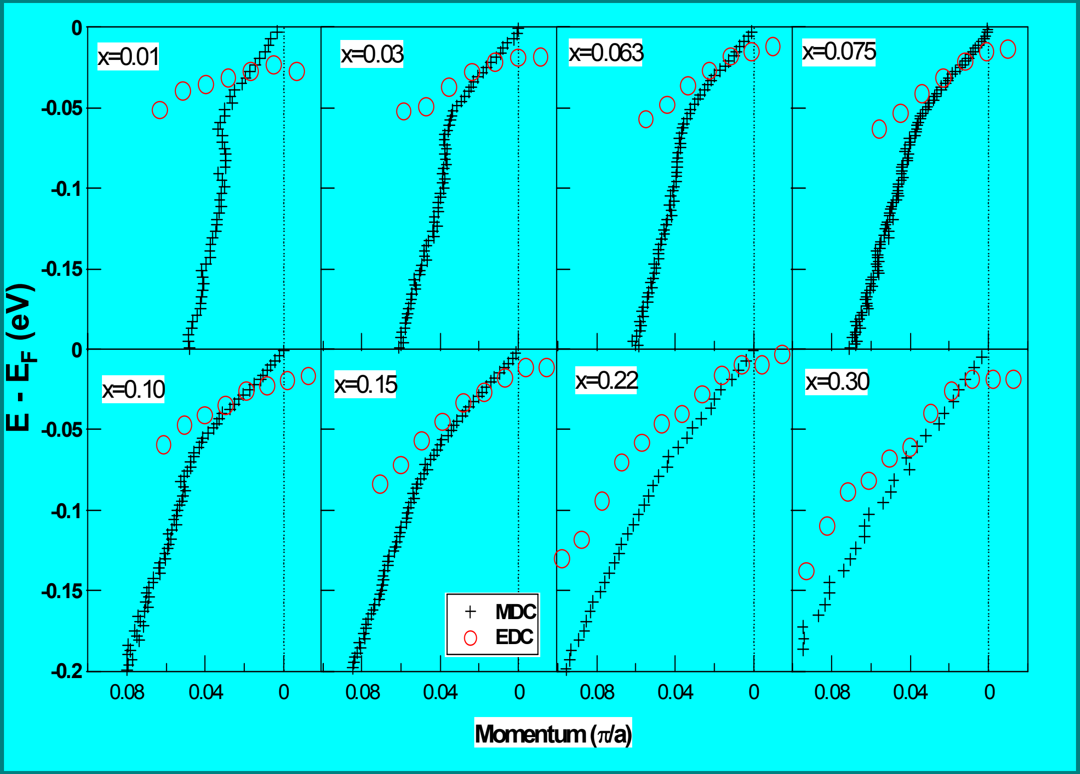

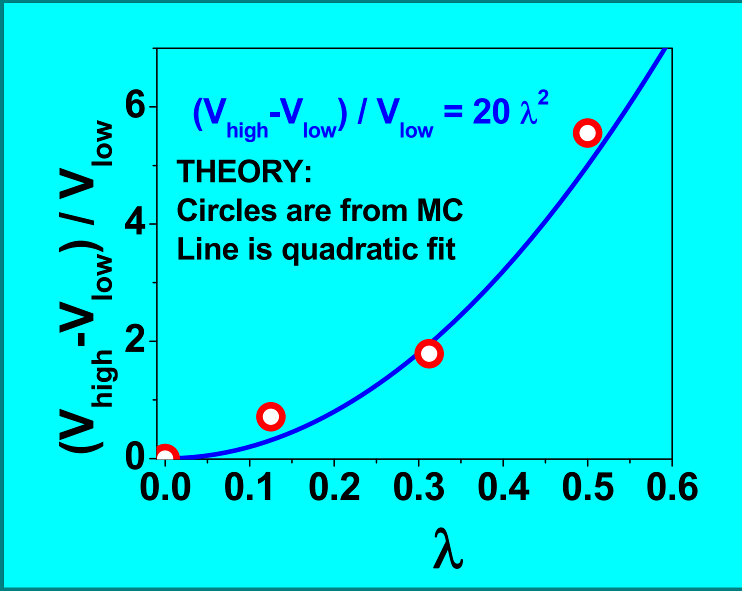

Dopping dependence of λ in LSCO

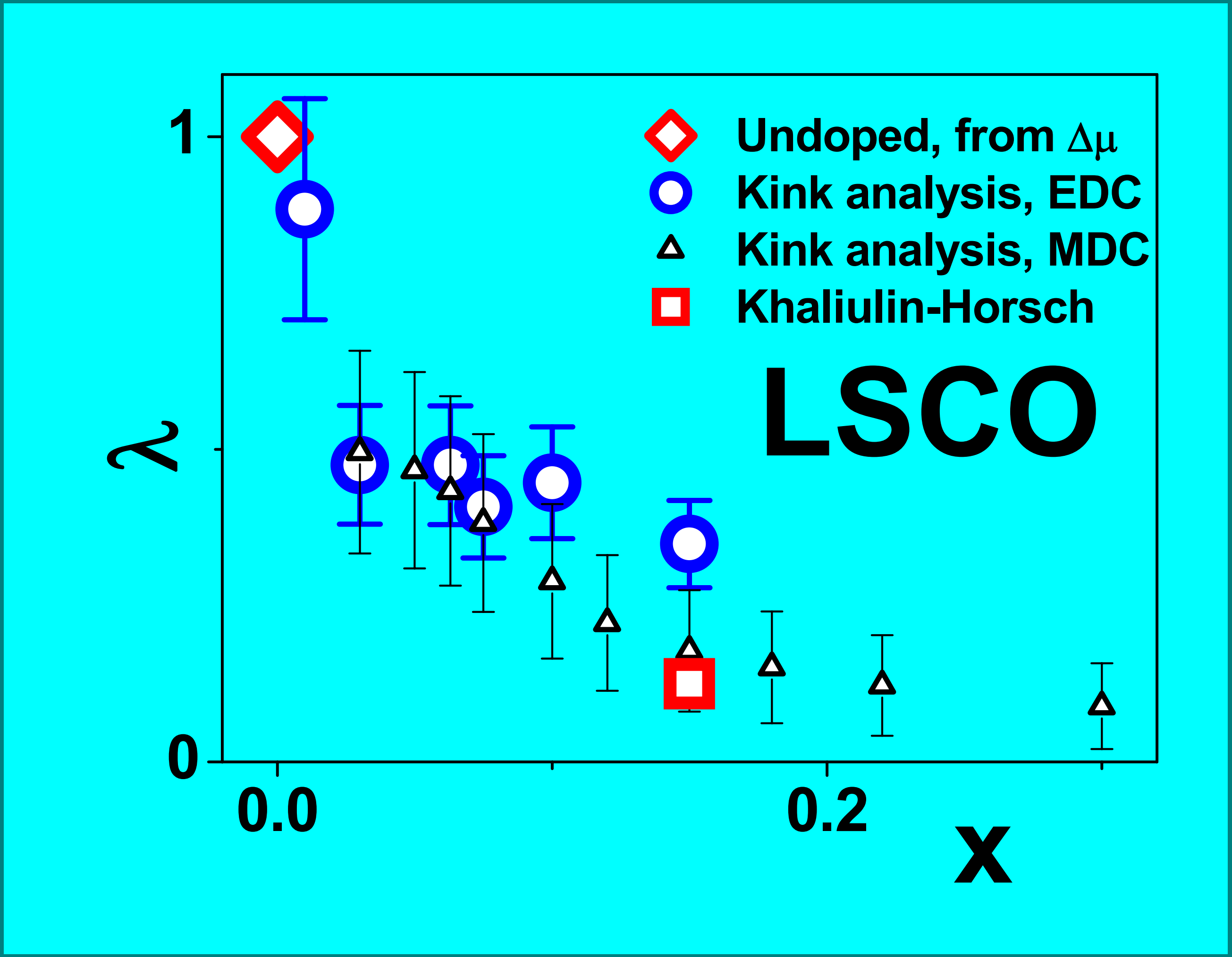

MIR in experiment

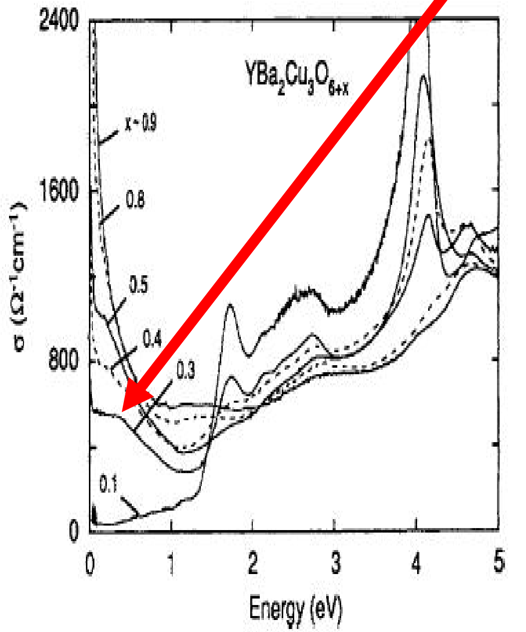

FIG. 10. In-plane ($E \perp c$) optical conductivity $\sigma(\omega)$ obtained from a Kramers-Kronig analysis of the reflectivity data for various compositions of $YBa_2Cu_3O_{6+x}$. Adapted from Cooper, Reznik, *et al.*, 1993.

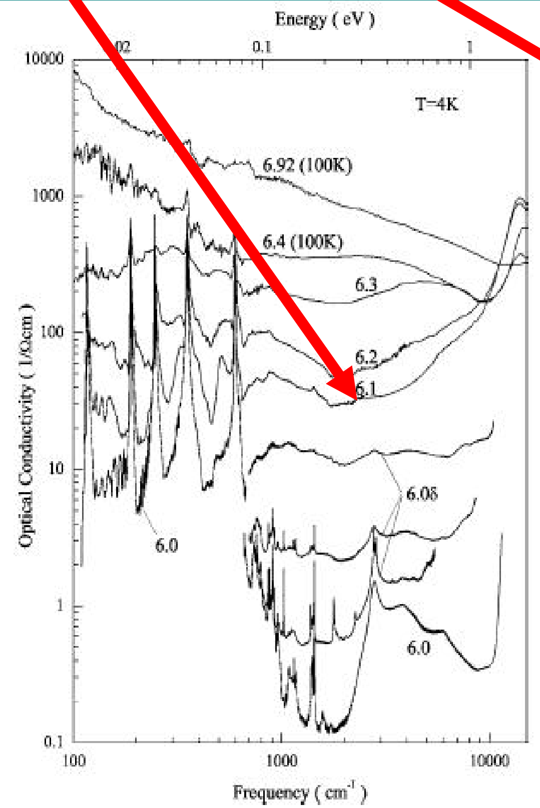

FIG. 9. Doping dependence of $YBa_2Cu_3O_x$ at 4 K (100 K for the superconducting samples with x=6.4 and 6.92). From Gruninger, 1999.

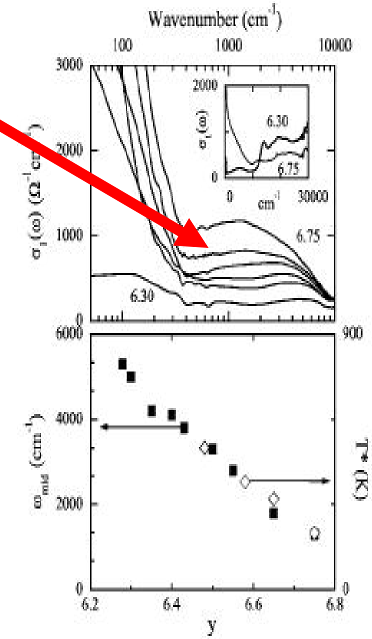

FIG. 5. (Top panel) Doping dependent $\sigma_1(\omega)$ at 10 K or at $T \simeq T_c$ for y=6.30, 6.35, 6.43, 6.50, 6.55, and 6.75. For clarity, the sharp phonon structures are removed. Inset shows the $\sigma_1(\omega)$ up to 30 000 cm^{-1} for y=6.30 and 6.75. (Bottom panel) Doping dependences of the peak position of mid-IR absorption ω_{mid} (solid square) and the pseudogap onset temperature T^* (open square) quoted from Ref. 22. The ω_{mid}/k_BT^* values are estimated to be 7–9.

Cooper, Reznik et al 1993

Gruninger 1999

Lee at al 2005

MIR – attempts of theoretical interpretation in the framework of the t-J model

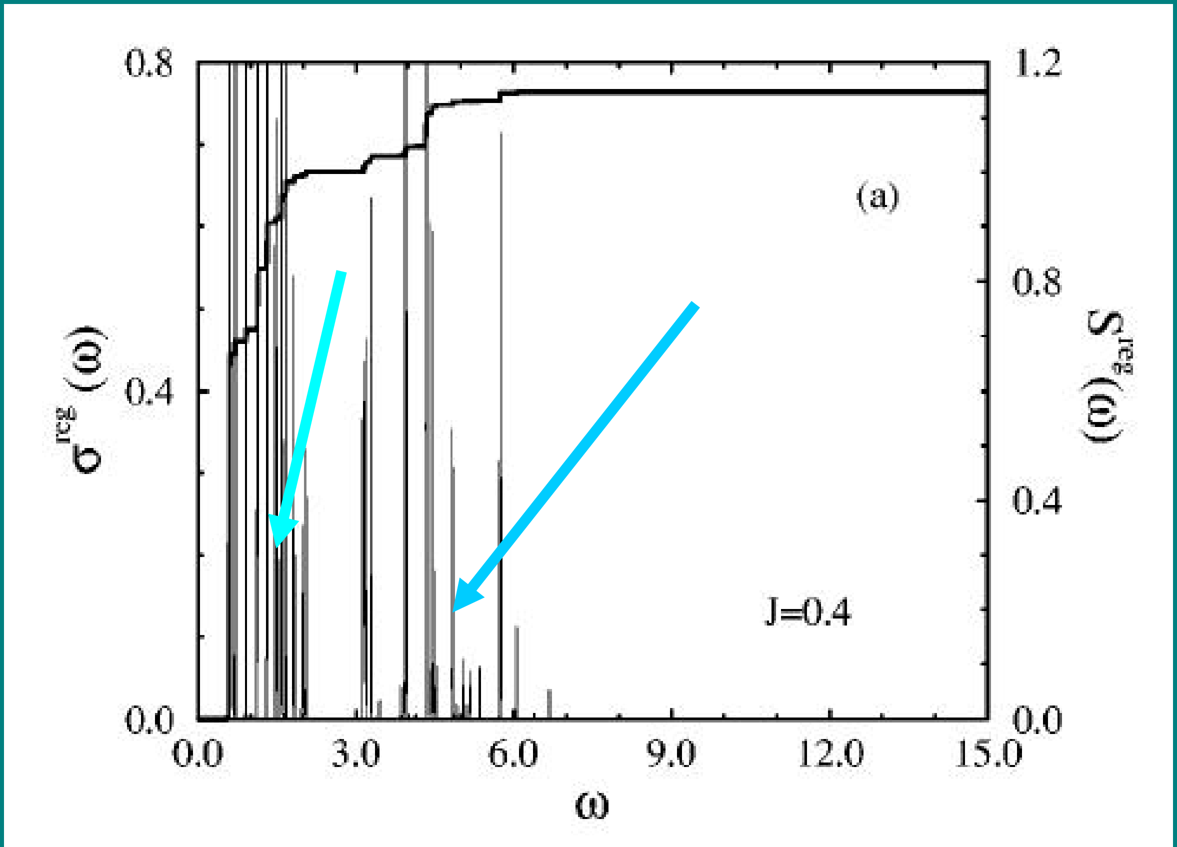

ED: Fehske, Poilblanc:

1. Main peak at 2J
2. Difficult to see secondary peak
3. Peak at 5t

MIR – contradictions between theory and experiment: 1

Theory

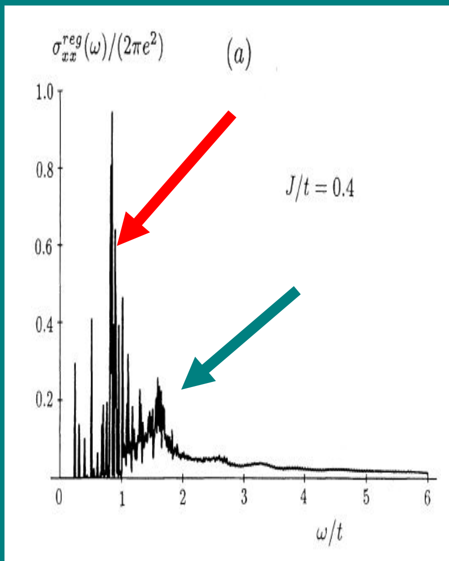

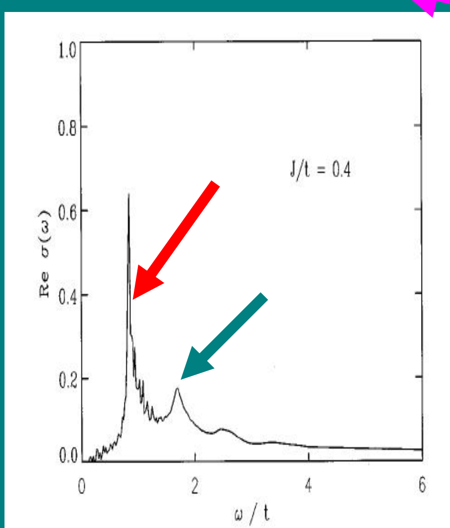

In experiment:
MIR energy = 0.5 eV at low doping

In theory:
t=0.4 eV, J=0.35t.
MIR energy = 0.28 eV

Experiment

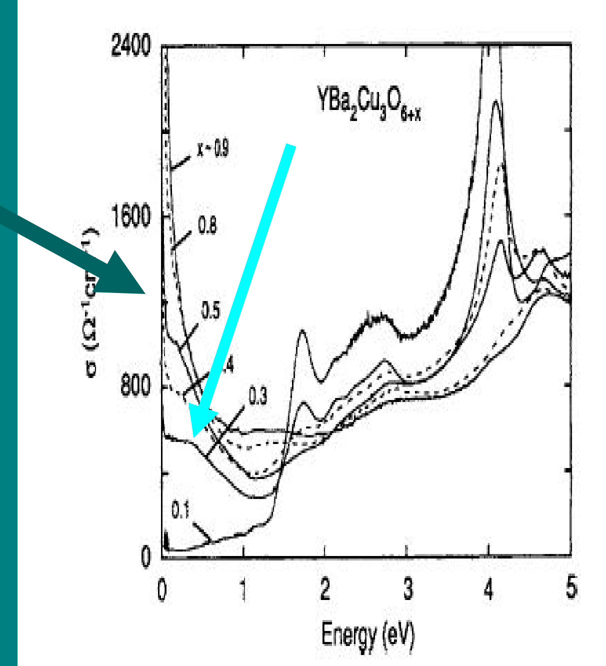

FIG. 10. In-plane ($E \perp c$) optical conductivity $\sigma(\omega)$ obtained from a Kramers-Kronig analysis of the reflectivity data for various compositions of $YBa_2Cu_3O_{6+x}$. Adapted from Cooper, Reznik, *et al.*, 1993.

MIR – contradictions between theory and experiment: 2

Theory

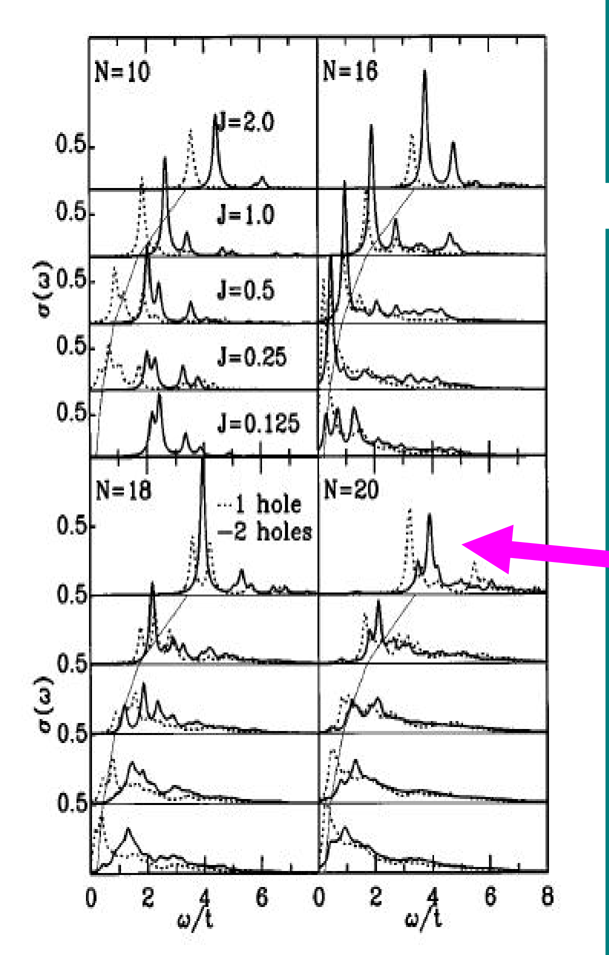

Experiment

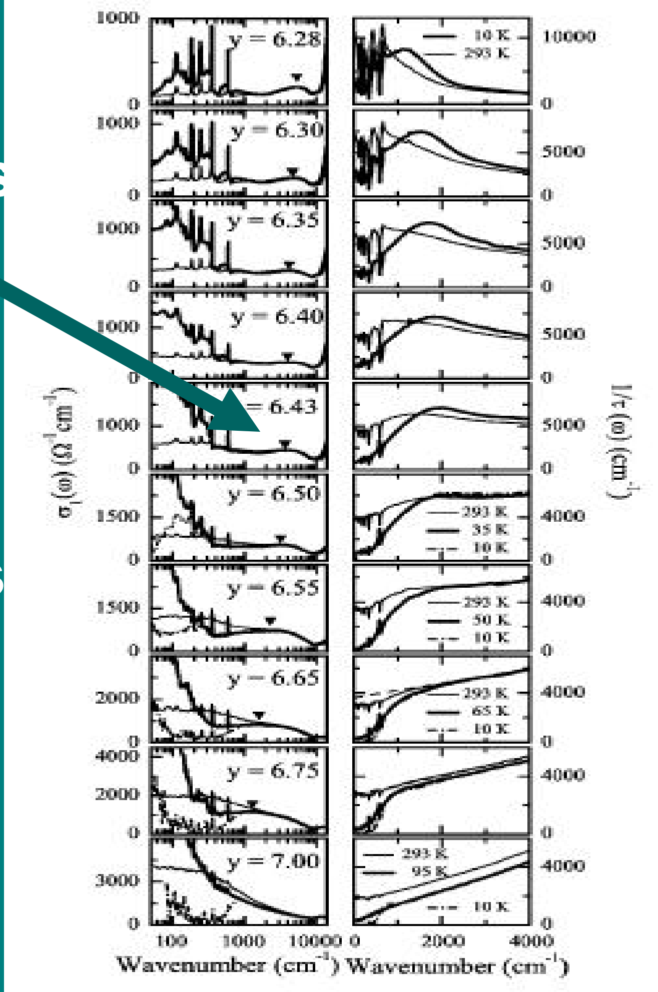

In experiment:
MIR energy decreases with increase of doping

In theory:
MIR energy increases with increase of doping

PHONONS?

DMC is better than ED and SCBA – infinite system, resolution.

SCBA

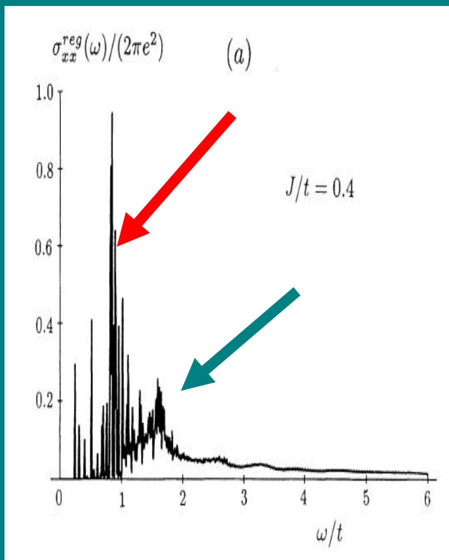

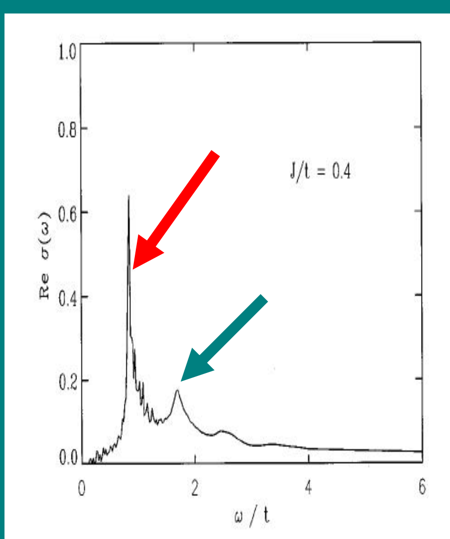

ED

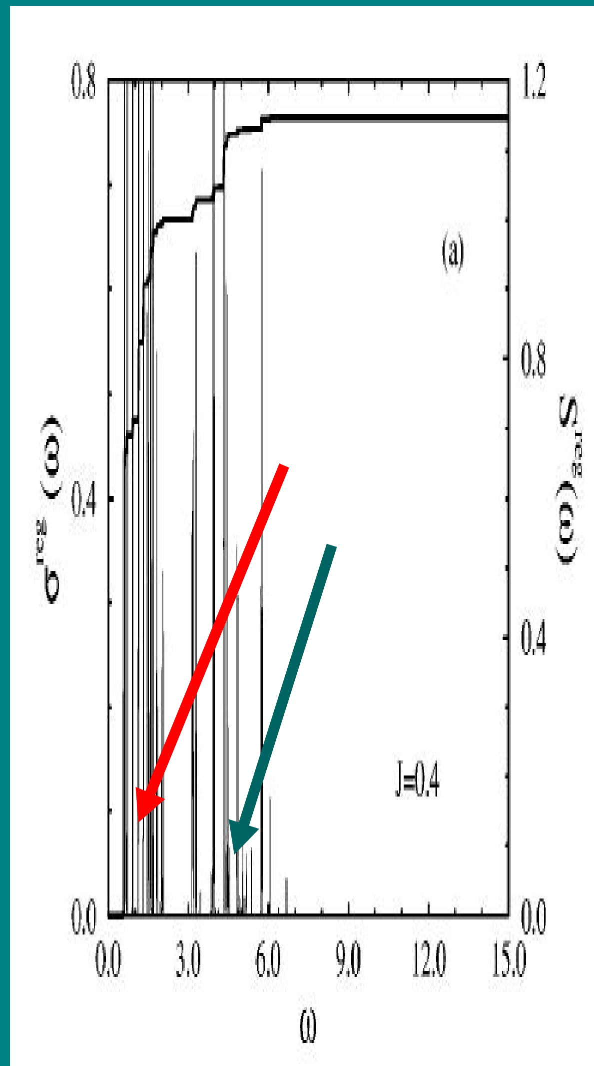

DMC t-J

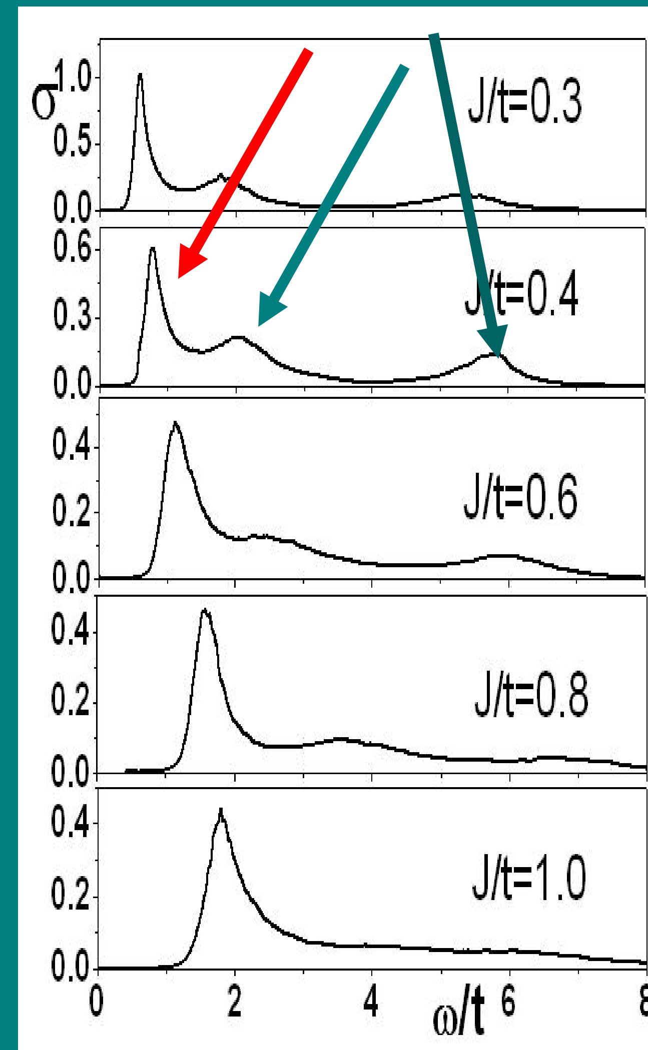

Phonon-scattering feature is known from experiment

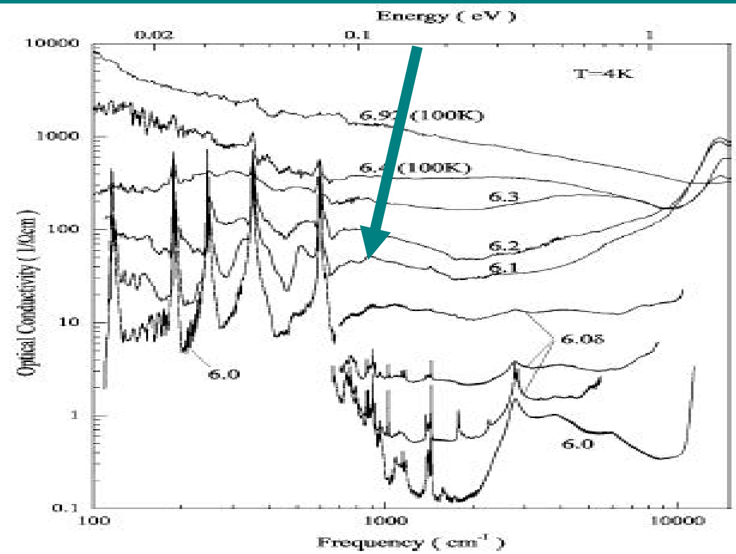

FIG. 9. Doping dependence of $YBa_2Cu_3O_x$ at 4 K (100 K for the superconducting samples with $x=6.4$ and 6.92). From Gruninger, 1999.

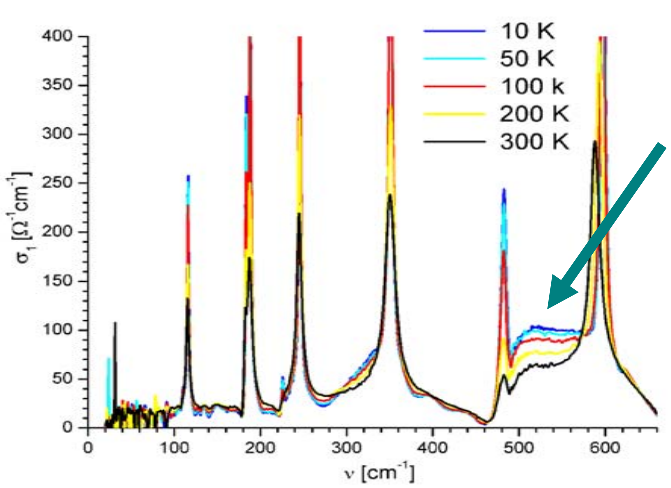

From C. Bernhard

DMC t-J-Holstein

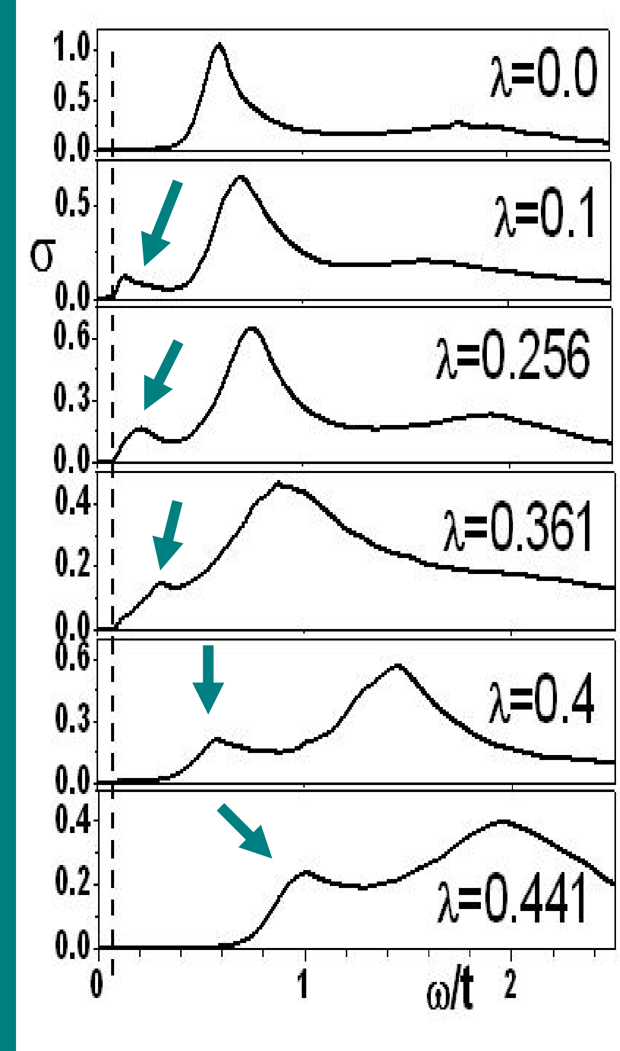

Doping dependence of effective electron-phonon coupling strength

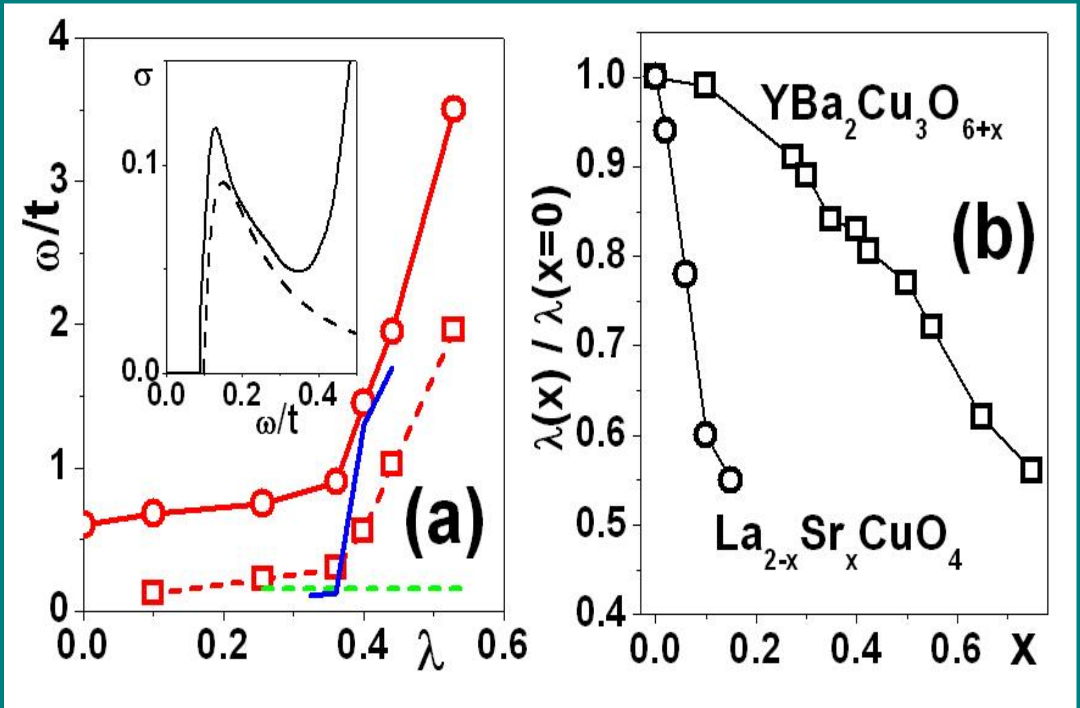

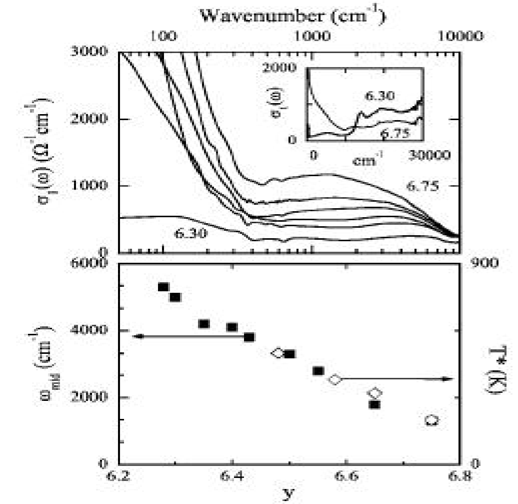

FIG. 5. (Top panel) Doping dependent $\sigma_1(\omega)$ at 10 K or at $T \simeq T_c$ for y=6.30, 6.35, 6.43, 6.50, 6.55, and 6.75. For clarity, the sharp phonon structures are removed. Inset shows the $\sigma_1(\omega)$ up to 30 000 cm^{-1} for y=6.30 and 6.75. (Bottom panel) Doping dependences of the peak position of mid-IR absorption ω_{mid} (solid square) and the pseudogap onset temperature T^* (open square) quoted from Ref. 22. The ω_{mid}/k_BT^* values are estimated to be 7–9.

Scaling $\lambda_c^{ttt\text{-}J} = 1.5\lambda_c^{t\text{-}J}$

We determine the effective coupling for given doping from the the experimental position of MIR.

Doping dependence of effective electron-phonon coupling strength

Optical conductivity

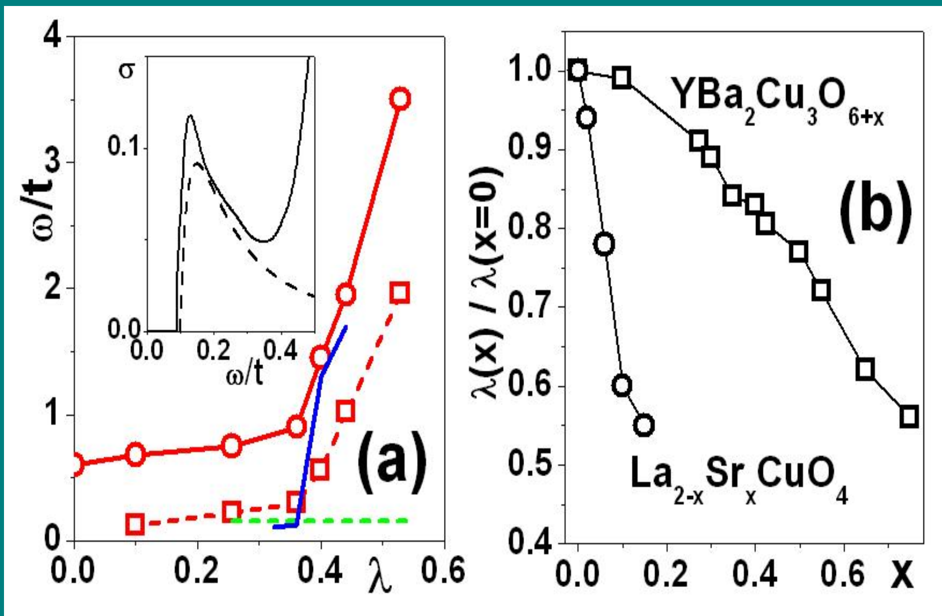

ARPES

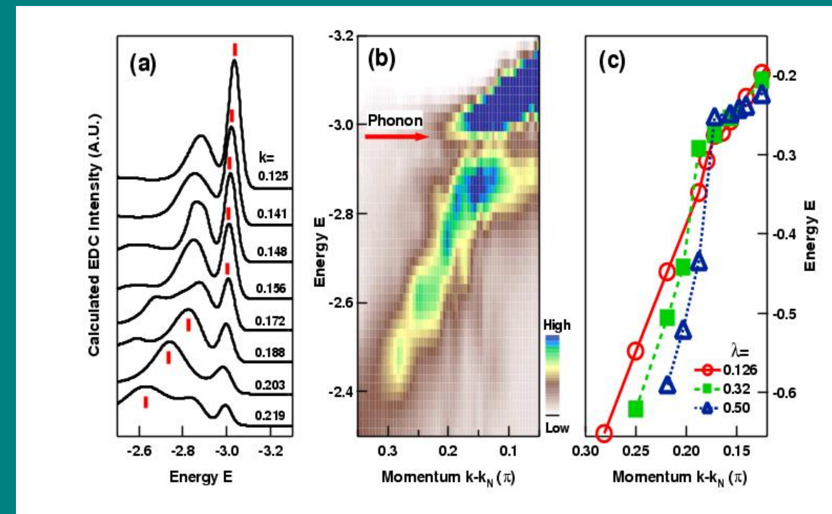

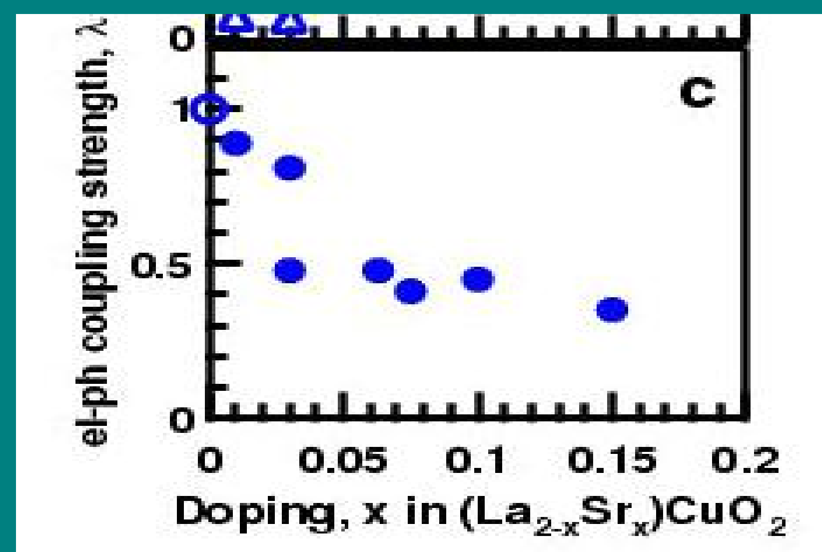

Doping dependence of effective electron-phonon coupling strength

Optical conductivity

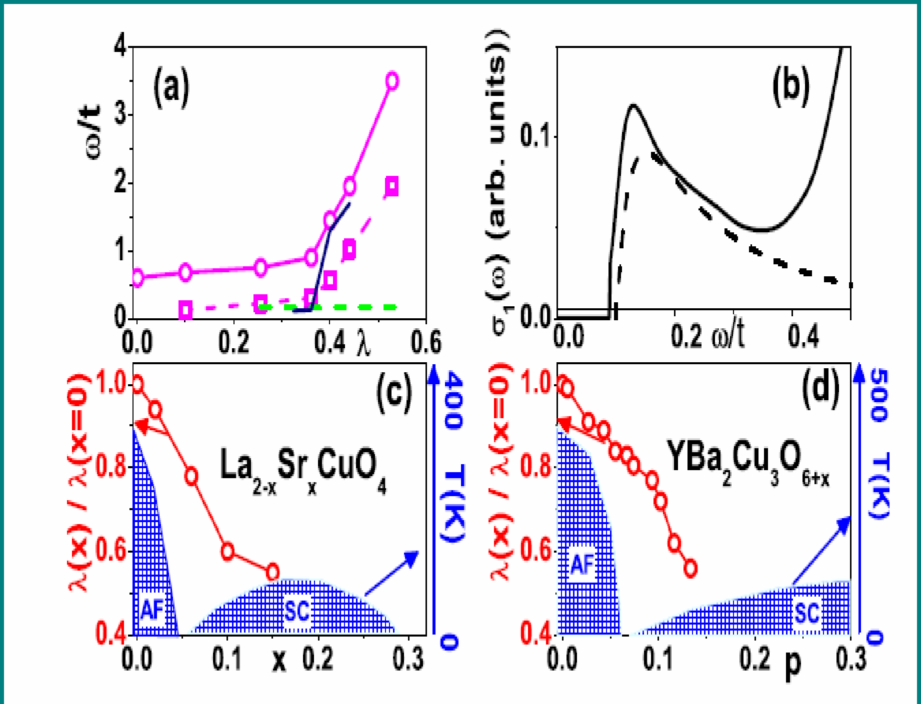

ARPES